LINKING PHOTOSYNTHESIS PHYSIOLOGY OF UPLAND HARDWOOD REPRODUCTION TO ECOLOGY AND SILVICULTURE IN THE ARKANSAS OZARKS

A Dissertation Submitted
to the Graduate School
University of Arkansas at Little Rock

in partial fulfillment of requirements
for the degree of

DOCTOR OF PHILOSOPHY

in Applied Science

in the Department of Applied Science
of the College of Science

May 2014

Kutcher Kyle Cunningham

Master of Science, Mississippi State University, 2003
Bachelor of Science, Mississippi State University, 2001

ProQuest LLC.
789 East Eisenhower Parkway
P.O. Box 1346
Ann Arbor, MI 48106 - 1346

This dissertation, “Linking Photosynthesis Physiology of Upland Hardwood Reproduction to Ecology and Silviculture in the Arkansas Ozarks”, by Kutcher Kyle Cunningham, is approved by:

Dissertation Advisor:	Stephen Grace Associate Professor of Biology
Dissertation Committee:	John Bush Associate Professor of Biology
	William Baltosser Professor of Biology
	Margaret McMillan Associate Professor of Earth Science
	Qingfang He Professor of Applied Science
Program Coordinator:	Tansel Karabacak Professor of Applied Science
Interim Graduate Dean:	Paula Casey Professor of Law

Fair Use

Duplication

LINKING PHOTOSYNTHESIS PHYSIOLOGY OF UPLAND HARDWOOD REPRODUCTION TO ECOLOGY AND SILVICULTURE IN THE ARKANSAS OZARKS by Kutcher Kyle Cunningham, May 2014

ABSTRACT

Oak (*Quercus*) forests in the Arkansas Ozarks have been important culturally, ecologically and environmentally for centuries. Historically these forests were fire dependent and dominated by oak species. In the past century, fire suppression and land management have caused these forests to densify. As a result, oaks are increasingly less abundant following disturbance in natural hardwood stands. Many applied ecological studies have explored methods and practices to maintain oak species in newly developing stands. This study attempted to link the mechanistic physiology of oak and non-oak reproduction to the applied ecological work. Varying stand conditions were generated in an undisturbed mature hardwood forest. Photosynthesis physiology was evaluated through direct and in-direct measures for six upland hardwood species in the Springfield Plateau of the Arkansas Ozarks. Environmental conditions, including sunlight canopy penetration, were significantly different based on treatment/slope position combinations. Corresponding differences in photosynthesis, development and abundance of hardwood reproduction were also significant across treatments, topographic position, and species. In conclusion, this study demonstrates that *in situ* measurements of photosynthetic performance are a valuable tool in predicting stand performance in oaks growing in their natural environment.

ACKNOWLEDGEMENTS

I would first like to Dr. Stephen Grace and Dr. John Bush for their unreserved assistance and guidance during my time at the University of Arkansas at Little Rock. I would like to acknowledge Dr. Bill Baltosser, Dr. Beth McMillan and Dr. Qingfang He for their assistance as committee members. I thank all my mentors for sharing their vast knowledge with me through the progression of my Ph.D. program.

Special thanks are extended to the Arkansas Forest Resources Center, the University of Arkansas – Division of Agriculture, and the University of Arkansas Livestock and Forestry Research Station at Batesville for the support and resources provided to complete my research. Special thanks to Don Hubbell, Station Director, and Mike McGowan, Station Forester, for their assistance with completing the field work for the research project. Furthermore, I would like to thank Dr. Tamara Walkingstick and Dr. Phil Tappe for their patience, support, and guidance as I worked through my Ph.D. program.

Furthermore, I wish to thank Beverly, my mother, and Sonny, my father, for their never ending support and understanding, when it was most needed. I am also grateful to Brant, my brother, and Christy, my sister, and their families for their support and encouragement through the Ph.D. process. Finally, I wish to thank my son, Caleb, and step-daughter, Brooklyne, for giving me purpose and keeping me motivated throughout my Ph.D. experience.

TABLE OF CONTENTS

LIST OF FIGURES AND ILLUSTRATIONS

LIST OF TABLES

CHAPTER I – INTRODUCTION

The Plant Ecophysiological Concept

Plant ecology is an experimental science that examines interactions of species within communities and the way in which populations of species adapt to a range of environments (Lambers et al. 2008). Ecological studies have been important for examining ecological processes in upland hardwood ecosystems. These processes may include: growth, survival, reproduction, and/or distribution of tree species. A number of applied ecological studies have examined reproduction dynamics in upland hardwood ecosystems and silvicultural methods for reestablishing important species, such as oak (*Quercus*) species, in hardwood forests across the eastern United States (*e.g.* Brose et al. 1999, Cunningham et al. 2011, Hicks et al. 2001, Hodges and Janzen 1986, Loftis 1990, Loftis 1993, Larsen and Johnson 1998, Rogers et al. 1993, Rogers Sander and Graney 1993and Johnson 1998).

Plant physiology is often concerned with the individual and physiological responses to its environment (Lambers et al. 2008). Physiological studies often provide insight to how an individual will respond to a change in a specific aspect of the environment. While there are often limitations on extrapolating responses under a controlled environment, physiological studies provide valuable insight to ecological processes (Lambers et al. 2008). A number of physiological studies have been conducted examining physiological processes in reproduction of hardwood species, including oak species (*e.g.* Abrams 1990, Bahari et al. 1985, Battaglia et al. 2000, Hinckley et al. 1978, Hodges and Gardiner 1993, Gardner and Hodges 1998, Lockhart and Hodges 2003, and Quero et al. 2008).

Plant ecophysiology is an experimental science that seeks to describe the physiological mechanisms underlying ecological observations. Ecophysiologists or physiological ecologists address ecological questions related to the controls over the growth, survival, reproduction, abundance, and geographical distribution of plants. The controls over these processes involve

interactions of plants with their physical, chemical, and biotic environment (Lambers et al. 2008). Tree growth (and subsequent survival) is a result of myriad interacting physiological processes influenced by inherited genetic traits and the ambient environment (Dixon, 1990).

When addressing questions about regeneration ecology in upland hardwood systems, physiological ecology involves using physiological mechanisms to assess how the reproduction of different tree species function in given environments. My study focused on photosynthesis physiology of oak and non-oak competitors in different understory light environments and attempts to link the physiological mechanistic responses to seedling growth, survival, competitiveness, and abundance.

Study Objectives

Treatments were established to generate contrasting mid-story/overstory density levels in an upland hardwood forest. Study variables for oak and non-oak reproduction analysis included:

1. Treatment effects on understory sunlight levels.
2. Treatment effects on hardwood reproduction size and abundance.
3. Methodology for analyzing photosynthesis physiology in the field.
4. Treatment, season, and species level effects on photosynthesis physiology.

The goal of the study was to further supplement our understanding of upland hardwood regeneration dynamics. To achieve this goal we attempted to link the relationships between the physiology, ecology, and silviculture of hardwood regeneration in the Arkansas Ozarks (Figure 1.).

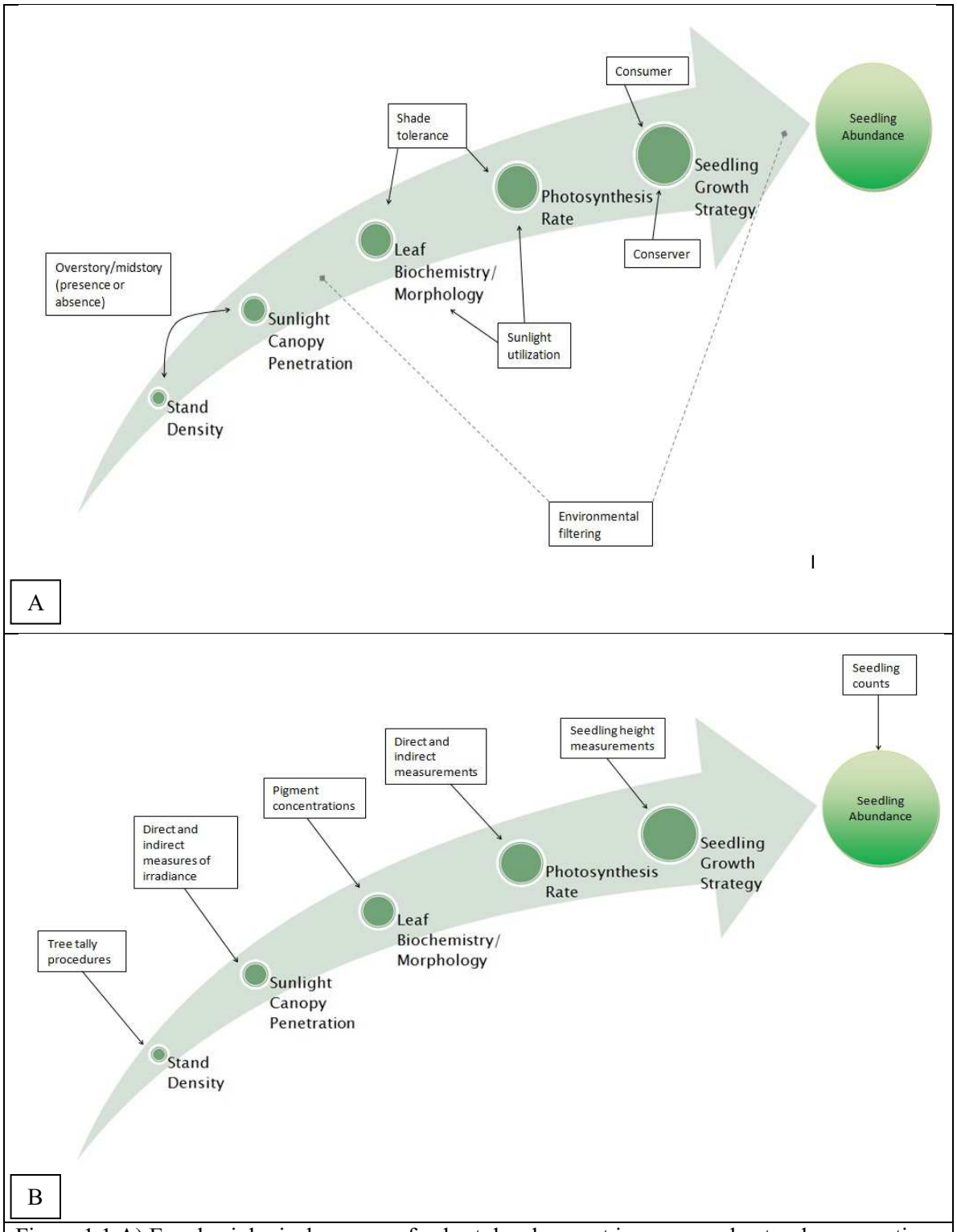

Figure 1.1 A) Ecophysiological process of cohort development in even-aged natural regeneration. B) Measurement methodology for variables examined.

Background

The hardwood forests of the Arkansas Ozarks have been dominated by oaks (*Quercus* spp.) since pre-settlement times. The forests also included hickories (*Carya* spp.), ash (*Fraxinus* spp.), blackgum (*Nyssa sylvatica*), elm (*Ulnus* spp.), maple (*Acer* spp.), other hardwoods, and a component of shortleaf pine (*Pinus enchinata* L.), as stated by Foti (2004). These oak dominated forests have provided resources to the region for hundreds of years including: timber, wildlife habitat (critical for many species), clean water and air, and aesthetic quality. They have influenced the economy, growth, culture, and landscape of the Ozarks prior to and since the early settlement era (Sabo et al. 2004).

Early survey records indicate that in pre-settlement times the region was much more open than today. The landscape was composed of barrens, prairies, oak savannahs, and oak forests. The factor that maintained these "open" systems was fire. In earlier times, the forests contained fire tolerant tree species such as oak, hickory, and pine that are moderately tolerant to intolerant of shade. The forests contained low percentages of shade tolerant species such as elm, maple, and dogwood (*Cornus* spp.) as stated by Foti (2004). Fire suppression over many decades has increased stand densities, greatly reducing light levels, and increased the amount of shade tolerant tree species in the mid-story and understory of oak dominated over-stories (Soucy et al. 2004). The result from this management shift is increasingly reduced levels of oak regeneration in newly established stands, which could have significant impacts on the ecology and utilization of Ozark upland forests.

The Natural Oak Regeneration Problem

Throughout the hardwood forests of North America, regenerating oak stands on productive upland sites presents a major problem to resource managers (Brose et al. 1999). The physiological and morphological adaptations of oak seedlings often narrow the environmental conditions in which they survive and grow. A basic assumption is that success in survival and

growth is influenced by: 1) microclimate and edaphic factors, 2) morphological and physiological characteristics of a particular species, and 3) interaction between the two (Hodges and Gardiner 1993). Understanding these relationships is key to understanding management strategies for perpetuating oaks into new forests.

Typically, most hardwood stands do not have enough light reaching the understory for the development of oak seedlings. Canham et al. (1990) found that closed-canopy hardwood forests in north Florida to have photosynthetic active radiation (PAR) transmittance to the forest floor from 0.4 to 2.5 percent of total available sunlight. Also, 48 to 69 percent of PAR transmittance occurs in sunflecks with 4 to 11 minute duration. Cunningham et al. (2011) found a closed canopied hardwood stand on a terrace topographical position to have PAR transmittance of 7 to 9 percent. These light conditions are unfavorable for oak seedling survival and growth. Low understory light levels in hardwood stands may be the most limiting factor to the establishment and growth of oak regeneration (Hodges and Gardiner 1993). Battaglia et al. (2000) stated that environmental factors such as light and soil moisture may have independent or interacting influence on hardwood seedling survival and growth. Quero et al. (2008) found that irradiance levels have greater impact on seedling growth than water supply.

Sources for hardwood regeneration include: seedlings, seedling sprouts, and stump sprouts. When present prior to harvest, these sources are known as advanced reproduction (Rogers et al. 1993). Growth and survival of new oak seedlings may be influenced by different factors than that of older seedlings. Early growth and survival of seedlings beneath a dense canopy are primarily dependent upon stored food reserves in acorns and not on current photosynthate production (Hodges and Gardiner 1993). The initial growth flush is determined by carbohydrate reserves in acorns (Richardson 1956). Under low light conditions, such as those common in many Ozark hardwood stands, seedlings must begin to produce sufficient photosynthate for survival as reserves are depleted. However, under low light conditions, new oak seedlings will typically only produce one growth flush (Phares 1971 and Crow 1988).

Problems with regenerating oaks are amplified by the recognition of most hardwood researchers that the more productive the site, the more difficult it is to regenerate oaks (Rogers et al. 1993). The commonly accepted theory is that as site productivity increases, such as the north facing, mid-to-lower slopes on upland hardwood sites, a higher level of competition exists for the crop trees. The less productive sites, such as the ridges and south facing slopes on upland hardwood sites, will produce less competition, and often oaks may maintain a competitive advantage on these topographic positions.

Upland Hardwood Natural Regeneration Methods

An increase of sunlight aids in promoting both the successful establishment and subsequent growth of advance oak regeneration in hardwood stands. However, too much light in the initial stages of development may hinder oak seedlings in that it will favor the faster growing, more shade intolerant, tree species and herbaceous vegetation (Hodges and Janzen 1986). Notably, the optimal level of sunlight to maximize cherrybark oak (*Quercus michauxii* L.) seedling height and root-collar growth is 53% sunlight, and when sunlight penetration is 27%, cherrybark oak seedling height and root-collar growth is adequate (Gardiner and Hodges 1998). Thus, the level of the partial overstory removal may affect the amount of advance reproduction present following harvesting activity as it impacts both the amount of site disturbance and the resulting available sunlight.

Shelterwood harvests may present the most flexible alternative to naturally regenerating desirable species such as oaks. A shelterwood harvest is a management system that promotes a standing crop of regeneration through a series of partial removals of the overstory (Smith *et al*. 1996).

An alternate version of the classical approach to shelterwood harvests may be required for the desirable oak species on the more productive sites. Combining herbicide treatments and/or

prescribed fire along with the shelterwood is being considered by many researchers (Hicks *et al*. 2001). As previously stated, fire has long been an integral component to successful oak regeneration in upland hardwoods (Rogers and Johnson 1998). Silvicultural applications including midstory/understory control and partial overstory removal are commonly applied to hardwood stands to enhance the survival and growth of oak regeneration. Cunningham et al. (2011) found that mid-story/understory removal, coupled with a partial overstory removal, generate sunlight conditions that favor the development of oak seedlings.

Although there are no universal prescriptions for the hardwood regeneration problem, modified shelterwood systems that remove canopy and sub-canopy individuals prior to overstory removal to increase light reaching the ground can increase seedling dominance and survival for desirable species such as the oaks. There have been many advances in our understanding of ecological and silvicultural requirements to promote oak regeneration. Linking this knowledge with existing physiological research and exploring methods for *in situ* analyses of seedling physiology should significantly increase our understanding of oak establishment, particularly in the absence of fire.

Physiological Assessment of Seedling Performance

An array of technology is currently available to obtain plant physiological data in the field. These methods include: 1) biochemical analysis, 2) gas exchange and 3) chlorophyll fluorescence. These methods have been utilized by researchers for a variety of forest assessments.

Biochemical analysis

Tree leaves contain many pigments, including: chlorophylls, carotenoids, and others. Pigments play a role in leaf function such as sunlight absorption and photo-protection. Chlorophylls (a and b) are the prominent pigments in sunlight absorption. Chlorophyll levels can provide useful physiological information that potentially allows inferences to plant responses in

varying environments. Levels of total chlorophyll, chlorophyll a, chlorophyll b and the a/b ratio have provided valuable insight to the photosynthetic performance of trees growing in different environments, such as in varying light conditions, nutrient availability, and soil moisture conditions (e.g. Lichtenthaler et al. 2007, and Mielke et al. 2010, Netto et al. 2005, Rossini et al. 2006 and Percival et al. 2008).

The SPAD 502 chlorophyll meter (Konica Minolta, Inc.) is a handheld instrument that allows for non-destructive chlorophyll measurements to be easily taken in the field. The SPAD 502 determines the relative amount of chlorophyll present in a leaf by measuring light attenuation at 650 nm (close to maximum total chlorophyll absorption) and at 950 nm (no absorbance by chlorophyll). Using the two absorbance measures of a leaf, the instrument calculates a numerical SPAD value that is proportional to the amount of chlorophyll in a leaf (Konica Minolta, Inc.). Correlations between SPAD 502 indices and chlorophyll content (obtained through UV-VIS spectroscopy; Lichtenthaler and Bushmann 2001) in tree leaves have been well documented (e.g. Mielke et al. 2010 and Netto et al. 2005).

Carotenoids are another set of pigments important in leaf physiology, particularly with photo-protection. Leaves cannot utilize all the sunlight absorbed under full sunlight conditions (Demmig-Adams and Adams 1996). Excess sunlight can cause stomata to close, reduce CO_2 concentrations, and create the risk of producing high-energy reactive oxygen species (ROS), such as superoxide and singlet oxygen (Lambers et al. 2008). A related process, photorespiration, occurs often in high sunlight and is caused by oxygenation of RuBP in the initial phase of the Calvin cycle, instead of carboxylation. The progression of the Xanthophyll cycle from neozanthin, anthrozanthin, to zeozanthin provides a pathway for excess energy to be emitted as heat (thermal decay or non-photo chemical quenching). Having detailed measurements of each carotenoid's presence or simply knowing the total carotenoids present can provide useful information about leaf physiology (Demmig-Adams and Adams 1996, Logan et al. 1998, and

Percival et al. 2008). In other studies, SPAD 502 measures have shown to strongly correlate with total carotenoids present in a leaf in field studies (Percival et al. 2008).

When combined with growth data and other physiological data, leaf pigment concentrations can further supplement our understanding of plant performance under specific environmental conditions (e.g. irradiance impacts, nutrient availability, or indicator of seedling stress). The SPAD 502 provides a rapid and non-destructive method for obtaining useful and informative pigment data in the field.

Chlorophyll fluorescence

All active light absorption and reactions occur in the chloroplasts of plants, primarily within mesophyll cells. Within the chloroplasts, light energy absorbed by a chlorophyll complex provides electrons to photosystem II (PSII) for linear electron transport through the photosynthetic apparatus by a series of oxidation/reduction reactions (Taiz and Zieger 2006 and Bradbury and Baker 1984; Figure 1.2).

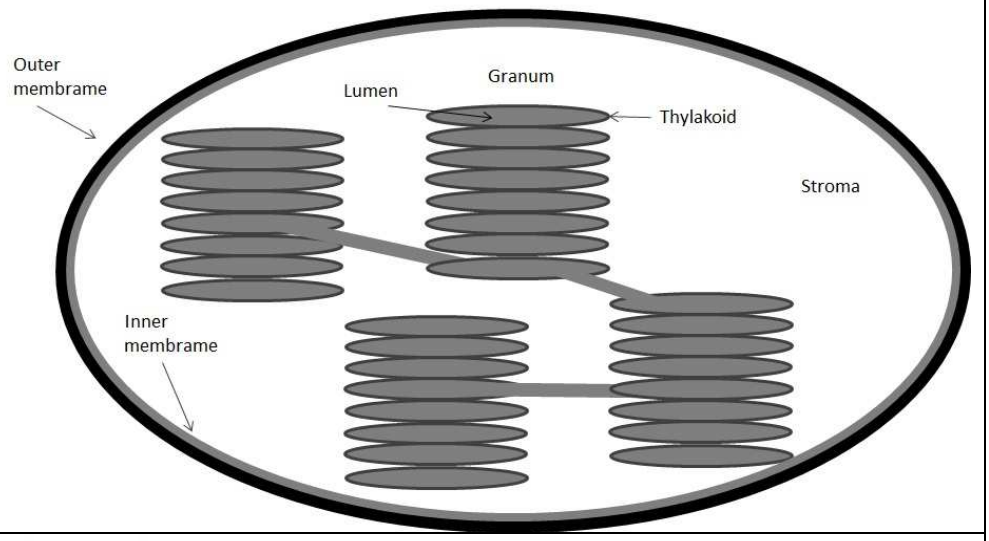

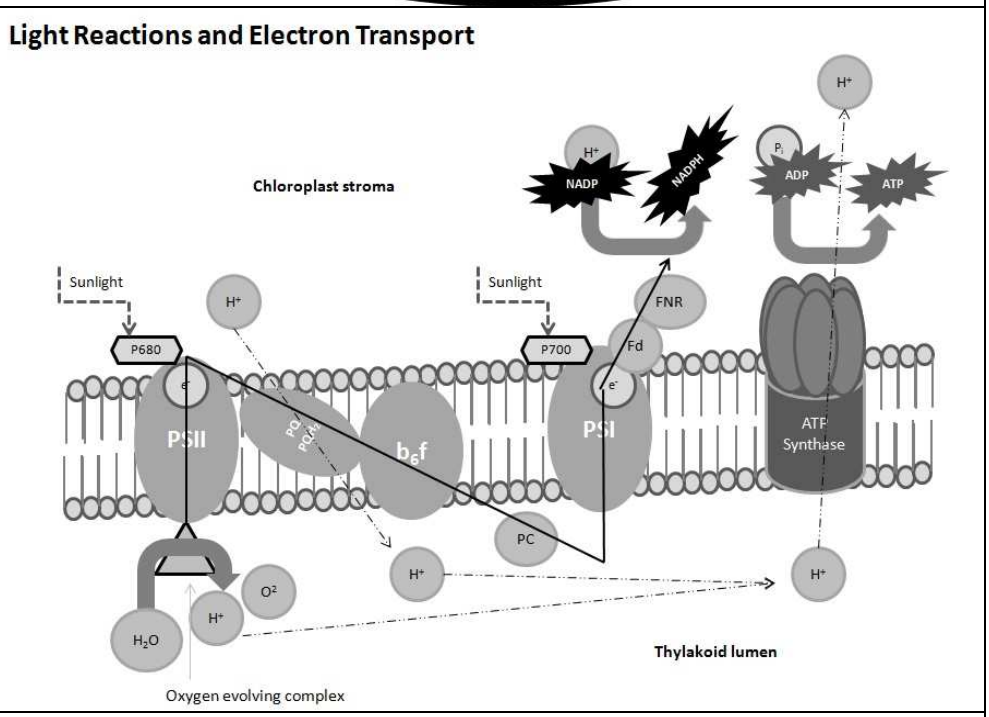

Figure 1.2. A. Illustration of a chloroplast in a leaf cell. B. Illustration of the photosynthetic apparatus located in the thylakoid membrame.

Energy from the light reactions may have four fates: 1. fluorescence, 2. heat dissipation, 3. energy transfer, or 4. photochemistry. Fluorescence, heat dissipation, and photochemistry are considered the three major de-excitation pathways. Figure 1.3 illustrates the four fates and the relationship between light absorption and emission. Light emission always occurs at longer wavelengths than absorption (Taiz and Zeiger 2006). The reemission of light (known as fluorescence) can be measured using a red light (~ 650 μmol m^{-2} s^{-1}), which coincides with the maximum absorption of chlorophyll *a* (Maxwell and Johnson 2000).

An excited chlorophyll molecule can also return to its "ground state" through heat dissipation or thermal decay and is a key factor in photo-protection in excess sunlight. Photochemistry is the process in which an excited state molecule causes chemical reactions to occur (Taiz and Zeiger 2006). A phenomenon known as the "Kautsky Effect" or fluorescence quenching was first discovered by Hans Kaustky in 1931 and describes the variation of fluorescence in plants when exposed to light. Kautsky found that dark adapted photosynthetic tissue will experience a brief increase in fluorescence yield when exposed to light, a consequence of reduction of the electron acceptor plastiquinone a. As enzymatic processes engage, causing electron transfer to increases, thermal decay efficiency increases and fluorescence quenching occurs. Through fluorescence measurements, these photochemical and non-photochemical quenching processes can be analyzed (Maxwell and Johnson 2000 and Kautsky et al. 1959).

In theory, these processes occur in competition to one another, and changes in one will have a known effect on the rate of the others (Maxwell and Johnson 2000). The theory does require that the rate constants do not change, which is not always true in the presence of light. Changes in rate constants for heat loss can occur; therefore, both photochemical and non-photochemical processes must be known to estimate PSII photochemistry (Baker 2008). Fortunately, these processes can be quantified through maximal plastiquinone a (Q_a, the initial electron acceptor from PSII) reduction through a rapid, large increase in light (Bradbury and

Baker 1981). Through this method, both photochemical and non-photochemical processes can be quantified (Bradbury and Baker 1984).

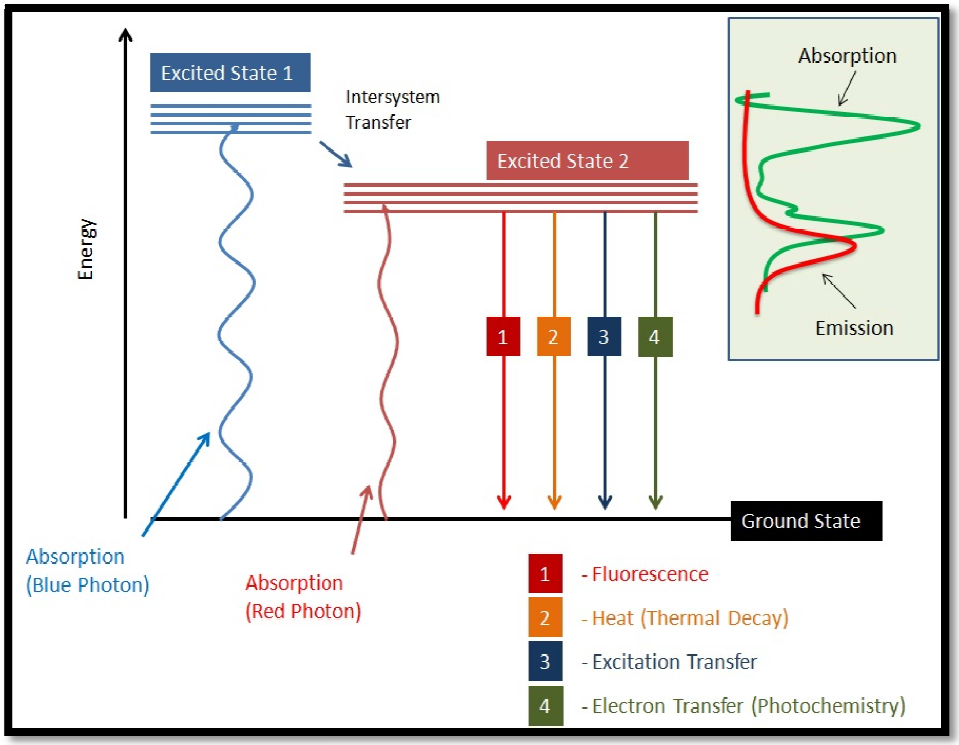

Figure 1.3. Conceptual illustration for the fates of excitation energy in the photosynthetic apparatus.

As stated, obtaining information on chlorophyll fluorescence, photochemistry, and thermal heat decay allows a comprehensive analysis of photosynthetic performance. Obtaining information about one of these parameters allows one to make inferences about the others (Figure 1.3). The development of chlorophyll fluoremeters that use pulses of modulated, strong light (pulse amplitude modulated light or PAM) have allowed the measurement of photochemical and non-photochemical processes (Genty and Baker 1989, and Krause et al. 1982). PAM fluoremeters use the saturated pulse method to assess photochemistry in PSII. The instrument utilizes two light signals, a measuring beam and a saturation pulse, through a fiber optic probe. The red (~ 650 µmol m^{-2} s^{-1}) measuring beam is rapidly switched on and off (modulated) and

allows the re-emitted light (~ 680 μmol m^{-2} s^{-1}) or fluorescence (exclusively from chlorophyll *a*) to be measured through a filter (Lichtenthaler et al. 1986). In dark adapted tissue, the fluorescence signal obtained by the measuring beam is termed F_o (Figures 1.3 and 1.4). In the presence of background light F_o becomes F'. This initial fluorescence is reflective of the reaction centers that are "open" or oxidized and available for electron transport. The application of an intense pulse of white light (~1s duration) saturates all reaction centers and they become "closed" or reduced and unavailable for electron transport. At this point, fluorescence is maximal and the fluorescence value represents F_m (or F_m' in the light). Knowing these basic fluorescence parameters allows derivation of calculated fluorescence parameters that provide information about photochemical and non-photochemical processes. The most direct and major parameter calculated is $F_v/F_m = (F_m - F_o)/F_m$. This parameter becomes F_q'/F_m' in the presence of background light (Table 1.1).

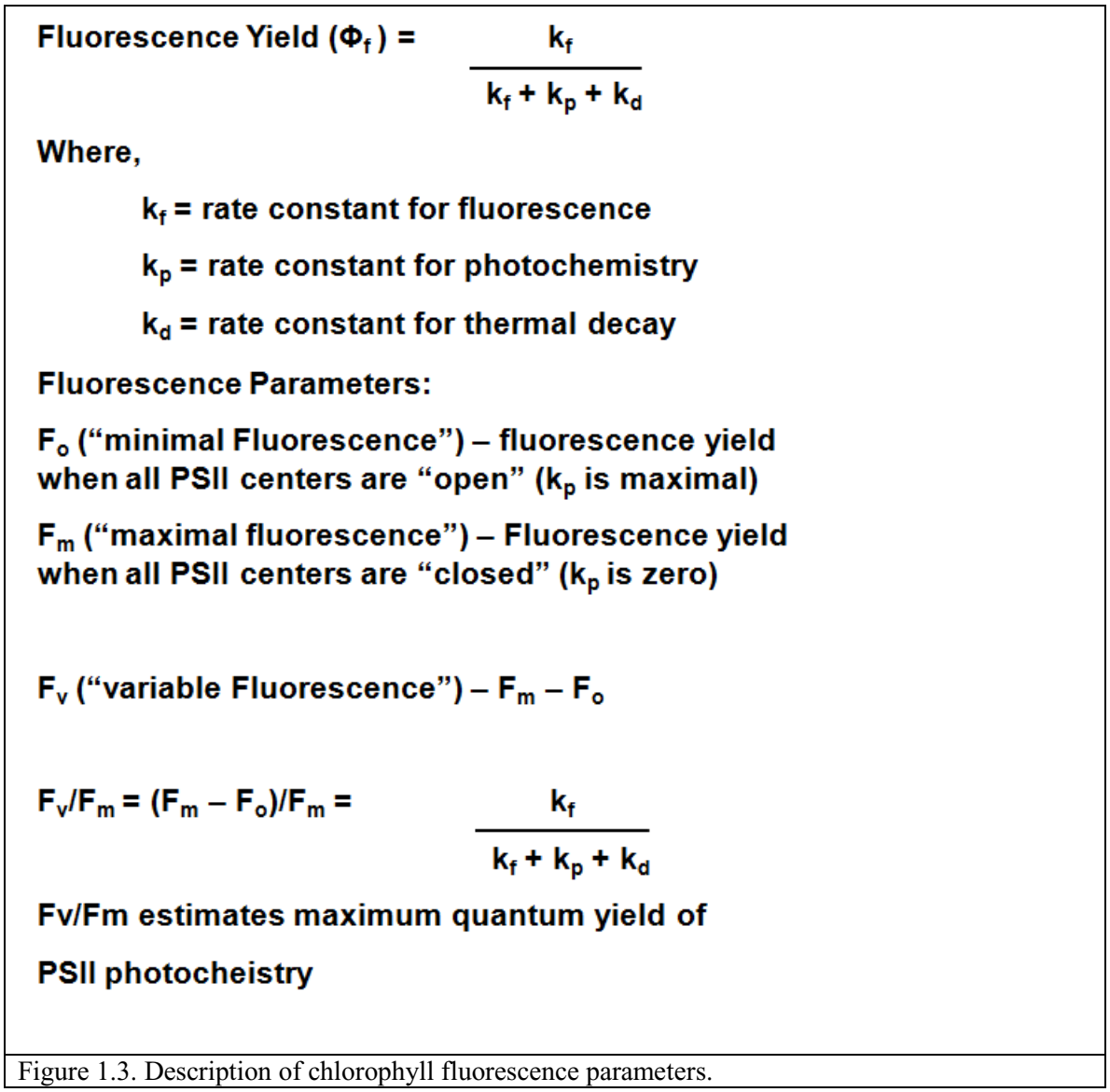

Figure 1.3. Description of chlorophyll fluorescence parameters.

The understanding of the photochemical and non-photochemical processes that create the quenching of fluorescence provide means for obtaining fluorescence parameters for both dark adapted and light adapted leaves (Maxwell and Johnson 2000 and Kautsky et al. 1959). Figure 1.5 illustrates the fluorescence parameters and the impact of increasing irradiance has on each parameter or the ability to attain or not attain a particular parameter.

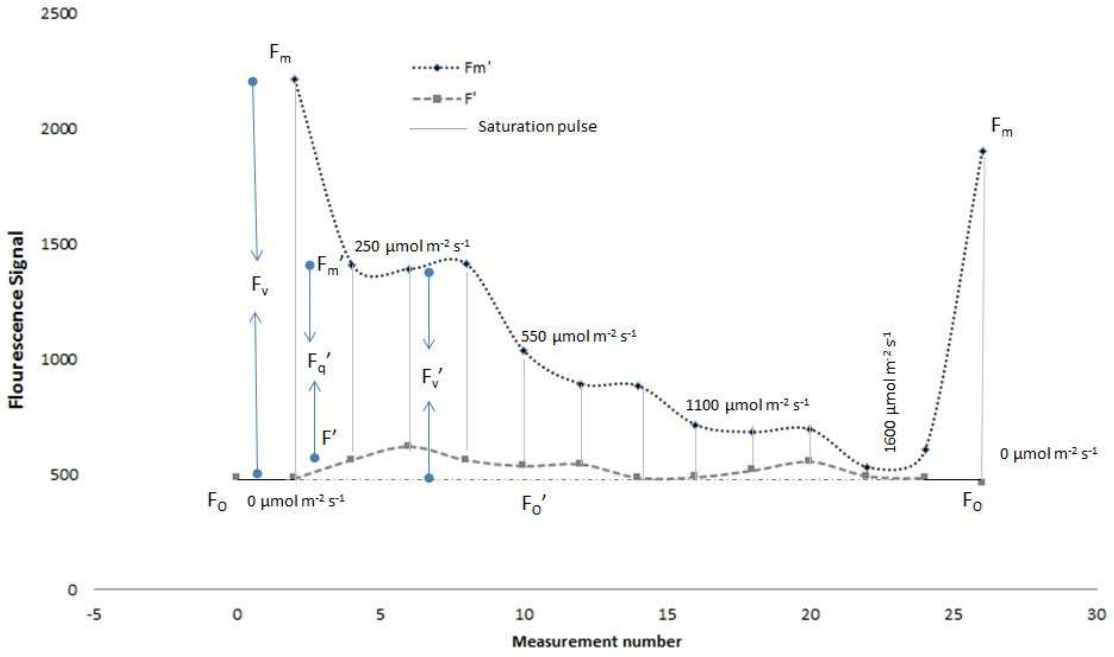

Figure 1.5. Basic fluorescence parameters obtained by a chlorophyll fluoremeter. Samples were acclimated to each light step for 1 minute prior to saturation pulse.

Table 1.2 illustrates four major calculated parameters that provide information on both photochemical and non-photochemical processes. As stated, F_v/F_m provides the maximum quantum efficiency of PSII photochemistry. Photochemical quenching (qP) provides the proportion of "open" PSII centers for electron transport. F_q'/F_m' provides the effective quantum yield of PSII photochemistry in the light. Non-photochemical quenching (NPQ) provides the proportion of absorbed light energy being released as heat. The result of the measures of fluorescence and calculation of photochemical quenching, quantum yield and NPQ is an assessment of the three major de-excitation pathways of absorbed light energy.

Table 1.1. Major chlorophyll fluorescence parameters.

Fluorescence Parameter	Definition	Formula
F_V/F_M	Maximum quantum efficiency of PSII photochemistry	$(F_M-F_o)/F_M$
qP	Photochemical quenching; proportion of "open" PSII centers (Q_A oxidized)	$(F_M'-F)/(F_M'-F_o')$
$F_{q'}/F_{m'}$ or ΦPSII	Actual quantum yield of PSII photochemistry	$(F_M'-F)/F_M'$
NPQ	Non-photochemical quenching (thermal energy dissipation)	$(F_M/F_M')-1$

Using F_q'/F_m', an apparent electron transfer rate (ETR) can be calculated, which potentially provides a proxy measure of photosynthetic performance. Each photon of light absorbed by the reaction center provides one electron to move through the electron transport chain. Therefore, a relative rate of electron transport can be calculated from the product of $F_{q'}/F_m'$ and the absorbed light. To calculate ETR, $F_{q'}/F_m'$ is multiplied by absorbed light (Formula 1.1). Absorbed light must be adjusted by a factor of 0.5 and 0.84, because it is assumed that half of absorbed light is partitioned between PSII and PSI and because only 84 percent of light is actually absorbed (16 percent is believed to be reflected or transmitted through a leaf). ETR can provide extremely valuable and useful information on photosynthesis physiology, because it has been proven, under the right conditions, to provide a "proxy" measure to photosynthesis. The ease at which fluorescence data can be collected (compared to gas exchange measurements) makes this relationship very important in ecophysiological studies.

Chlorophyll fluorescence provides potentially valuable information on the status of PSII in a leaf. This assessment can provide insight into photosynthesis, nutrient availability, and plant stress levels. The development of miniaturized pulse amplitude modulation has allowed chlorophyll fluorescence measures to be obtained in the field and have become important components of ecophysiological plant research (Maxwell and Johnson 2000 and Bilger et al. 1995). These instruments, such as the MiniPAM 2000 (Walz, Inc., Germany), have made collecting non-destructive fluorescence sampling in the field possible.

Advances in instrumentation available (e.g. Orgen and Baker 1985, Schreiber et al. 1993, Schreiber 1986 and Schreiber et al., 1986) and methodology (e.g. Bradbury and Baker, 1981; Krause et al. 1982, Bilger et al. 1989 and Genty et al. 1989) have linked basic and applied chlorophyll fluorescence ecophysiological research in recent decades (e.g. Kooten and Snel, 1990, and Maxwell and Johnson 2000). For field analysis, the Mini-PAM 2000 (Walz, Inc.) provides a rugged, non-destructive, portable instrument for obtaining chlorophyll fluorescence data *in situ*.

Chlorophyll fluorescence analysis has become one of the most powerful and widely used techniques available to plant physiologists and ecophysiologists (Maxwell and Johnson 2000). Perhaps the single greatest advantage of fluorescence is that it can be performed in the field using a portable chlorophyll fluoremeter. While chlorophyll fluorescence has been utilized extensively *in vivo* and in numerous plant ecophysiological analyses, it is somewhat new to field-based forest studies. The majority of forest ecophysiology studies have relied on gas exchange in leaves (Ball et al. 1994). There have been a limited number of studies in forest ecology and in urban forests (e.g. Epron et al. 1992 and Schindler and Lichtenthaler 1996). A need exists to explore methods for incorporating chlorophyll fluorescence into a forest ecophysiology context. Maxwell and Johnson (2000) further state that, often, CF experiments include a gas exchange analysis to obtain a more complete picture of the response of plants to their environment.

Gas exchange

Gas exchange has long been an essential tool for plant physiologists and ecophysiologists. Photosynthesis is unique in that it is a sensitive indicator for limitations of physiological processes that can be continuously monitored (Long et al. 1996). Forty years ago, a publication by Sestak et al. (1971) provided a manual of methods for photosynthesis measurements. At that time, to obtain photosynthesis measurements in the field was difficult, tedious, and basically required a lab be set up on site. Today, an array of portable photosynthesis analyzers are available that allow one to obtain real-time measurements of leaf photosynthetic CO_2 uptake, transpiration, leaf conductance, and intercellular CO_2 mole fraction with little knowledge required of the system and calculations involved (Long et al. 1996). Because of portable photosynthesis systems, such as the LI-6400xt photosynthesis system (LI-COR, Inc.), obtaining photosynthesis information can be easily achieved in the field.

Forest ecophysiologists have utilized gas exchange for examining forest condition (e.g. Ogaya and Peñuelas 2003), impacts of elevated atmospheric CO_2 on forests (e.g. Curtis 1996 and Hamilton et al. 2002), tree seedling performance (e.g. Lockhart and Hodges 1994), and other aspects of forest function. Lockhart and Hodges 1994 utilized gas exchange to evaluate cherrybark oak seedlings from different sources of seedling stock (planted vs. natural). Additional forest ecophysiology studies have utilized gas exchange to examine irradiance and edaphic factors influence on oak reproduction survival and growth (e.g. Gardiner and Krauss 2001). Furthermore, gas exchange has been used to evaluate carbon gain by northern red oak advanced reproduction in the presence or absence of competing competition (Nilsen et al. 2009).

Maxwell and Johnson (2000) stated that gas exchange remains at the heart of ecophysiological research. Furthermore, chlorophyll fluorescence analysis should include a component of gas exchange analysis for validation. The observations of Kautsky and Hirsch (1931) first demonstrated that changes in fluorescence of dark adapted leaves by light could be correlated to changes in CO_2 assimilation. The principles, equipment, and procedures for

measuring leaf level gas exchange and chlorophyll fluorescence have been well defined and simultaneous measurement of their responses provide valuable information about photosynthesis physiology *in vivo* (Long and Bernacchi 2003).

The ability to obtain reliable photosynthesis rates in the field has increased our capabilities in field research. However, to be more useful to ecophysiologists, certain parameters of photosynthesis analyses should correlate to overall plant growth. The work of Quero et al. (2008), involving four *Quercus* species, demonstrated that multiple factors drive differences in absolute seedling growth and relative growth rate (RGR) in contrasting irradiance and water supplies. They utilized the gas exchange light curve variables quantum yield (Φ), maximum photosynthetic rate (A_{max}), curvature (θ), and dark respiration (R_d) to calculate net assimilation rate (NAR) (as described by Thornley, 1976). The authors stated that leaf-level carbon gain or net assimilation rates can predict RGR across species and can do so across contrasting light and water availabilities. Shipley (2006) found in a meta-analysis of growth including 614 species that in general, NAR was the best predictor of RGR. Quero et al. (2008) further state that in the four *Quercus* species, gross maximum photosynthetic rate ($A_{max.g}$) did not prove to be a good predictor of RGR or absolute seedling growth.

Literature Cited

Abrams, M. D. (1990). Adaptations and responses to drought in *Quercus* species of North America. *Tree Physiology*, *7*(1-2-3-4), 227-238.

Bahari, Z. A., Pallardy, S. G., & Parker, W. C. (1985). Photosynthesis, water relations, and drought adaptation in six woody species of oak-hickory forests in central Missouri. *Forest Science*, *31*(3), 557-569.

Baker, N. R. (2008). Chlorophyll fluorescence: a probe of photosynthesis in vivo. *Annual Review of Plant Biology*, *59*, 89-113.

Ball, M.C., Butterworth, J.A., Roden, J.S. Christian, R. and Egerton, J.G. (1994). Applications of chlorophyll fluorescence to forest ecophysiology. *Australian Journal of Plant Physiology* 22:311-319.

Battaglia, L. L., Foré, S. A., & Sharitz, R. R. (2000). Seedling emergence, survival and size in relation to light and water availability in two bottomland hardwood species. *Journal of Ecology*, *88*(6), 1041-1050.

Bilger W. and Bjorkman, O. (1989) Light-induced spectral absorbance changes in relation to photosynthesisand the epoxidation state of the xanthophyll cycle components in cotton leaves. *Plant Physiology* 91: 542

Bilger, W., Schreiber, U., & Bock, M. (1995). Determination of the quantum efficiency of photosystem II and of non-photochemical quenching of chlorophyll fluorescence in the field. *Oecologia*, *102*(4), 425-432.

Bradbury, M. and Baker, N.R. (1981) Analysis of the slow phases of the in vivo chlorophyll fluorescence induction curve. Changes in the redox state of Photosystem II electron acceptors and fluorescence emission from Photosystems I and II. *Biochimica et Biophysica Acta*635:542-551.

Bradbury, M. and Baker, N.R. (1984) A quantitative determination of photochemical and non-photochemical quenching during the slow phase of the chlorophyll fluorescence induction curve of bean leaves. *Biochimica et Biophysica Acta* 765:275-281.

Brose, P., Van Lear, D., & Cooper, R. (1999). Using shelterwood harvests and prescribed fire to regenerate oak stands on productive upland sites. *Forest Ecology and Management*, *113*(2), 125-141.

Canham, C. D., Denslow, J. S., Platt, W. J., Runkle, J. R., Spies, T. A., & White, P. S. (1990). Light regimes beneath closed canopies and tree-fall gaps in temperate and tropical forests. *Canadian Journal of Forest Research*, *20*(5), 620-631.

Crow, T.R. (1988) Reproductive Mode and Mechanisms for Self Replacement of Northern Red Oak (*Quercus rubra*) – a review. *Forest Science*, 34(1): 19-40.

Cunningham, K. K., Peairs, S. E., Ezell, A. W., Belli, K. L., & Hodges, J. D. (2011). Understory Light Conditions Associated with Partial Overstory Removal and Midstory/Understory Control Applications in a Bottomland Hardwood Forest. *Forests*, *2*(4), 984-992.

Curtis, P.S. (1996) A Meta-analysis of Leaf Gas Exchange and Nitrogen in Trees Grown Under Elevated Carbon Dioxide. *Plant, Cell and Environment* 19, 127 -137.

Demmig-Adams B. and W.W.Adams, W.W. (1996) The role of xanthophyll cycle carotenoids in the protection of photosynthesis. *Trends in Plant Science* 1:21-26.

Dixon, R.K. (1990) Process modeling of forest growth responses to environmental stress. Eds: Dixon, R.K., Meldahl, R.S., Ruark, G.A., and W.G. Warren. Timber Press. Portland, Oregon pp. 441.

Epron, D., Dreyer, E. and Breda, N. (1992). Photosynthesis of oak trees [*Quercus petraea* (Matt.) Liebl.] during drought under field conditions: diurnal course of net CO_2 assimilation and photochemical efficiency of photosystem II. *Plant, Cell and Environment* 15:809-820.

Foti, L.T. (2004) Upland hardwood forests and the related communities of the Arkansas Ozarks in: The early 19th century. p. 21 – 29. In: Spetich, M.A., ed. Upland oak ecosystem symposium: history, current conditions, and sustainability. Gen. Tech. Rep. SRS-73. Asheville, NC: US Department of Agriculture, Forest Service, Southern Research Station. 311.

Gardiner, E.S., and Hodges, J.D. (1998) Growth and biomass distribution of cherrybark oak (*Quercus pagoda* Raf.) seedlings as influenced by light availability. *Forest Ecology and Management* 108:127-34.

Gardiner, E. S., & Krauss, K. W. (2001). Photosynthetic light response of flooded cherrybark oak (Quercus pagoda) seedlings grown in two light regimes.*Tree physiology*, *21*(15), 1103-1111.

Genty, B., Briantais, J., and N.R. Baker, N.R. (1989) The relationship between the quantum yield of photosynthetic electron transport and quenching of chlorophyll fluorescence. *Biochimica et Biophysica Acta (BBA) - General Subjects* 990(1) 87-92.

Hamilton J.G., DeLucia,E.H., George, K., Naidu, S.L., Finzi, A.C., and Schlesinger W.H. (2002). Forest Carbon Balance Under Elevated CO_2. *Oecologia*. 131 (2), 250-260.

Hicks R.R., Kennard D.K., Rauscher H.M., Schmoldt D.L., and Flebbe P.A. (2001)

Hinckley, T. M., Aslin, R. G., Aubuchon, R. R., Metcalf, C. L., & Roberts, J. E. (1978). Leaf conductance and photosynthesis in four species of the oak-hickory forest type. *Forest Science*, *24*(1), 73-84.

Hodges, J.D., and Gardiner, E.S. (1993) Ecology and physiology of oak regeneration. In: Loftis, D.L., McGee, C.E. (Eds.), *in* Oak regeneration, serious problems, practical recommendations, Loftis, D.L., and C.E. McGee (eds.). USDA Forest Serv. Gen. Tech. Report SE-84. 54-65.

Hodges, JD, and G.C. Janzen GC. (1986) Studies on the biology of cherrybark oak: recommendations for regeneration. *in* Proc. Fourth Bienn. South. Silvic. Res. Conf., Phillips, D.R. (ed.). USDA For. Serv. Gen. Tech. Rep. SE-42.1986; 133-138.

Kautsky H., and Hirsch, A. (1931) Neue versuche zur kohlensaureassimilation. Naturwissenchaften 19:964.

Kautsky, H., Appel, W., & Amann, H. (1959). [Chlorophyll fluorescence and carbon assimilation. Part XIII. The fluorescence and the photochemistry of plants.]. *Biochemische Zeitschrift*, *332*, 277-292.

Krause G.H., Briantais J.M. and C. Vernotte. 1982. Photo-induced quenching of chlorophyll fluorescence in intact chloroplasts and algae. Resolution into two components. Biochim. Biophys. Acta. 679: 116-124.

Lambers, H., Chapin III, F.S., and Pons, T.L. (2008) Plant Physiological Ecology.

Larsen, D. R., & Johnson, P. S. (1998). Linking the ecology of natural oak regeneration to silviculture. *Forest Ecology and Management*, *106*(1), 1-7.

Lichtenthaler, H. K., Buschmann, C., Rinderle, U., & Schmuck, G. (1986). Application of chlorophyll fluorescence in ecophysiology. *Radiation and Environmental Biophysics*, *25*(4), 297-308.

Lichenthaler, H.K., Alexander A., Marek, M.V., Kalina, J., and Urban, O. (2007) Differences in pigment composition, photosynthetic rates and chlorophyll fluorescence images of sun and shade leaves of four tree species. *Plant Physiology and Biochemistry* 45:577-588.

Lichenthaler, H.K. and Buschmann, C. (2001) Chlorophylls and carotenoids: measurement and characterization by UV-VIS spectroscopy. *Current Protocols in Food Analytical Chemistry* F4.3.1-F4.3.8.

Lockhart, B.R., and J.D. Hodges, J.D. (1994) Comparitive gas-exchange in leaves of intact and clipped, natural and planted cherrybark oak (*Quercus pagoda* Raf.) seedlings. *Proceedings of the Arkansas Academy of Science*, Vol. 48.

Loftis, D. L. (1990). A shelterwood method for regenerating red oak in the southern Appalachians. *Forest Science*, *36*(4), 917-929.

Loftis, DL. (1993). Regenerating northern red oak on high quality sites in the southern Appalachians. In: Loftis, D.L. and McGee C.E. eds. Oak Regeneration: Serious Problems Practical Recommendations (Symposium Proceedings) Gen.Tech. Rep. SE-84. Asheville, NC: U.S. Department of Agriculture, Forest Service, Southeastern Forest Experiment Station. 202 – 210.

Logan, B. A., Demmig-Adam, B., & Adams, W. W. (1998). Antioxidants and xanthophyll cycle-dependent energy dissipation in Cucurbita pepo L. and Vinca major L. upon a sudden increase in growth PPFD in the field. *Journal of Experimental Botany*, *49*(328), 1881-1888.

Long, S. P., & Bernacchi, C. J. (2003). Gas exchange measurements, what can they tell us about the underlying limitations to photosynthesis? Procedures and sources of error. *Journal of Experimental Botany*, *54*(392), 2393-2401.

Maxwell M. and Johnson G.N. (2000). Chlorophyll fluorescence—a practical guide *Journal of Experimental Botany* 51(345): 659-668.

Mielke, M.S., Schaffer, B. and Li, C. (2010) Use of a SPAD meter to estimate chlorophyll content in *Eugenia uniflora* L. leaves as affected by contrasting light environments and soil flooding. *Photosynthetica* 48(3):332-338.

Netto, A.T., Campostrini, Oliveira, J.G., and Bressan-Smith, R.E. (2005) Photosynthetic pigments, nitrogen, chlorophyll a fluorescence, and SPAD 502 readings in coffee leaves. *Scientia Horticulturea* 104:199-209.

Nilsen, E. T., Lei, T. T., & Semones, S. W. (2009). Presence of Understory Shrubs

Constrains Carbon Gain in Sunflecks by Advance-Regeneration Seedlings: Evidence from Quercus rubra Seedlings Growing in Understory Forest Patches with or without Evergreen Shrubs Present. *International Journal of Plant Sciences*, *170*(6), 735-747.

Ogaya, R., & Peñuelas, J. (2003). Comparative field study of Quercus ilex and Phillyrea latifolia: photosynthetic response to experimental drought conditions. *Environmental and Experimental Botany*, *50*(2), 137-148.

Orgen E. and Baker N.R. (1985). Evaluation of a technique for the measurement of chlorophyll Fluorescence from leaves exposed to white light. *Plant Cell and Environment* 8: 539-547.

Quero, J.L., Villar, R., Maranon, T., Zamora, R., Vega, D, and Sack, L. (2008) Relating leaf photosynthetic rate to whole-plant growth: drought and shade effects on seedlings of four Quercus species. *Functional Plant Biology* 35:725-737.

Percival, G.C., Keary, I.P., and Noviss, K. (2008) The potential of a chlorophyll SPAD meter to quantify nutrient stress in foliar tissue of sycamore (*Acer psuedoplatanus*), English oak (*Quercus robur*), and European beech (*Fagus sylvatica*). *Aboriculture and Urban Forestry* 34(2):89-100.
Springer 1-91.

Phares, R. E. (1971). Growth of red oak (*Quercus rubra L.*) seedlings in relation to light and nutrients. *Ecology*, 669-672.

Rogers, R., and Johnson, P.S. (1998) Approaches to modeling natural regeneration in oak-dominated forests. *Forest Ecology and Management* 106: 45-54.

Rogers, R., Johnson, P.S., and Loftis, D.L., (1993) An overview of oak silviculture in the United States: the past, present, and future. *Ann. Sci. For.* 50: 535-542.

Rossini M., Panigada, C., Meroni, M., and R. Columbo. 2006. Assessment of oak forest condition based on leaf biochemical variables and chlorophyll fluorescence. *Tree Physiol.* 26(11): 1487-1496.

Sabo G.,Lockhart, J.J. and J.E. Hilliard. (2004) The forest as a resource: from prehistory to history in the Arkansas Ozarks. p. 30 – 35. In: Spetich, M.A., ed. 2004. Upland oak ecosystem symposium: history, current conditions, and sustainability. Gen. Tech. Rep. SRS-73. Asheville, NC: US Department of Agriculture, Forest Service, Southern Research Station. 311.

Sander, I.L. and Graney, D.L. 1993. Regenerating oaks in the central states. in: Loftis, D. and McGee, C.E. (eds.)Oak regeneration: Serious problems, practical recommendations. Symposium Proceedings; 1992 Sept. 8-10; Knoxville, TN. Presented by the center for oak studies. Gen. Tech. Rep. SE-84, Ashville, NC: U.S. Department of Agriculture, Forest Service, Southeastern Forest Experiment Station: 174-183.

Shipley, B. (2006) Net assimilation rate, specific leaf area and leaf area and leaf area mass ratio: which is most closely correlated with relative growth rate? A meta-analysis. *Functional Ecology* 20: 565-574.

Schreiber U. (1986) Detection of rapid induction kinetics with a new type of high frequency modulated chlorophyll fluoremeter. *Photosynthesis Resource* 10: 51-62.

Schreiber, U., Schliwa, U. and Bilger, W. (1986) Continuous recording of photochemical and non-photochemical chlorophyll fluorescence quenching with a new type of modulation fluoremeter. *Photosynthesis Research* 10: 51-62.

Schreiber, U., Neubauer, C. and Schilwa, U. (1993) PAM fluorometer based on medium-frequency pulsed Xe-flash measuring light: A highly sensitive new tool in basic and applied photosynthesis research. *Photosynthesis Research* 36(1):65-72.

Schindler, C. and H.K. Lichtenthaler, H.K. (1996) Photosynthetic CO_2 assimilation, chlorophyll fluorescence and zeaxanthin accumulation in field grown maple trees in the course of a sunny and a cloudy day. *Journal of Plant Physiology* 148:399-412.

Sestak, Z., Catský, J., & Jarvis, P. G. (1971). Plant photosynthetic production. Manual of methods. *Plant photosynthetic production. Manual of methods.*

Smith, D.M., Larson, B.C., Kelty, M.J. and Ashton, P.M.S. (1996) *The practice of silviculture: applied forest ecology*. Ninth Edition. 537.

Soucy, R., Heitzman, E. and Spetich, M. (2004) Age distribution of oak forests in North-central Arkansas. 53 – 61. In: Spetich, M.A., ed. Upland oak ecosystem symposium: history, current conditions, and sustainability. Gen. Tech. Rep. SRS-73. Asheville, NC: US Department of Agriculture, Forest Service, Southern Research Station. 311.

Taiz L. and Zeiger, E. (2006). *Plant Physiology*. 4th Edition. Sinauer 126-156.

Thornley, JHM. (1976) Mathematical models in plant physiology. Academic Press: New York

Van Kooten, O., & Snell, J. F. H. (1990). Progress in fluorescence research and nomenclature for quenching analysis. *Photosynth Res*, *25*, 147-150.

CHAPTER II – APPLIED ECOLOGICAL METHODOLOGY

Study Site

The study site was located in the Ozark Mountains of Arkansas, within the Highly Dissected Springfield Plateau physiographic province. The predominant soils were listed as Clarksville very cherty silt loam with 20 to 40 percent slopes and Clarksville very cherty silt loam with 8 to 20 percent slopes. These soils are described as deep, somewhat excessively drained, low available water capacity, low organic matter content, and strongly acidic (Ferguson et al., 1982). The description provided is a general soil description based on broad ranges of slope positions. The area selected for my study was only on north aspects, which potentially have somewhat higher organic matter, higher moisture content, and generally considered more productive than ridge-tops and south-facing slopes.

Site indices (a measure of site quality) were determined by collecting age and height data for white oak, black oak, and northern red oak dominant and co-dominant trees and determining mean tree heights at base age 50 using the models of Graney and Bower (1971). Site indices range from 18 m on upper slopes to 21 m on lower slopes for white oaks. Site indices for northern red and black oak were 20 m on upper slopes to 23 m on lower slopes. These site indices represent moderately productive hardwood sites.

Over-story measurements were taken from two (one upper slope and one lower slope) fifth acre circular plots (r = 16.3 m). Over-story measurements include: species, DBH, merchantable height, log grade, damage, and number of epicormic branches (lateral branching). Mid-story measurements are taken from 20^{th} acre circular plots (r = 8.2 m). Mid-story measurements include: species and total height. Initial over-story, mid-story, and understory measurements were taken in the summer of 2009.

Initial over-story mean basal area (cross-sectional area of a tree bole at 1.4 m above ground in square meters) of treatment replicates was 21.5 m^2 per hectare (h) (± 1.97 m^2 h^{-1} at α =

0.05), representing a fully stocked to slightly overstocked stand. Initial over-story species composition was dominated by approximately 75 percent oak species. Initial mean mid-story density was 766 trees per hectare (TPH). Species composition in the mid-story was dominated by non-oak, shade tolerant species. Mean understory (regeneration source) density included 1,166 oak seedlings per hectare (SPH) (± 363 SPH $\alpha = 0.05$) and 6,256 non-oak SPH (± 904 SPH $\alpha = 0.05$) Species composition in the under-story was dominated by shade tolerant species. Red maple, winged elm, and hickory comprised 48 percent of understory, while oaks, collectively, comprised 15 percent (Figure 2.1).

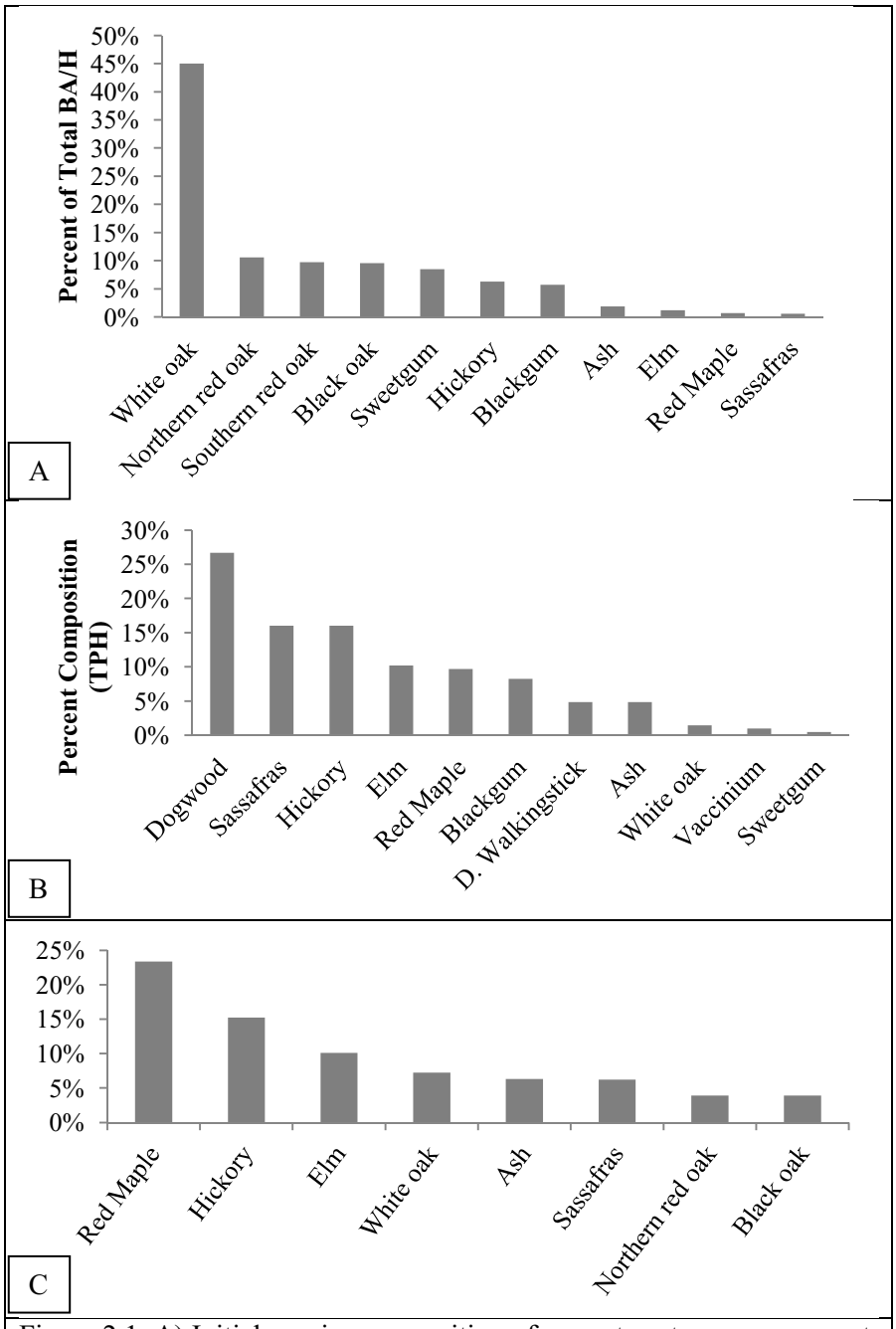

Figure 2.1. A) Initial species composition of over-story trees as a percent of total basal area per hectare. B) Initial species composition of mid-story trees of total trees per hectare (TPH). C) Initial species composition of understory (regeneration) of total seedlings per hectare (SPH) (minimum 5% of total).

Stand Treatments

Studies have suggested that the best environment for oak seedling growth and development is a partial sun and shade environment resulting in an average of 40 to 50 percent full sunlight to optimize oak seedling growth and development. This environment has been most often generated utilizing mid-story removal, over-story removal, or a combination of the two. Therefore, this study utilized two primary treatments that incorporate the two methods to generate a potentially adequate to optimum environment for oak seedling establishment and development. A third treatment is a control, where no stand manipulation has occurred, designed to illustrate an inadequate sunlight condition (Table 1).

Table 2.2 Study Treatments.	
BA11	Partial over-story removal to basal area 11.5 m^2 h^{-1}.
BA11 + MR	Partial over-story removal to basal area 11.5 m^2 h^{-1} plus complete mid-story removal of non-oak species.
NHC	No stand manipulation or non-harvested control

Mid-story removal treatments were applied from November 2008 to February 2009. Follow-up treatments were applied in July 2009. Mid-story, non-oak species were removed using herbicide injection. One milliliter of an aqueous solution of 25 percent imazapyr and 75 percent water was injected at 7.6 cm intervals around tree trunks.

The mechanical thinning operation was applied to treatments 1 and 2 from October 2009 through March 2010. The target residual basal was 11.5 m^2 h^{-1}. Residual trees were selected for 1) oak species and 2) large vigorous crowns.

Experimental Layout and Field Measurements

Initially, the experimental design was to be a randomized complete block (RCB) with four replicates of each treatment. However, a physical constraint on randomization was generated by the necessity to facilitate the partial overstory removal and remove the potential for sunlight canopy penetration interaction between treatment replicates. Therefore, a completely randomized design of four replicates per treatment was utilized. However, complete randomization was not truly achieved. BA11 and BA11 + MR replicates were randomized within the harvest area and the NHC replicates were located to the exterior of the harvest area. The author believes this constraint did not impact study results at the treatment level. The forest stand has developed under the same conditions, with no stand management occurring for nearly a century. The uniformity across the study area in soils, aspect, and slope position, along with statistically similar initial over-story, mid-story, and understory densities across treatments minimized the potential impacts of the physical constraint on randomization.

There are three treatments, with four replicates that are two hectares in size each. Each replicate contains 12, 4,000th hectare circular regeneration sample plots (r = 3.6 m) spaced on a grid along the slope gradient, allowing plots to be split into upper slope and lower slope samples. Reproduction measurements at each plot include: species and height class (< 0.3 m, 0.3 to 0.9 m., and >0.9 m). This sample pool was used for overall species composition and height class analysis.

Within the species suite, six were selected for photosynthesis physiological analysis: northern red oak (*Quercus rubra* L.), black oak (*Quercus velutina* L.), white oak (*Quercus alba* L.), red maple (*Acer rubrum* L.), winged elm (*Ulmus alata* Michx.) and black cherry (*Prunus serotina* L.). Sixteen individual seedlings from each treatment for each species were selected for analysis. Morphological data collected on these sample seedlings included: species, ground line diameter (GLD), height, and leaf area. Leaf level physiological data collected included: photosynthetic pigment levels, specific leaf area, and chlorophyll fluorescence. Gas exchange was

incorporated in the 2012 growing season for a subset of photosynthesis sample seedlings for each species. The protocols for each measurement type are described in more detail in their respective study chapters.

Chlorophyll fluorescence, sunlight canopy penetration, and leaf pigment content sampling began in 2010. Chorophyll fluorescence and sunlight canopy penetration were obtained in early, mid, and late growing season through 2012, representing year 1, year 2, and year 3 post-harvest measurements, respectfully.

Climatic data presented were from a National Oceanic and Atmospheric Administration (NOAA) weather station located approximately 1km from study site. The weather station provided detailed measurements for temperature, relative humidity, precipitation, solar radiation, and soil moisture in the area. Climatic data presented represent mid-day values. Mid-day was defined in this study as the hours between 10:00 am and 3:00 pm, which were the peak times of diurnal sunlight and the subsequent time window for photosynthesis data collection.

CHAPTER III – ENVIRONMENTAL RESULTS AND DISCUSSION

Climatic Conditions

Table 3.1 illustrates the mean maximum daily temperature (MDT, ^{0}C) for each month during the growing season. Growing season MDTs were above average all three years following treatment applications. 2010 exhibited the highest average MDT of 29.3^0, which was 1.9^0 above average for the season. However, 2012 (year 3 post treatment) experienced the highest monthly MDTs, including a time period from mid-June to the end of July where MDTs were consecutively above 37^0. While there existed several excessive heat periods during the study, the period of time from June through July 2012 significantly impacted seedling physiology more than any other period during the study. A compounding factor during this time period was that it followed early season precipitation rates well below normal. The coupled impacts of high MDTs and low precipitation rates were evident in data collection during 2012.

Table 3.1. Growing season monthly average maximum daytime temperatures (^{0}C) and departure from annual average temperature for respective months.

		2010		2011		2012	
Month	Annual average	Max daily temp.	Departure	Max daily temp.	Departure	Max daily temp.	Departure
April	21	23.4 (3.2)	2.4	23.2 (3.9)	2.2	23.1 (3.9)	2.1
May	26	26.1 (3.8)	0.1	24.1 (5.2)	-1.9	28.8 (3.5)	2.8
June	30	33.2 (2.3)	3.2	32.8 (1.7)	2.8	32.4 (2.4)	2.4
July	33	33.4 (1.7)	0.4	34.6 (2.3)	1.6	36.5 (3.6)	3.5
August	32	34.9 (2.8)	2.9	34.0 (3.6)	2	33.4 (3.5)	1.4
September	28	28.9 (3.9)	0.9	27.4 (4.9)	-0.6	28.0 (5.1)	0.0
October	22	25.2 (3.8)	3.2	22.6 (5.2)	0.6	20.4 (5.1)	-1.6
Average	27.4 (4.7)	29.3 (3.1)	1.9	28.4 (3.8)	1.0	28.9 (4.2)	1.5

Note: Standard deviation of daily maximum temperature in parenthesis. Data were obtained from a NOAA weather station located on the LFST (within 1km of study site).

Post-Treatment Stand Conditions

Treatment applications had significant impact on residual over-story and mid-story conditions. BA11 and BA11 + MR, post-treatment basal areas ranged from 10.3 to 12.6 $m^2 h^{-1}$, resulting in approximately a 55 percent reduction in over-story density. NHC remained at initial basal area levels (21.5 $m^2 h^{-1}$).

BA11 mid-story density was approximately 761 TPH for upper slope plots and 1,161 TPH for lower slope plots. The mean post-treatment mid-story density for BA11 was 480 TPH, resulting in approximately a 51 percent reduction from initial mid-story density. BA11 + MR mid-story trees were near 100 percent removed from chemical injection treatments (~ 766 TPH). NHC mid-story densities were approximately the same as initial stand conditions. Reproduction analyses are discussed in Chapter IV.

Treatment Level Sunlight Conditions

Pre-treatment sunlight canopy penetration averaged below 10 percent of full sunlight (~ 2,000 μmol $m^{-2} s^{-1}$) for all treatments. Post-treatment sunlight environments ranged from 5 percent of full sunlight for the NHC treatment up to 42 percent of full sunlight for BA11 + MR (Figure 3.1). Sunlight environments varied by topographic position across treatments as well. Upper slope positions exhibited higher sunlight levels than lower slope positions Figure 3.2. Sunlight results are discussed in more detail in Chapter IV.

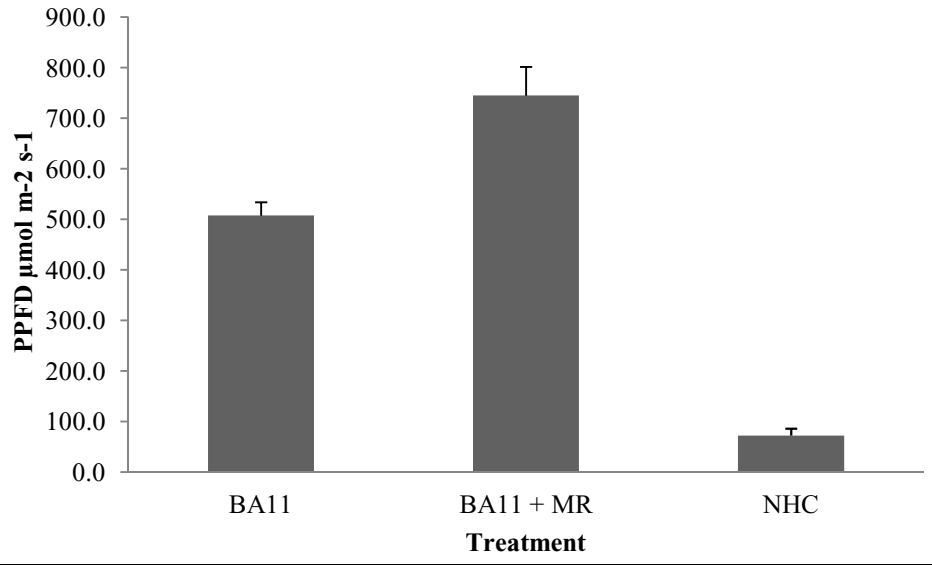

Figure 3.1. Three year mean irradiance levels for BA11, BA11 + MR, and NHC.

Values represent readings taken using a leveled micro-quantum sensor and calibrated against a Delta OHM LP 471 quantum sensor. Measurements were taken in late summer of each year, during mid-day hours and under clear to mostly sunny atmospheric conditions.

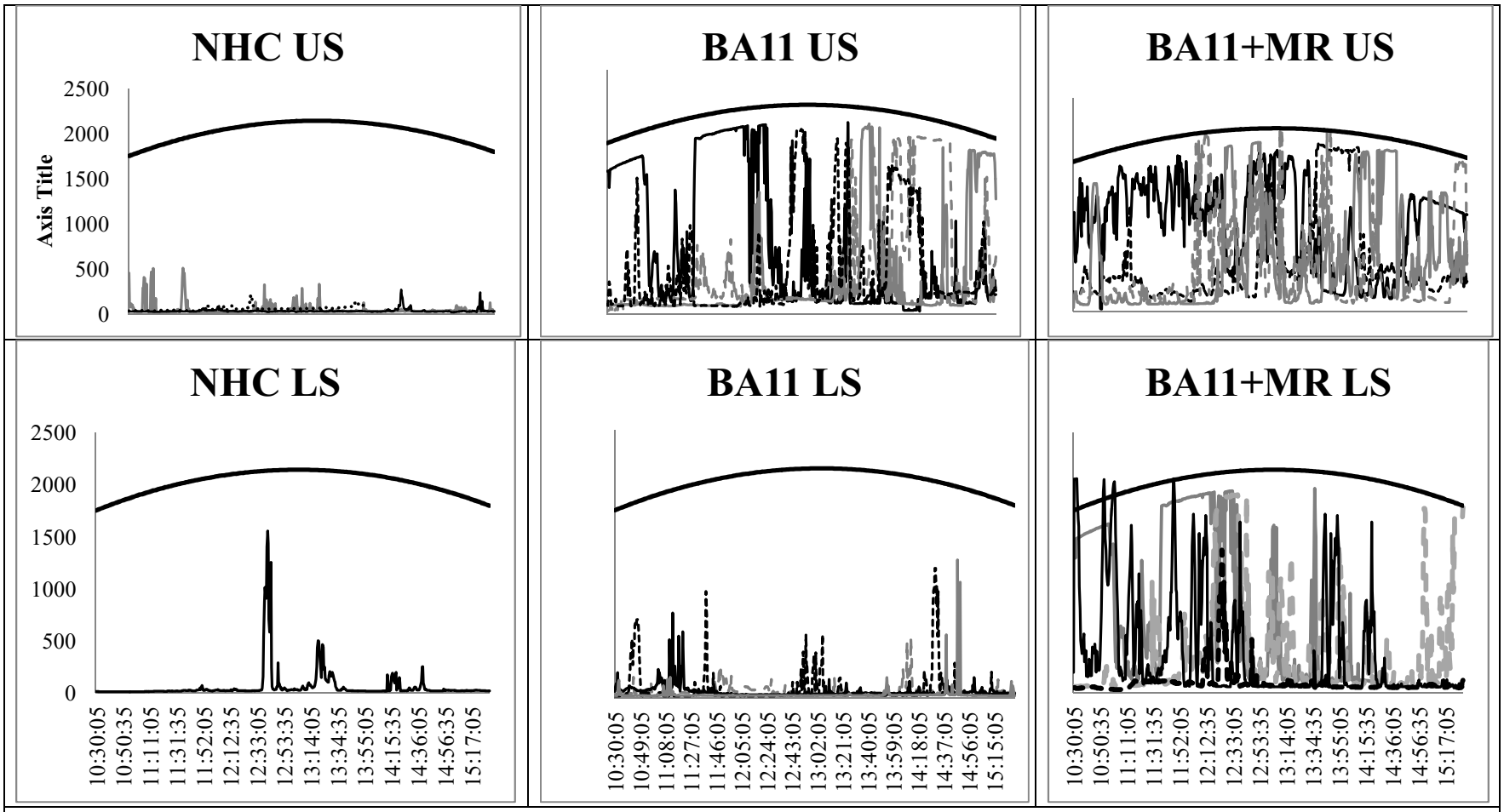

Figure 3.2. Understory level sunlight log for slope positions 1 and 3 in treatments NHC, BA11, BA11+MR. Sunlight data were logged at slope positions 1 and 3 for each replicate. Data were logged in 30 second intervals. Sunlight data were collected using a cosine corrected quantum sensor (400 to 700 nm spectral range) connected to a Delta OHM 2102.2 irradiance data logger. The sensor was leveled and placed 1.2 m above ground level. Data were collected between 10:00 and 16:00 hours. Maximum PAR values were obtained in open areas adjacent to treatments.

CHAPTER IV – SUNLIGHT AND REPRODUCTION ANALYSIS

Abstract

A study evaluating the response of oak natural reproduction to a shelterwood harvest and midstory competition control in an upland hardwood stand within the Ozark highlands of Arkansas was conducted. Two-hectare treatment plots were established within a 57 hectare shelterwood harvest on north-facing slopes (SI 26 – 30 m for oaks) in a 110 year old upland hardwood stand. The overstory was dominated by white oak (Quercus alba L.), black oak (Quercus velutina Lam.), and northern red oak (Quercus rubra L.). Treatments include: 1) shelterwood harvest to 11 m^2/h (BA11), 2) shelterwood harvest to 11 m^2/h plus injection of non-oak midstory trees (2.5 – 12.7 cm DBH; BA11+MR); and 3) non-harvested control (NHC). Initial mean oak seedlings per hectare (SPH) were 761 (±121), 1,515 (±316), 1,354 (±177) for BA11, BA11+MR, and NHC, respectively. Year 3 post treatment mean oak SPH were 4,195 (±901), 7,586 (±1,996), 8,253 (±2,446). A significant difference was detected between initial vs. year 3 values for all three treatments ($p = 0.003, 0.008, 0.007$; Student's t-test, $\alpha = 0.05$). No differences in total oak SPA were detected between treatments within year 3. Year 3 total abundance numbers were impacted by a heavy seedling crop and environmental factors. Significant differences were detected between initial and year 3 oak SPH by height class for BA11 and BA11+MR. BA11+MR exhibited the greatest changes in oak seedling height growth.

Introduction

Throughout the hardwood forests of North America, regenerating oak stands on productive upland sites presents a major problem to resource managers (Brose et al. 1998). The physiological and morphological adaptations of oak seedlings often narrow the environmental conditions in which they survive and grow. A basic assumption is that success in survival and growth is influenced by: 1) microclimate and edaphic factors, 2) morphological and physiological characteristics of a particular species, and 3) interaction between the two (Hodges and Gardiner 1993). Understanding these relationships is important to understanding management strategies for perpetuating oaks into new forests. Most hardwood stands do not have adequate sunlight penetration through the upper canopy for the development of oak seedlings. Undisturbed, "closed" canopies often result in sunlight canopy penetration to the ground level of less than ten percent (Canham et al. 1990 and Cunningham et al. 2011). Low understory light levels in hardwood stands may be the most limiting factor to the establishment and growth of oak reproduction (Hodges and Gardiner 1993). Battaglia et al. (2000) stated that environmental factors such as light and soil moisture may have independent or interacting influence on hardwood seedling survival and growth. Quero et al. (2008) found that irradiance levels have greater impact on seedling growth than water supply.

An increase of sunlight aids in promoting both the successful establishment and subsequent growth of oak advanced reproduction in hardwood stands. However, too much light in the initial stages of development may hinder oak seedlings by favoring faster growing, more shade intolerant tree species, and herbaceous vegetation (Hodges and Janzen 1986). Hodges and Gardener (1993) observed that sufficient sunlight levels for growth and survival of cherrybark oak (*Quercus pagoda* Raf.), under controlled conditions, occurred at 27 percent of total available photosynthetically active radiation (PAR) and optimal growth conditions occured at 53 percent of total available PAR.

Recent advances in applied research for oak natural regeneration have established combinations of partial overstory harvests and midstory competition control to improve environmental conditions for developing oak reproduction (Loftis 1990, Loftis, 1993, Larsen and Johnson 1998, and Cunningham et al. 2011). Sources for hardwood reproduction include: seedlings, seedling sprouts, and stump sprouts. Seedlings present prior to harvest are known as advanced reproduction (Rogers et al. 1993). The level of partial overstory removal may affect the amount of advance reproduction present following harvesting activity as it impacts both the amount of site disturbance and resulting available sunlight. Shelterwood harvests may present the most flexible option for naturally regenerating desirable species such as oaks. A shelterwood harvest is a management method that promotes a standing crop of reproduction through a series of partial removals of the overstory (Smith et al. 1996). An alternate version of the classical approach to shelterwood harvests may be required for desirable oak species on more productive sites. Combining herbicide treatments and/or prescribed fire along with the shelterwood has been evaluated by many researchers (Hicks et al. 2001).

Although there are no universal prescriptions for the hardwood regeneration problem, modified shelterwood methods that remove canopy and sub-canopy individuals prior to overstory removal to increase light reaching the forest floor can increase seedling dominance and survival for desirable species such as oaks. This study attempts to further supplement our knowledge of oak natural regeneration by evaluating irradiance effects and hardwood reproduction response to two shelterwood methods.

Materials and Methods

The study site is located in the dissected Springfield Plateau physiographic province on the University of Arkansas – Division of Agriculture Livestock and Forestry Research Station near Batesville, AR. The predominant soils are Clarksville very cherty silt loam with 8 to 20

percent slopes and Clarksville very cherty silt loam with 20 to 40 percent slopes. These soils are described as deep, somewhat excessively drained, low available water, low organic matter content, and strongly acidic (Ferguson et al. 1982). The description provided is a general soil description based on broad ranges of slope positions. The areas selected for this study were only on north aspects, which potentially had somewhat higher organic matter, higher moisture content, and generally considered more productive than ridge-tops and south facing slopes. Site indices for white oak, black oak, and northern red oak dominant and co-dominant trees were calculated from equations developed by Graney and Bower (1971). Site indices for oaks were 26 meters on upper slopes to 30 meters plus on lower slopes.

Three treatments with four replicates were incorporated into a completely randomized design. Treatments included: 1. shelterwood harvest to BA 11 m^2/h (BA11), 2. shelterwood harvest to BA 11 m^2/h plus injection of non-oak stems between 2.5 and 12.7 cm DBH (BA11+MR) and 3. non-harvested control(NHC). Mid-story removal treatments were applied from November 2008 to February 2009. Follow-up treatments were applied in July 2009. Mid-story removal was performed using herbicide injection. 1 ml of an aqueous solution of 25 percent imazapyr and 75 percent water was injected for every 7.5 cm of diameter around tree trunks. A partial overstory harvest operation was applied to the BA11 and BA11+MR from October 2009 through March 2010. The target residual basal area was 11 m^2/h. Desirable residual tree characteristics were 1. oak species and 2. large vigorous crowns.

A physical constraint on randomization was unavoidable with regard to treatment replicates. BA11 and BA11+MR were both randomly assigned within a harvested area. The NHC was restricted to the exterior of the harvested area, resulting in the constraint on randomization. It was believed that if NHC replicates were within the harvest boundary, data integrity may be jeopardized by inadvertently altering sunlight penetration between harvested and non-harvested treatment replicates. However, the author feels confident that there was no impact on study results, because: 1. all replicates were located on the same aspect, soil type, and were in close

proximity and 2. there were no significant differences detected in initial stand values for overstory, mid-story or reproduction stems per hectare between treatments.

Each treatment replicate contained twelve 250th hectare circular (r = 3.6 m) reproduction sample plots spaced on a grid along the slope gradient (six upper slope and six lower slope plots). Reproduction measurements at each plot included species and height class (<0.3 m, 0.3 to 0.9 m, and > 0.9 m). Over-story measurements were taken from two (one upper slope and one lower slope) 13th hectare circular (r = 16 m) plots. Over-story measurements included species, DBH, merchantable height, log grade, damage, and number of epicormic branches. Mid-story measurements were taken from two, 50th hectare circular (r = 8 m) plots. Mid-story measurements included species and total height. Initial over-story, mid-story and understory measurements were taken in the summer of 2009.

Photosynthetic Photon Flux Density (PPFD) was measured at each of the twelve reproduction plots per replicate. PPFD was measured at plot center using a micro-quantum sensor attached to a Mini-PAM 2000 (WALZ, Inc.). Mini-PAM light readings were calibrated against an additional quantum light sensor (Delta OHM LP 471, □400 to 700 nm) for accuracy. The sensor was mounted to a leveled tripod at each measurement point. Sunlight observations were taken at mid-day (10:30 – 15:30 hrs) under mostly clear to clear sky conditions in September of each growing season. Open sky readings were taken prior to and after replicate light measurements were obtained. Open sky values were used to calculate percent of full sunlight values.

All statistical analyses were performed in Sigma Plot 11.0. All data were tested for normality and equal variances. When necessary, reproduction data were square root transformed to meet required assumptions. If assumptions were still not met, non-parametric analyses were conducted. Sunlight level and reproduction response were analyzed for treatment differences using analysis of variance (ANOVA). Individual means separation was conducted using the Holm-Sidak method. If a Kruskal Wallis ANOVA on ranks was required, means separation was

conducted using an Student Newman Kuels (SNK) on ranks test. All statistical tests were performed at the alpha 0.05 level.

Results

Initial over-story mean basal area of treatment replicates was 21.5 m^2/h (± 1.9 m^2), representing a fully stocked to slightly overstocked stand. Initial over-story species composition included approximately 75 percent oak species. Initial mean mid-story density was 766 trees per hectare (TPH) and included primarily non-oak, shade tolerant species. An appreciable portion of the midstory consisted of large crowned flowering dogwood (*Cornus florida* L.). Mean understory density included 1,174 oak SPH (± 363) and 6,256 non-oak SPH (± 904). Species composition in the under-story was also dominated by shade tolerant species. Red maple (*Acer rubrum* L.), winged elm (*Ulmus alata* Michx.), and hickory (*Carya* spp.) comprised 48 percent of understory, while oaks comprised 15 percent.

Treatment applications had appreciable impact on residual over-story and mid-story conditions. For BA11 and BA11+MR, post-treatment basal areas ranged from 10.3 to 12.6 m^2/h, resulting in a 55 percent reduction in overstory density. The NHC remained at initial basal area levels (~ 21.5 m^2/h). The BA11 midstory density was approximately 309 TPH for upper slope plots and 470 TPH for lower slope plots. The mean post-treatment, midstory density for BA11 was 388 TPH, resulting in approximately a 51 percent reduction from initial mid-story density. The BA11+MR mid-story trees were approximately 100 percent removed (~ 766 TPH). The NHC mid-story densities were approximately the same as initial stand conditions.

Irradiance

Mean mid-day photosynthetic photon flux densities (PPFDs) following treatment applications were 507, 744.5 and 72.1 µmol m^{-2} s^{-1}, respectively for BA11, BA11+MR, and NHC (Figure 4.1a.). Sunlight canopy penetration to ground level was 28, 42, and 5 percent of full sunlight for BA11, BA11+MR, and NHC. A one-way analysis of variance detected significant differences to exist ($p = 0.003$) for treatment effects. A Holm-Sidak means analysis detected significant differences to exist between all 3 treatments.

Sunlight levels increased from lower slope to upper slope positions for all treatments (Figure 4.1b.). A significant difference ($p = 0.02$) was detected between upper slope (527.2 µmol m^{-2} s^{-1}) versus lower slope (355.3 µmol m^{-2} s^{-1}). In terms of percent sunlight, BA11 exhibited 19 and 39 percent of available sunlight for the lower (positions 1 and 2) and upper (positions 3 and 4) slope positions. BA11+MR had 36 percent of full sunlight on lower slopes and 47 percent of full sunlight on upper slopes. The NHC treatment included 4 percent of full sunlight on lower slopes and 5 percent on upper slopes.

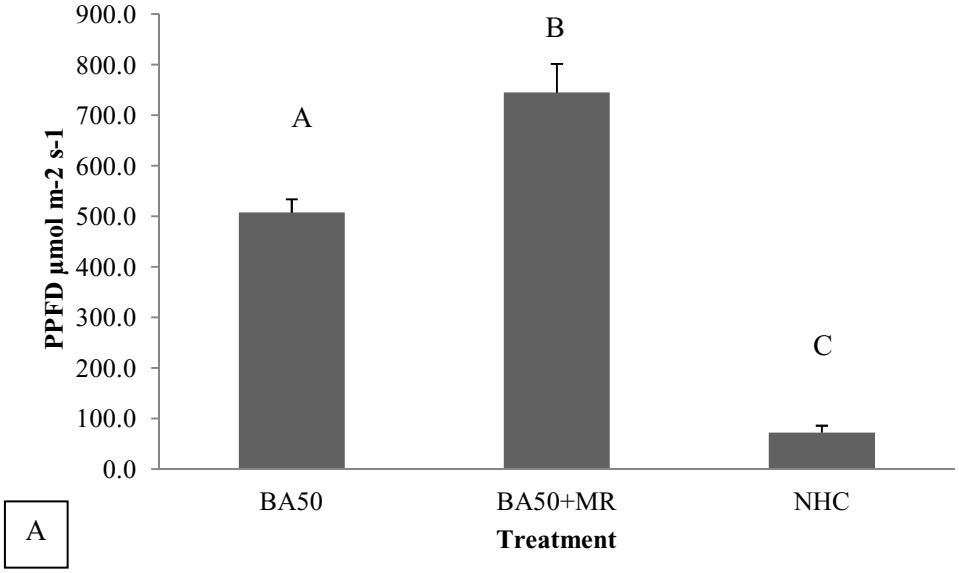

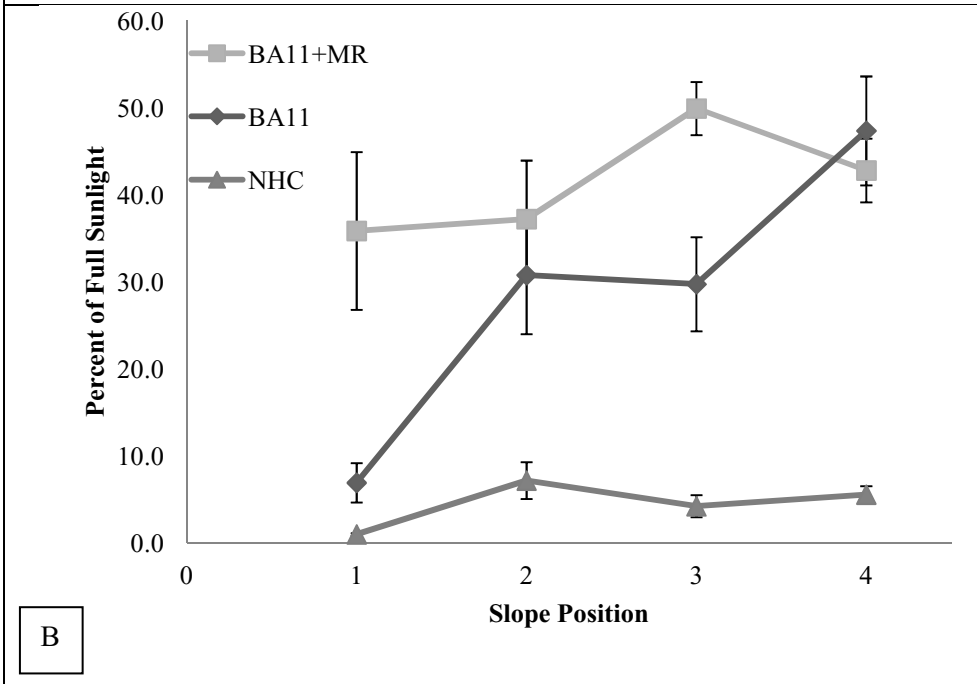

Figure 4.1. A) Sunlight levels at the forest floor by treatment. B) Percent of full sunlight at the forest floor by treatment and slope position.

Means followed by the same letter do not significantly differ (Holm-Sidak method; $\alpha = 0.05$). Error bars = ±1SE.

Regeneration

Year 3 mean oak SPH for BA11, BA11+MR, and NHC were 4,196, 7,586, and 8,253 SPH, respectively (Figure 2a.). Final oak SPH numbers represented an increase from initial numbers of 3,432, 6,068, and 6,899 for BA11, BA11+MR, and NHC, respectively (Table 1). Student's t-test comparisons detected a significant difference between initial versus year 3 oak SPH for BA11, BA11+MR, and NHC ($p = 0.003$, 0.008, and 0.007). A one-way analysis of variance for year by combined treatment detected significant differences between years ($p < 0.001$). A Holm-Sidak means separation procedure detected significant differences between year 3 versus years 2, 1, and initial oak SPH, and year 2 versus year 1 and initial oak SPH. No differences were detected between year 1 and initial oak SPH. A one-way analysis of variance established differences among treatments, across years ($p = 0.003$) for mean oak SPH. A Holm-Sidak means analysis detected significant differences between year 3 BA11+MR and NHC versus all treatments by year (Figure 4.2a.).

Year 3, post-harvest mean non-oak SPH were 9,928, 10,615, and 7,445 SPH for BA11, BA11+MR, and NHC treatments, respectively (Figure 4.2b.). This was an increase in mean non-oak SPH of 3855, 3,879, and 1,480 for BA11, BA11+MR, and NHC treatments, respectively. Primary non-oak species were winged elm, red maple, black cherry *(Prunus serotina* EhRh.*),* blackgum *(Nyssa sylvatica* Marsh.*),* hickory species and flowering dogwood. Year 3 mean non-oak SPH for BA11 were 1,658, 3,104, and 5,166 SPH for height classes 1, 2 and 3, respectively. Year 3, mean non-oak SPH for BA11+MR were 2,204, 3,845, and 4,566 SPH for height classes 1, 2 and 3, respectively. Year 3, mean non-oak SPH for NHC were 2,293, 2,792, and 2,360 SPH for height classes 1, 2, and 3, respectively.

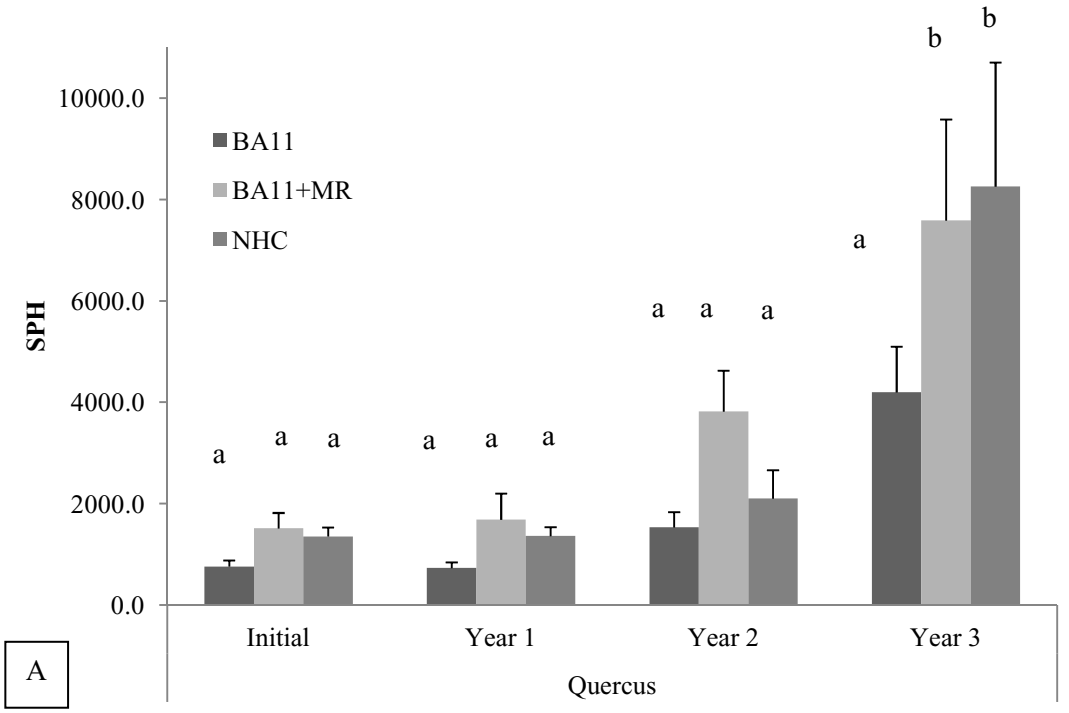

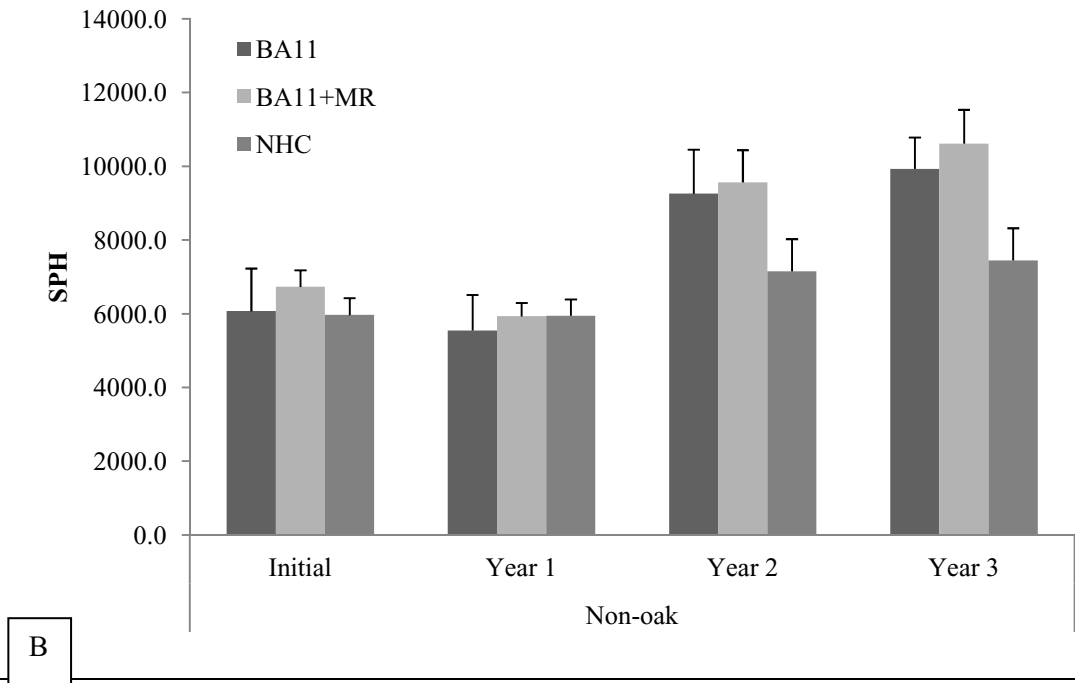

Figure 4.2.A. Oak SPH by year and treatment. B. Non-oak SPH by year and treatment. Means followed by the same letter do not significantly differ; Square root transformed, Holm-Sidak method, α=0.05; Error bars = ±1SE.

Year 3, mean oak SPH for BA11 were 3,345, 689, and 160 SPH for height classes 1, 2, and 3, respectively. This was an increase of 2,624, 366, and 94 SPH over initial values for height classes 1, 2, and 3. Student's t-test detected significant differences between year 3 versus initial oak SPH for all three height classes in BA11 ($p = 0.01$, 0.04, and 0.007). Year 3, mean oak SPH for BA11+MR were 5,201, 1,843, and 538 SPA for height classes 1, 2, and 3, respectively. This was an increase of 4,465, 1,215, and 390 SPH over initial values for BA11+MR oak (Table 4.1.). Paired t-test detected significant differences for all height classes between initial and year 3 values ($p = 0.04$, 0.03, and 0.04,). Year 3, mean oak SPH for NHC were 7683, 561, and 10 oak SPH for height classes 1, 2, and 3, respectively. This was a change of 6,775, 227, and -5 oak SPH for height class 1, 2, and 3 in the NHC treatment. There were no significant differences found between initial versus year 3 oak SPH by height class for the NHC treatment.

Table 4.1. Initial versus year 3 mean *Quercus* SPH by treatment and height.

Height	**BA11**		**BA11+MR**		**NHC**	
	Initial	Final	Initial	Final	Initial	Final
< 0.3 m	721.5 [162]	3,345 [907] (0.01)	736 [242]	5,202 [1789] (0.04)	906 [180]	7,682 [2,516] (0.07)
0.3 to 0.9 m	323.7 [54]	689 [168] (0.04)	627.7 [151]	746 [405] (0.03)	294 [72]	561 [119] (0.11)
> 0.9 m	67 [7.4]	161 [84] (0.007)	148 [57]	539 [140] (0.04)	15 [10]	10 [10] (0.82)

Data were square root transformed, Student's t-test, $\alpha = 0.05$; () = p-values, [] = ± 1SE.

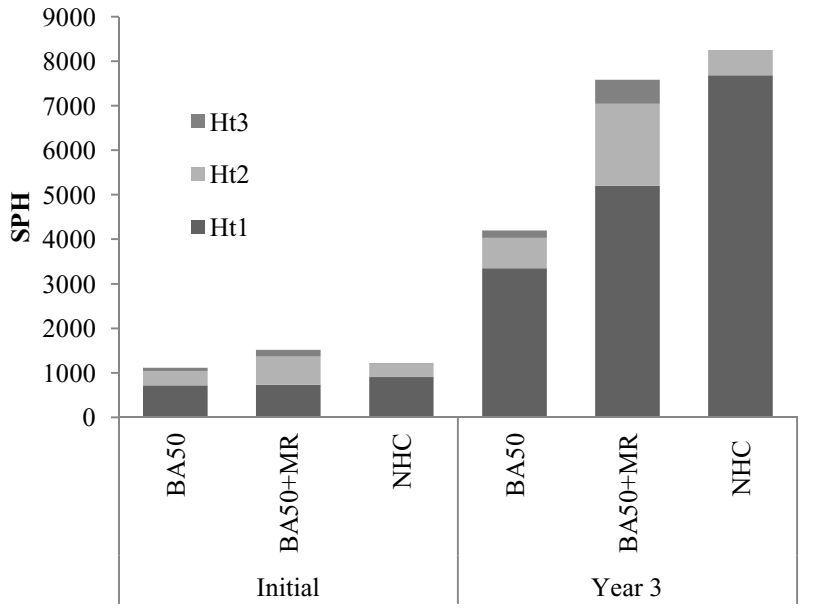

Figure 4.3. Oak SPH by treatment and height class for initial versus year 3 data.

Reproduction analysis by slope position

Mean oak SPH were 4,185 (±1,512) and 8,424 (± 2,599) for lower and upper slope positions. A significant difference was observed in Year 3 total oak SPH by slope position for all treatments combined (square root transformed; Student's t-test; $p = 0.014$). A one-way analysis of variance for treatment by slope position revealed significant differences between NHC upper slope versus NHC and BA11 lower slope means (Figure 4.4a.).

No significant differences were observed between treatment by slope position for height class 1 ($p = 0.07$). The highest amount of oak SPH were observed in NHC upper (11,799) and BA11+MR (7,048). The lowest number of oak SPH for height class 1 was observed in BA11 lower slope position (2,553; Figure 4.4b.).

In height class 2, BA11+MR contained the highest oak seedling abundance, with 1,739 and 1,946 oak SPH in lower and upper slope positions, respectively. Significant differences were detected between treatments and slope positions for height class 2 ($p = 0.006$). BA11+MR upper

slope was determined to be significantly different than all other treatment by slope combinations. NHC lower slope was also determined to be different than all other treatment by slope combinations. BA11 lower slope was similar to BA11+MR lower and BA11 upper slope. There was also no difference between BA11+MR lower slope, BA11 upper slope and NHC upper slope for height class 2 (Figure 4.4c.).

In height class 3, BA11+MR contained the highest oak seedling abundance, with 641 and 381 oak SPH in lower and upper slope positions, respectively. A one-way analysis of variance detected significant differences among treatments by slope position ($p < 0.001$). BA11+MR lower, and NHC lower were determined similar. BA11 upper and BA11+MR upper were also similar. BA11+MR lower was determined to be different than BA11 lower, NHC lower, and NHC upper (Figure 4.4d.).

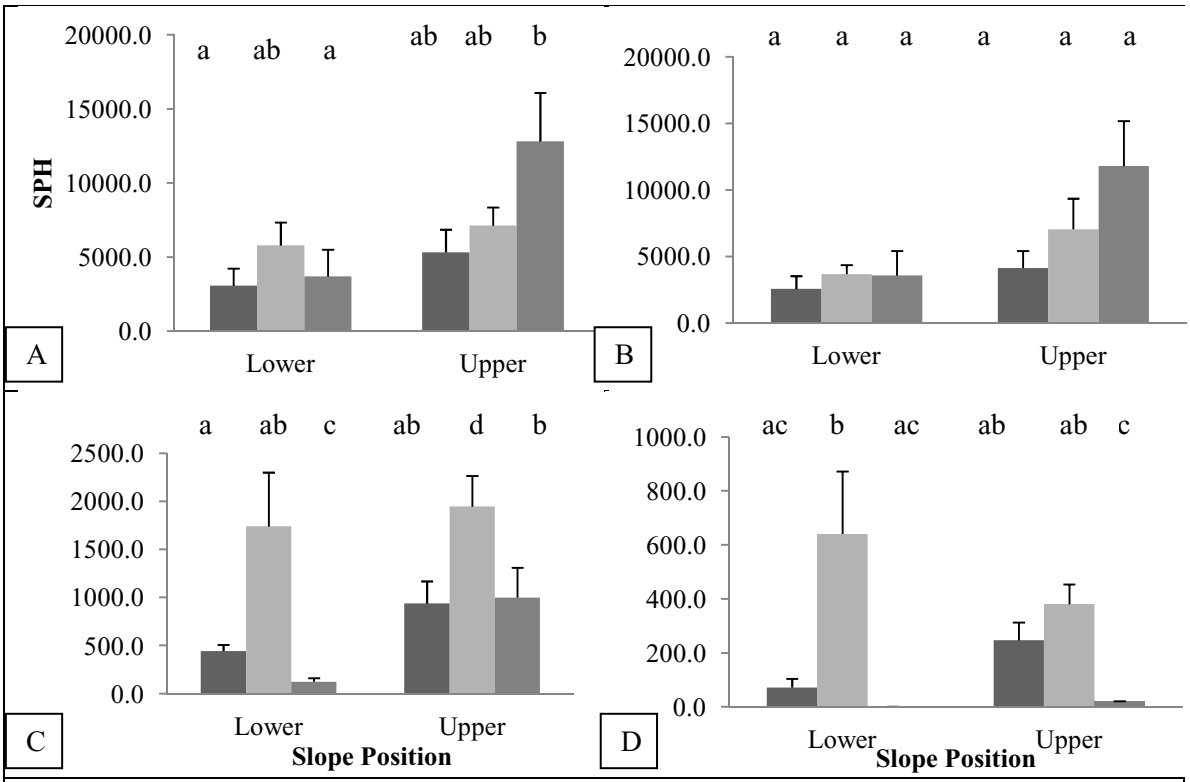

Figure 4.4. Year 3 mean oak SPH by treatment, slope position, and height class (A = total , B = height class 1, C = height class 2, and D = height class 3).
A., B., and D. One-way analysis of variance, Holm-Sidak method, α = 0.05, error bars = ±1SE.
C. Kruskal-Wallis one-way analysis of variance on ranks, SNK on ranks method, α=0.05, error bars = ±1SE.

Discussion

Sunlight canopy penetration to the forest floor was significantly impacted by treatment. BA11+MR provided 14 percent additional sunlight over BA11 and 37 percent more sunlight than the NHC treatment. BA11+MR provided light levels in the optimal range for oak seedling establishment and growth. Non-oak midstory removal in BA11+MR helped to establish uniform light conditions from lower slope to upper slope. BA11 provided adequate light levels for oak seedling development. However, there was a gradient in sunlight levels from lower slope to upper slope in BA11. This effect was attributed to harvest damage to midstory trees. This resulted in areas where light conditions ranged from optimal to adequate to inadequate for oak seedling

development within BA11. Sunlight levels remained inadequate for oak seedling development across all slope positions in the undisturbed stand conditions present in the NHC treatment.

Oak reproduction was also significantly impacted by treatment applications. BA11+MR provided the greatest increase in oak reproduction abundance coupled with height growth. BA11+MR increased oak reproduction in height classes 2 and 3 by 193 and 263 percent. This increase was greater than BA11, which exhibited increases of 112 and 140 percent for height class 2 and 3 oaks. The NHC treatment did have a 90 percent increase in oak reproduction in height class 2, but exhibited a 33 percent decline in height class 3. Increases in height classes 2 and 3 are of great importance because these are the seedlings that have potential to become "free to grow" and contribute to future stand stocking through recruitment into the overstory (Belli et al. 1999).

The NHC treatment did provide a glimpse into seedling flux in undisturbed hardwood stands. Oak reproduction remained somewhat constant from initial through year 2 post-treatment abundance numbers. However, year 3 post-treatment abundance values spiked for NHC with a total of 8,253 oak SPH, which was an increase of 6,899 oak SPH over the previous season and the highest of any treatment in year 3. The increase was attributable to a heavy white oak acorn crop observed in fall 2011 (year 2). Conventional wisdom dictates that the majority of these seedlings will not persist into the future if stand conditions remain constant.

An additional question arose as to why the influx of new seedlings was not as substantial in harvested treatments versus the NHC. The author attributes this phenomenon to two factors: 1) environmental conditions and 2) competition from non-oak competitors. The final year (3) was a season with extreme temperatures and severe drought in the region. With the capacity of upland sites in the Springfield Plateau region to become very dry, the harvest areas were exposed to higher sunlight levels and temperatures compared to the NHC treatment. Also, while partial overtory harvests and midstory removal demonstrated improved sunlight conditions for oak seedling development. There remains significant competition from non-oak reproduction,

suggesting additional competition control operations such as prescribed burning could be a beneficial additional treatment those presented in this study (Figure 4.5a – 4.5f).

The most important determinant in whether an applied silvicultural treatment could be considered successful is the influx of seedlings into the upper height class (> 0.9 m). As previously stated, oak seedlings greater than 1 meter in height have the highest potential to become “free to grow” seedlings and compete well in a developing hardwood stand. BA11+MR exhibited the largest influx of oak seedlings into height class 3 (Figures 4.5c and 4.5d). The largest increases in oak SPH for BA11 height class 3 occurred in black and white oaks (Figures 4.5a and 4.5b). NHC treatment exhibited a negative change in oaks larger than 0.9 m (Figure 4.5e and 4.5f).

An additional point of discussion is the apparent impact slope position played in sunlight canopy penetration and the resulting oak seedling growth response. BA11 averaged ~19 percent of full sunlight at ground level for the lower slope position. BA11+MR averaged ~36 percent of full sunlight at ground level for the lower slope position (Figure 1b). The oak reproduction growth response appeared to be impacted by slope position and sunlight level. In BA11, 77 percent of the year 3 post-harvest, large oak SPH occurred on the upper slope position. Conversely, 65 percent of year 3, large oak SPH occurred on the lower slope in BA11+MR. BA11+MR also exhibited increases in northern red oak reproduction, where BA11 did not. The increase in height class 3 northern red oak in BA11+MR occurred primarily on the lower slope (~ 71 percent of total). The author feels confident the increased sunlight levels combined with better site conditions for northern red oak (micro-site conditions) present in the lower slope position of BA11+MR played a primary factor in the influx of large northern red oak seedling in that treatment.

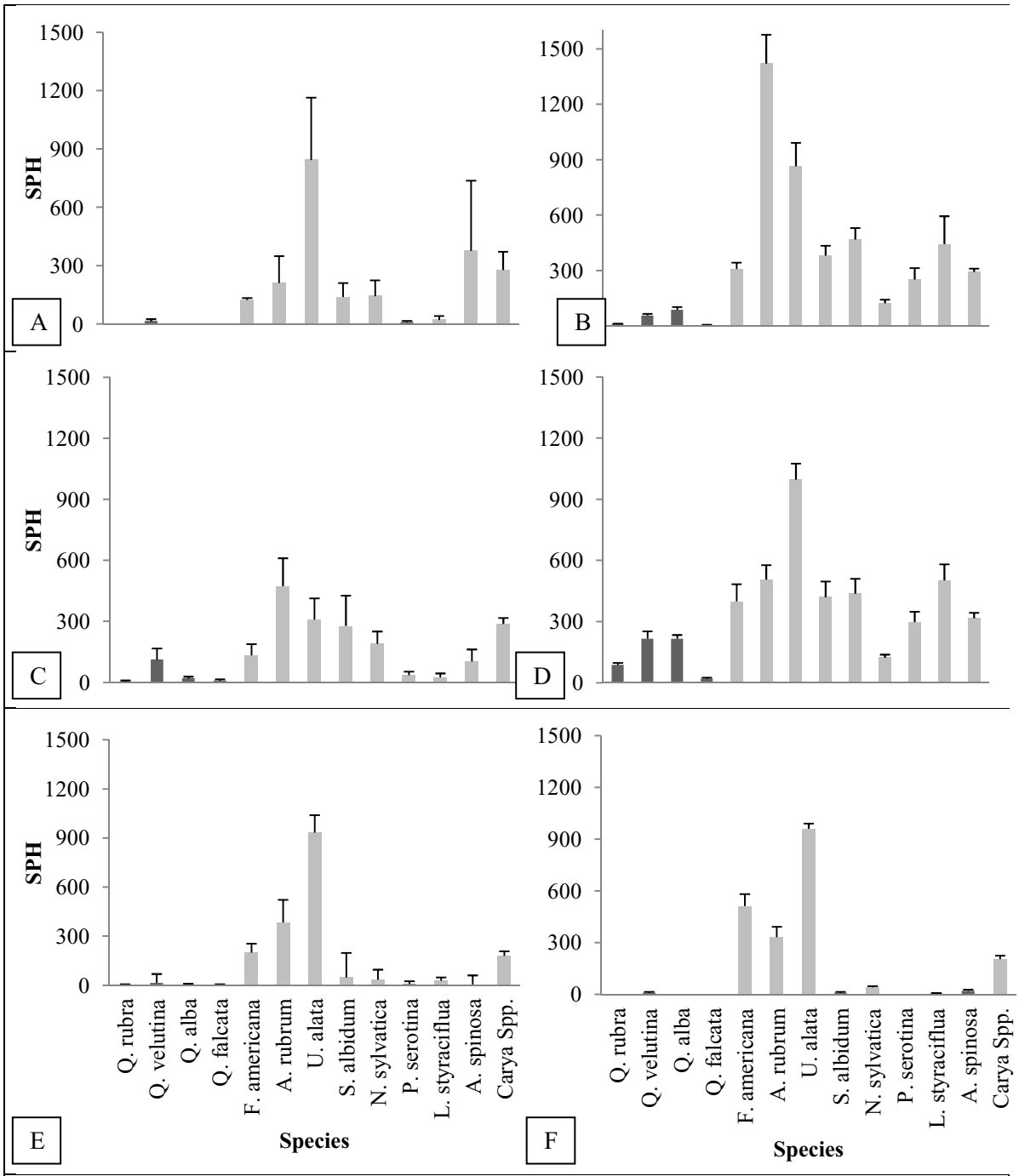

Figure 4.5. Mean SPH for height class 3 in: A. BA11initial, B. BA11 year 3, C. BA11+MR initial, D. BA11+MR year 3, E. NHC initial, and F. NHC year 3.

Conclusions

Undisturbed stand conditions did not allow growth of oak reproduction into taller height classes, keeping them in a poor position to compete with other species. A shelterwood harvest alone (BA11) created variable sunlight conditions at ground level, with only a portion of its area exhibiting adequate sunlight for oak seedling growth and survival. Year 3 results show that a modified shelterwood, combining partial overstory and non-oak midstory removal, generated optimal sunlight conditions for oak seedling development. While the partial overstory removal coupled with midstory removal created conditions beneficial to oak seedling development, non-oak species in these environments remain strong competitors. Additional treatments, such as prescribed burning, could provide additional benefit to oak reproduction.

Literature Cited

Battaglia, L.L., Fore, S.A, and R.R. Sharitz. 2000. Seedling emergence, survival, and size in relation to light and water availability in two bottomland hardwood species. J. Ecol. 88:1041-1050.

Belli, K.L., Hart, C.P., Hodges, J.D., and J.A. Stanturf. 1999. Assessment of the regeneration potential of red oaks and ash on minor bottoms of Mississippi. South. J. Appl. For. 23(3):133-138.

Brose, P., D. Van Lear, and R. Cooper. 1998. Using shelterwood harvests and prescribed fire to regenerate oak stands on productive upland sites. Forest Ecology and Management.113: 125-141.

Canham, C.D., Denslow, J.S., Platt, W.J., Runkle, J.R., Spies, T.A., and P.S. White. 1990. Light regimes beneath closed canopies and tree fall gaps in temperate and tropical forests. Can. J. For. Res. 20:620-631.

Cunningham, K.K., Peairs, S.E., Ezell, A.W., Belli, K.L., and J.D. Hodges. 2011. Understory Light Conditions Associated with Partial Overstory Removal and Midstory/Understory Control Applications in a Bottomland Hardwood Forest. ***Forests 2***, 984-992.

Ferguson, D.V., Lowrance, J.S., and C.E. McFadden. 1982. Soil Survey of Independence County, Arkansas. USDA Soil Conservation Service 148 p.

Graney D.L. and D.R. Bower. 1971. Site Index Curves for Red and White Oaks in the Boston Mountains of Arkansas. Res. Note SO-121. New Orleans, LA: U.S. Department of Agriculture, Forest Service, Southern Forest Experiment Station. 4.

Hicks, R.H., D.K. Kennard, H.M. Rauscher, D.L. Schmoldt, and P.A. Flebbe. 2001. Silviculture and management strategies applicable to southern upland hardwoods. *in*: Proceedings, Southern Forest Science Conference. 8 p.

Hodges, J.D., and E.S. Gardiner. 1993. Ecology and physiology of oak regeneration. *In*: Loftis, D.L., McGee, C.E. (Eds.), p. 54-65 *in* Oak regeneration, serious problems, practical recommendations,

Loftis, D.L., and C.E. McGee (eds.). USDA Forest Serv. Gen. Tech. Rep.

Hodges, J.D., and G.C. Janzen. 1986. Studies on the biology of cherrybark oak: recommendations for regeneration. p. 133-138 *in* Proc. Fourth Bienn. South. Silvic. Res. Conf., Phillips, D.R. (ed.). USDA For. Serv. Gen. Tech. Rep. SE-42.

Larsen, D.R. and P.S. Johnson. 1998. Linking the ecology of natural regeneration to silviculture. For. Ecol. and Man. 106(1):1-7

Loftis, D.L. 1990. A shelterwood method for regenerating red oak in the southern Appalachians. For.Sci. 36(4): 917-929.

Loftis, D.L. 1993. Regenerating northern red oak on high quality sites in the southern 20 Appalachians. *In*: Loftis, D.L. and C.E. McGee. eds. Oak Regeneration: Serious

Problems Practical Recommendations (Symposium Proceedings) Gen.Tech. Rep. SE-84. Asheville, NC: U.S. Department of Agriculture, Forest Service, Southeastern Forest Experiment Station. pp. 202 – 210.

Rogers, R., Johnson, P.S., Loftis, D.L., 1993. An overview of oak silviculture in the United States: the past, present, and future. Ann. Sci. For. 50: 535-542.

Quero, J.L., Villar, R., Maranon, T., Zamora, R., Vega, D, and L. Sack. 2008. Relating leaf photosynthetic rate to whole-plant growth: drought and shade effects on seedlings of four Quercus species. Functional Plant Biology, 35:725-737.

Smith, D.M., B.C. Larson, M.J. Kelty, and P.M.S. Ashton. 1996. The practice of silviculture: applied forest ecology. Ninth Edition. 537 p.

CHAPTER V – CHLOROPHYLL FLUORESCENCE SAMPLING METHODS

Abstract

The ability to collect non-destructive chlorophyll fluorescence (CF) data in the field using miniaturized pulse-amplitude modulated photosynthesis analyzers has improved our ability to conduct ecophysiological studies. This study explored methods for obtaining CF measurements in the field and categorized appropriate methods for CF data analysis. Ambient samples were obtained from a homogeneous sample pool of hardwood advanced reproduction (Amb1) and from a single seedling (Amb2) in normal sunlight conditions. CF samples were also collected from dark adapted seedlings using actinic light steps. Non-linear regression procedures were used to establish light curves for each sampling method. Amb1 and Amb2 light curves were similar for Q. rubra, Q. velutina, and U. alata. Amb1 light curves generated a higher ΦPSII response than did Amb2 for Q. alba, A. rubrum, and P. serotina. ΦPSII values from dark adapted samples were paired with photosynthesis yield values from CO_2 exchange samples to evaluate the relationships between chlorophyll fluorescence and carbon fixation for the seedlings included in the study. Linear and curvi-linear relationships existed between CF and CO_2 quantum yields. Gradients occurred at lower light intensities and were likely the product of competing processes to photosynthesis for electrons, such as photorespiration.

List of Abbreviations: F_v/F_m = maximum quantum yield, $F_{q'}/F_{m'}$ = effective quantum yield, ETR = electron transfer rate, PPFD = photosynthetic photon flux density, PSII = photosystem II, CF = chlorophyll fluorescence, ETR_{max}, Amb1 = Ambient 1 sampling method, Amb2 = Ambient 2 sampling method, DA = dark adapted samples.

Introduction

Assimilatory photochemistry in a leaf can be measured directly by an analysis of carbon uptake (gas exchange analysis) or indirectly by an analysis of non-cyclic electron transport in the photosynthetic apparatus. A method using chlorophyll fluorescence to calculate electron transport through PSII has proven valuable in assessing photosynthesis physiology. Chlorophyll fluorescence analysis (CF) has become one of the most powerful and widely used techniques available to plant physiologists and ecophysiologists (Maxwell and Johnson 2000). Perhaps the greatest advantage of CF is that it can be performed non-destructively in the field using a portable chlorophyll fluoremeter. However, caution must be taken when conducting a chlorophyll fluorescence study in the field or results may be misleading (Rasher et al. 2000). There are competing processes to carbon fixation for electrons, such as photorespiration and nitrogen fixation. Often, CF studies include analyses of carbon fixation and foliar pigment composition. Furthermore, inspection of automatic calculation of fluorescence parameters performed by the instrument software is necessary to ensure data integrity (Logan et al. 2007).

In addition to biochemical concerns, the proper selection of leaves to be measured is important. Leaves with similar development histories should be utilized to help ensure they are similar in pigment compositions and cuticular properties. Furthermore, leaves should have similar sun exposure periods. When proper steps are taken in leaf selection, leaves from different trees can be matched to yield similar results (Logan et al. 2007).

A large amount of work has been conducted to quantify the important parameters of CF techniques (e.g. Schreibner and Bilger 1993 and Schribner, Bilger and Neubauer 1995). The use of CF measurements to obtain important parameters such as effective quantum yield (ΦPSII) of photosystem II (PSII), photo-inhibition, maximum electron transfer rate (ETRmax), and saturating photosynthetic photon flux density (PPFDsat) (Rasher et.al. 2000). The latter two parameters are given by light response curves. Light response curves may provide a deeper insight into the characteristic parameters of an investigated plant, which are not related to the

momentary ambient conditions, but rather the ontogeny of a leaf and the range of physiological plasticity of a plant, resulting in “cardinal points” of light response curves that can be important in ecophysiological research (Rasher et.al. 2000). These comparative parameters may include effective quantum yield, maximum electron flow or CO_2 assimilation under saturated conditions.

There are two types of CF sampling that may be used to generate light response curves: ambient sampling and sampling of dark adapted seedlings under actinic light steps. The resulting light curves will be referred to as ambient light curves (Amb) and rapid light curves or in this study dark adapted light curves (DA). These measurements would be most accurate when obtained under steady state conditions, a scenario that may not always be achievable in field work.

As described by Rasher et al. (2000), to compare measurements taken under ambient conditions (solar irradiation = infinite distance) to those taken using the actinic light provided by the fiber-optics, caution must be taken into account for the fact that the micro-quantum sensor of the leaf clip is not on the same plane as the leaf (Figure 5.1). Though a short distance (less than 2mm), Rasher et al. (2000) illustrated that differences in light intensity can occur between the leaf plane and quantum sensor.

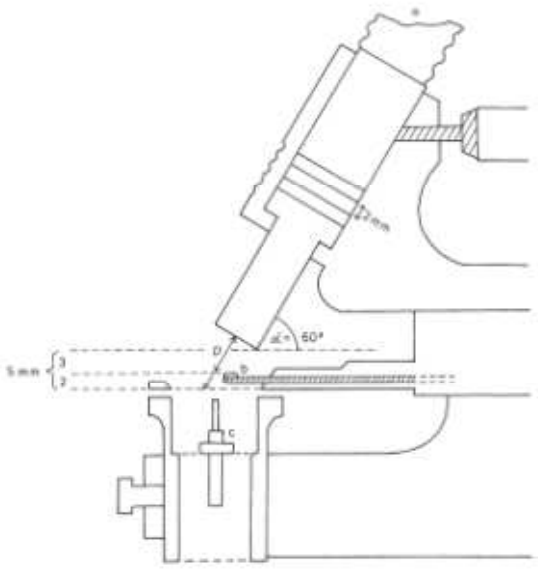

Figure 5.1. Leaf clip holder of the Mini-PAM (a. fiber optics; b. diffuser disc of light sensor; c, thermocouple for leaf temperature).

(Figure from Rasher et. al. 2000)

Materials and Methods

Chorophyll Fluorescence Sampling

Chlorophyll fluorescence samples were taken with a Mini-PAM 2000 (Walz inc., Germany) field fluoremeter. Sunlight values recorded by the Mini-PAM were calibrated against a quantum light sensor (Delta OHM LP 471, □400 to 700 nm) for accuracy (Figure 5.2). All samples were obtained between 10:30 and 15:30 hrs on clear to mostly clear days. Samples were taken in May 2012. CF parameters F_v/F_m, $F_{q'}/F_{m'}$, and ETR were calculated according to the equations in Table 1.1.

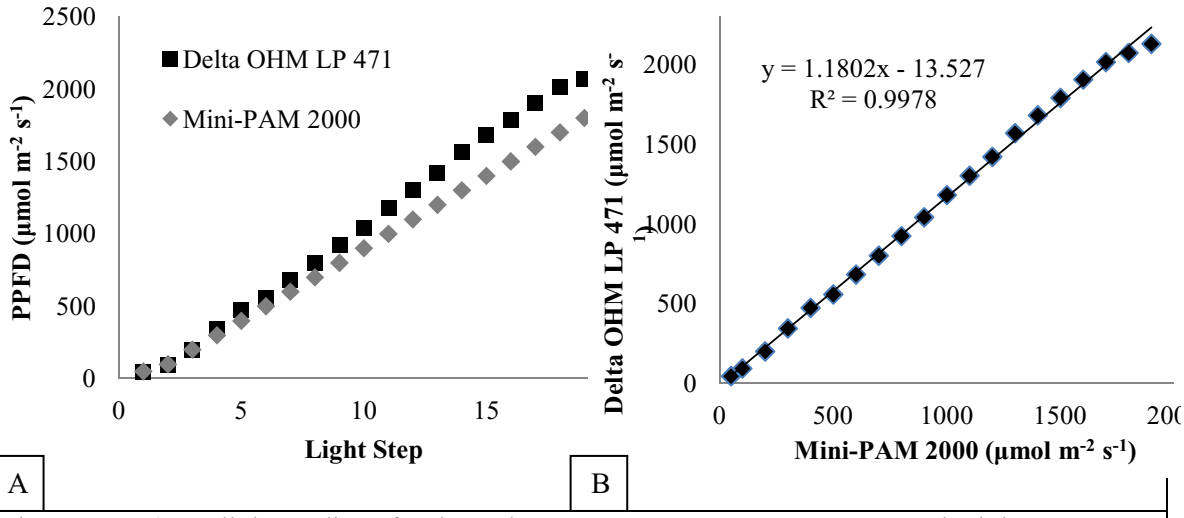

Figure 5.2. A) Sunlight readings for the Delta OHM LP 471 quantum sensor and mini-PAM 2000 micro-quantum sensor B) Relationship between Delta OHM LP 471 and mini-PAM 2000 light readings.

Sunlight readings were obtained under non-obstructed, clear skies, with each sensor leveled and fixed in position side-by-side. Light steps were in 100 µmol m^{-2} s^{-1} increments.

Ambient 1 CF sampling method

Twenty four sample seedlings were selected from the reproduction pool for each species in BA11 and BA11+MR to obtain Ambient 1 (Amb1) samples. At least three CF samples were obtained from each seedling, resulting in a minimum of 72 CF samples per species. The youngest, fully developed leaves present on a seedling were selected for measurement. In addition, leaves on a horizontal plane receiving uniform sunlight (leaves receiving full sunlight were selected first) across the adaxial surface were utilized.

Ambient 1 CF samples were utilized in a broader study examining CF variables in varying stand densities (and subsequent light environments), where maximum photosynthesis rate was the primary variable of interest. Therefore, the youngest, fully developed leaves were of most interest in Amb1 sampling. Differences in sunlight environments were solely the product of varying shading levels from canopy trees present on the broader study. The result was a

homogeneous sample pool of CF data representing low to high ambient sunlight conditions that could be used to generate ambient light curves.

Ambient 2 CF sampling method

One representative seedling from the Amb1 sample pool was selected for each species to generate Ambient 2 light curves (Amb2). Amb2 sample seedlings were all located on the same plot in the same replicate of the partial harvest treatment area. A pool of CF samples was obtained from leaves of each seedling receiving varying levels of sunlight. As in Amb1 samples, only fully mature leaves were selected. However, the remaining rules of leaf selection for Amb1 were not followed in Amb2 sampling. This lax in leaf selection criteria was necessary to obtain CF samples at varying sunlight intensities from a single seedling under ambient conditions.

Dark adapted CF sampling under an actinic light source

The same set of seedlings utilized for Amb2 samples were used to obtain dark adapted samples (DA). For this method, seedlings were dark adapted under a shade cloth for 30 minutes. After dark adaptation was complete, the actinic light source of the mini-PAM was activated. Light levels were increased in eight steps from 0 to 1800 μmol m^{-2} s^{-1}. Light step widths were set at one minute. Light intensities were adjusted based on the recommendations of Rasher et al. (2000). The process was repeated a minimum of three times for each sample seedling. F_v/F_m was the first measure obtained in DA samples at light intensity zero. However, the remaining samples represent $F_{q'}/F_{m'}$, which is the label used in figures related to DAs.

CO_2 exchange sampling method

Leaves used to sample dark adapted CF measures were sequentially sampled for CO_2 exchange rates. Gas exchange measurements were taken using a LiCor 6400xt portable photosynthesis system (LiCor, Inc., Lincoln, NE). The 6400xt was connected to a sensor head containing two infrared gas analyzers (IRGAs) to conduct photosynthesis measurements. The sensor head contained a sample and a reference IRGA. The sample IRGA was incorporated in a 2 x 3 cm^2 leaf chamber. During operation of the LiCor 6400 system the CO_2 concentration of gas entering the chamber was controlled by injecting CO_2 into air drawn through a gas scrubber. Reference CO_2 concentration was set at 400 μL L^{-1}, resulting in sample CO_2 concentrations at 390 uL $L^{-1.}$ The leaf chamber was illuminated with a LiCor 6400-02B light source utilizing red (peak spectral output = 670 nm) and blue (peak spectral output = 465 nm) light emitting diodes (LEDs). The LED light source was turned off and dark respiration was recorded manually after photosynthesis rate stabilized. Light was then increased in steps including 250, 750, 1250, and 1800 μmol m^{-2} s^{-1}. After photosynthesis rates stabilized at 1800 μmol m^{-2} s^{-1}, the light curve program was initiated. The light curve program recorded photosynthesis at decreasing light interval steps, including: 1800, 1250, 750, 450, 300, 150, and 50 μmol m^{-2} s^{-1}. Air flow through the chamber was set at a constant value of 250 μmol s^{-1} during light curve sampling. Temperature and relative humidity were at ambient conditions. The LiCor 6400 stability indicator option was activated and measurements were only recorded when the coefficients of variation of the measures CO2 concentrations in the sample stream and photosynthetic rates over the preceding 10 s were less than 1% and the rate of change in values was less than 1% per minute. IRGA's were matched automatically by the 6400XT if needed.

Net assimilation rate (NAR) was calculated by the 6400xt software by calculating the differences between CO_2 in the reference IRGA and the CO_2 in the sample IRGA times the

difference between the H_2O in the reference IRGA and the H_2O in the sample IRGA, all adjusted by the flow per leaf area.

CO2 yield was calculated by:

$$CO_2\ yield = \frac{(NAR+R_d)}{(PPFD*0.84)} \qquad \text{Formula 5.1}$$

Curve fitting procedure

Non-linear regression procedures were utilized for Amb1, Amb2, DA, and CO_2 samples. Quantum yields were fit to a two parameter hyperbolic decay function (Formula 5.2). Electron transfer rates and photosynthesis rate curves were fit to a two parameter, single rectangular curve (Formula 5.3). All curves were fit to datasets using SigmaPlot 11.0. These two curves were utilized for all sampling methods because they worked well for all the methods used, provided physiologically relevant relationships, and helped provide homogeneity in curve fitting across sampling methods. Often, electron transfer rate and photosynthesis rate curves are described by a non-rectangular hyperbola described by Ogren and Evans (1993). However, the method did not fit the ambient sample datasets well in this study and therefore was not used.

CF Quantum yield regression:

$$\Phi PSII\ line = \frac{ab}{b+x} \qquad \text{Formula 5.2.}$$

Where,

a = regression intercept coefficient (approximates F_v/F_m)

b = regression curvature coefficient

x = PPFD

ETR and CO_2 light curve regression:

$$ETR\ line = \frac{ax}{b+x}$$ Formula 5.3.

Where,

a = regression coefficient (magnitude of curve)

b = regression curvature coefficient

x = PPFD

Comparing CF and CO_2 samples

Three sets of paired DA and CO_2 samples for light steps 50, 150, 300, 450, 750, and 1200 μmol m^{-2} s^{-1} were collected for each species. Photosynthesis yield from CO_2 exchange (Formula 5.1) was plotted against $F_{q'}/F_{m'}$ (fluorescence yield, Formula 5.2) values. Regression analysis was performed for the paired DA and CO_2 samples. Regressions were performed using a 2 parameter power function in SigmaPlot 11.0.

Results

Mean SPAD chlorophyll indices ranged from 30.1 for *Q. rubra* to 39.1 for *P. serotina*. Leaf temperatures ranged from 32.9^0 to 42.7^0 C for DA chlorophyll fluorescence samples. For CO_2 samples, leaf temperature ranged from 33.4^0 to 40.1^0 C. Leaf temperatures were similar between samples for each species. Seedling heights ranged from 1.2 m for *Q. rubra*, *Q. velutina and P. serotina*, to 1.8 m for *U. alata* (Table 5.1).

Table 5.1. Descriptive seedling characteristics for the DA, Amb2 and CO_2 samples.

	SPAD Chlorophyll	Measured Chlorophyll (g/cm^2)	CF Leaf Temp.	CO_2 Leaf Temp.	Seedling Height (m)
Q. rubra	30.1 (0.4)	14.4	34 (0.9)	33.4 (2.5)	1.2
Q. velutina	35.7 (0.2)	19.2	33.5 (2.8)	34.8 (1.4)	1.2
Q. alba	31.7 (1.3)	15.6	34.7 (4.3)	33.6 (1.3)	1.3
A. rubrum	32.2 (0.4)	32.2	42.7 (0.03)	38.4 (1.5)	1.4
U. ulata	36.6 (0.3)	20.0	32.9 (1.4)	34 (1.3)	1.8
P. serotina	39.1 (0.3)	22.7	40.8 (0.9)	40.1 (0.4)	1.2

() = ± SE, measured chlorophyll described in Appendix IV.

Figure 5.4 illustrates the $F_{q'}/F_{m'}$ versus PPFD for *Quercus* and non-*Quercus* species. Maximal fluorescence yield (F_v/F_m) ranged from 0.681 to 0.805 for *Quercus* species and 0.674 to 0.775 for non-*Quercus* species. Q. rubra produced the highest effective quantum yield ($F_{q'}/F_{m'}$) values for Quercus species. *U. alata* produced the highest effective quantum yield for non-*Quercus* species. The two parameter, hyberbolic decay regression fit the DA sample data well with adjusted R^2 values of 0.95, 0.90, and 0.94 for *Quercus* species and 0.97, 0.77, and 0.90 for non-*Quercus* species. Regression parameters were significant for all samples (Table 5.2).

Table 5.2. Quantum yield regression parameters for DA sample curves.

Sample	Variable	Coefficient	Std. error	t	p
Q. rubra	a	0.746	0.009	83.0	< 0.001
	b	1226.4	71.2	17.2	< 0.001
	n = 21, Adj. R^2 = 0.95, F = 651, P < 0.0001				
Q. velutina	a	0.757	0.024	33.8	< 0.0001
	b	793.8	87.5	9.07	< 0.0001
	n = 21, Adj. R^2 = 0.90, F = 231.7 , P < 0.0001				
Q. alba	a	0.747	0.021	35.9	< 0.0001
	b	446.9	40.2	11.1	< 0.0001
	n = 21, Adj. R^2 = 0.94, F = 404.7 , P < 0.0001				
A. rubrum	a	0.649	0.03	21.8	< 0.0001
	b	229.5	29.6	7.8	< 0.0001
	n = 21, Adj. R^2 = 0.90, F = 221.9, P < 0.0001				
U. alata	a	0.745	0.01	72.1	< 0.0001
	b	909.7	51.6	17.6	< 0.0001
	n = 21, Adj. R^2 = 0.97, F = 742.1, P < 0.0001				
P. serotina	a	0.705	0.03	20.4	< 0.0001
	b	470.7	77.7	6.0	< 0.0001
	n = 21, Adj. R^2 = 0.77, F = 115.1 , P < 0.0001				

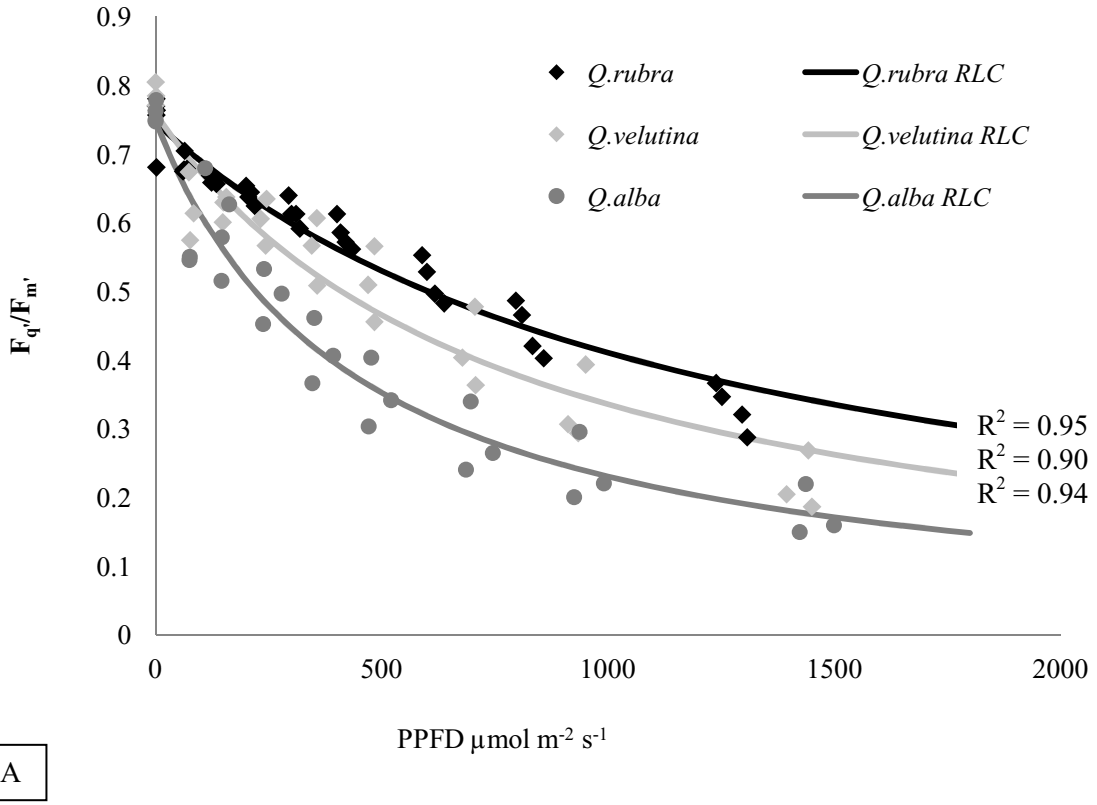

A

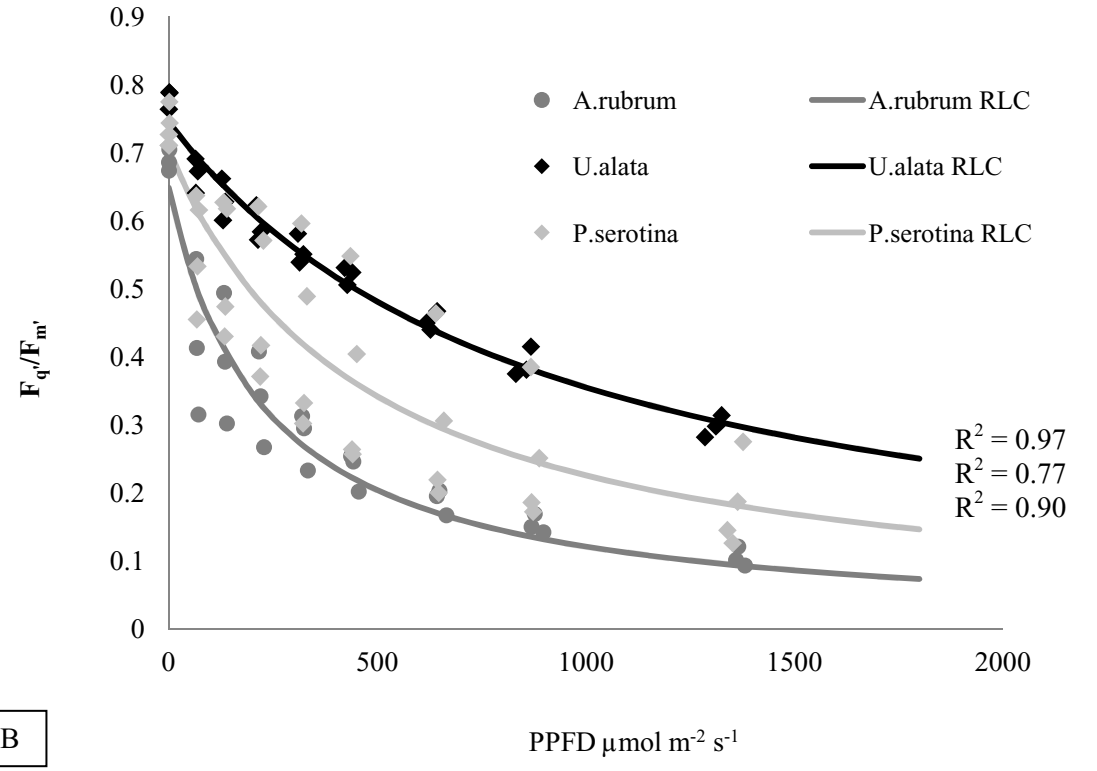

B

Figure 5.3. F_q'/F_m' versus PPFD for *Quercus*. B. F_q'/F_m' versus PPFD for non-*Quercus*.

Figure 5.4. illustrates the relationships between CO_2 exchange samples and DAs. R^2 values ranged from 0.6 to 0.8 for the six sample species (Table 5.3). All regression parameters were determined significant. *Q. rubra*, *Q. velutina*, and *U. alata* exhibited curvilinear relationships, while *Q. alba*, *A. rubrum*, and *P. serotina* exhibited linear relationships. Paired samples by species fit a two parameter power function well.

Table 5.3. Two parameter power regression analysis for paired effective quantum yields between DA and CO_2 samples [$\Phi CO_2 = c*(F_{q'}/f_{m'})$ ^d].

Sample	Variable	Coefficient	Std. error	t	p
Q. rubra	c	0.16	0.07	2.36	0.03
	d	3.07	0.93	3.28	0.005
	n = 18, Adj. R^2 = 0.60, F = 23.1, P = 0.0002				
Q. velutina	c	0.13	0.03	3.77	0.0017
	d	2.13	0.49	4.26	0.0006
	n = 18, Adj. R^2 = 0.68, F = 32.3 , P < 0.0001				
Q. alba	c	0.09	0.01	5.7	< 0.0001
	d	1.15	0.24	4.8	0.0002
	n = 18, Adj. R^2 = 0.69, F =35.8, P < 0.0001				
A. rubrum	c	0.19	0.04	5.0	0.0001
	d	1.24	0.19	6.4	< 0.0001
	n = 18, Adj. R^2 = 0.77, F = 55.6, P < 0.0001				
U. alata	c	0.18	0.040	4.53	< 0.0001
	d	2.42	0.427	5.66	< 0.0001
	n = 18, Adj. R^2 = 0.78, F = 58.0, P < 0.0001				
P. serotina	c	0.13	0.02	4.8	0.0003
	d	1.30	0.25	5.1	0.0002
	n = 15, Adj. R^2 = 0.74, F = 37.8, P < 0.0001				

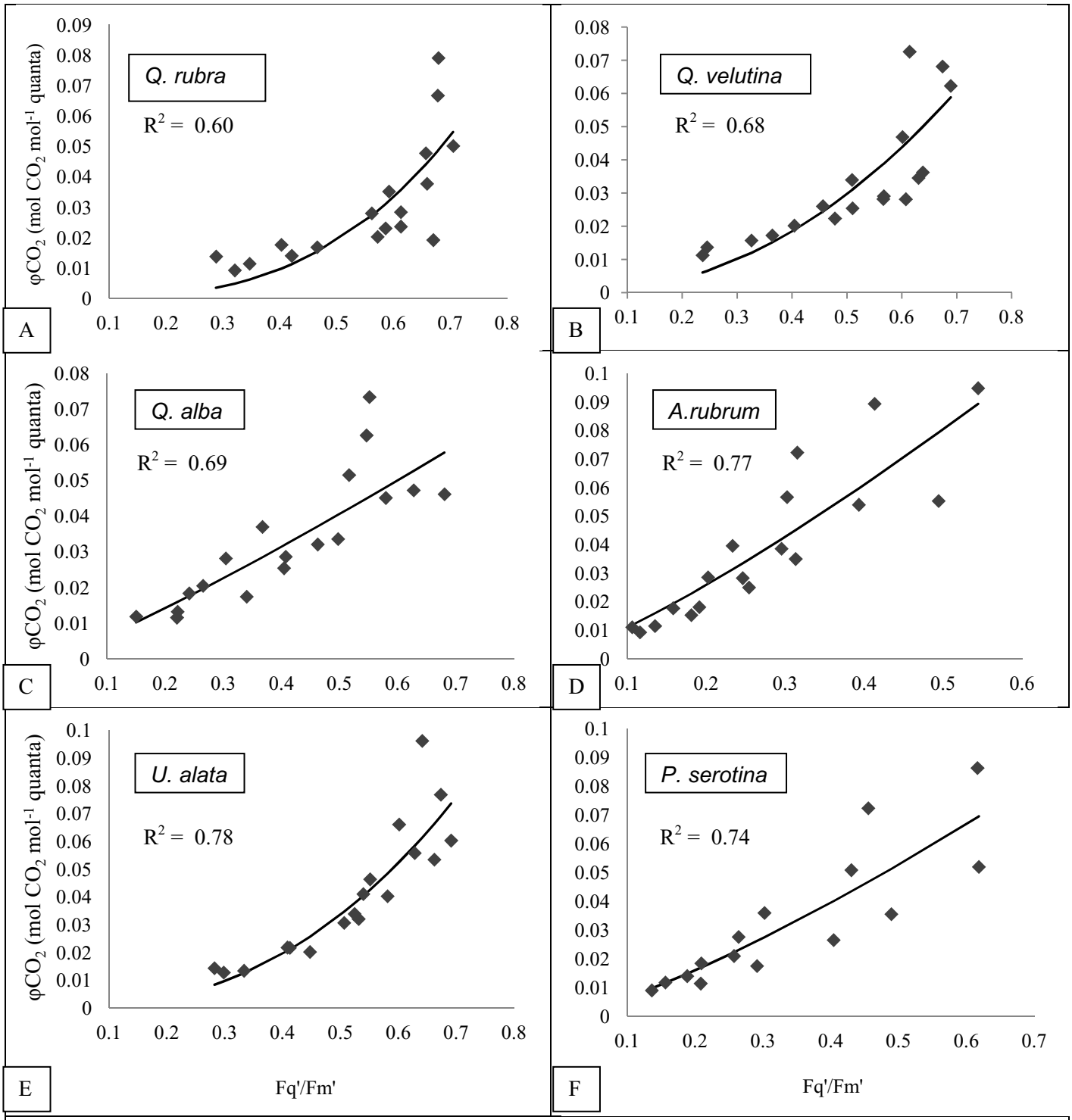

Figure 5.4. CO_2 effective quantum yield versus $F_{q'}/F_{m'}$ in spring 2012. A) Q. rubra, B) Q. velutina, C) Q. alba, D) A. rubrum, E) U. alata, and F) P. serotina.

All regressions were fit to a 2 parameter power function: $\Phi CO_2 = c*(F_{q'}/F_{m'})^{\wedge}d$.

Figure 5.5 illustrates the comparisons between Amb1 and Amb2 curves for F_q'/F_m' values per sunlight quanta for each of the six species sampled. Two parameter, hyperbolic decay regressions resulted in adjusted R^2 values from 0.87 to 0.94 for Amb1 samples and 0.71 to 0.90 for Amb2 samples. Regression parameters were significant for all samples (Table 5.4).

Table 5.4. Non-linear regression analysis for Amb1 F_q'/F_m' samples.

Sample	Variable	Coefficient	Std. error	t	p
Q. rubra	a	0.79	0.02	51.3	< 0.0001
	b	473.2	42.1	11.2	< 0.0001
	n = 131, Adj. R^2 = 0.90, F = 1163.9, P = <0.0001				
Q. velutina	a	0.79	0.007	106.1	<0.0001
	b	562.5	26.5	21.2	<0.0001
	n = 204, Adj. R^2 = 0.94, F = 3023.4, P <0.0001				
Q. alba	a	0.82	0.01	75.2	<0.0001
	b	461.8	23.5	19.6	<0.0001
	n = 188, Adj. R^2 = 0.94 , F = 2724.2 , P <0.0001				
A. rubrum	a	0.81	0.0086	94.1	<0.0001
	b	530.9	23.4	22.6	<0.0001
	n = 214, Adj. R^2 = 0.94, F = 3252.1, P <0.0001				
U. alata	a	0.79	0.008	96.3	<0.0001
	b	678.7	28.9	23.5	<0.0001
	n = 213 , Adj. R^2 = 0.93, F = 2958.7, P <0.0001				
P. serotina	a	0.79	0.02	48.3	<0.0001
	b	579.7	42.24	13.7	<0.0001
	n = 152, Adj. R^2 = 0.87, F = 1039.7, P <0.0001				

Table 5.5. Non-linear regression analysis for Amb2 $F_{q'}/F_{m'}$ samples.

Sample	Variable	Coefficient	Std. error	t	Prob.
Q. rubra	a	0.76	0.03	25.4	< 0.0001
	b	563.3	57.3	9.8	< 0.0001
	n = 94, Adj. R^2 = 0.82, F = 431.1, P < 0.0001				
Q. velutina	a	0.72	0.04	16.4	< 0.0001
	b	840.3	129.1	6.5	< 0.0001
	n = 50, Adj. R^2 = 0.71, F = 123.6, P < 0.0001				
Q. alba	a	0.78	0.03	26.8	< 0.0001
	b	575.9	56.1	10.3	< 0.0001
	n = 80, Adj. R^2 = 0.84, F = 421.9, P < 0.0001				
A. rubrum	a	0.71	0.02	34.7	< 0.0001
	b	850.9	78.0	10.9	<0.0001
	n = 65 , Adj. R^2 = 0.87, F = 433.1, P < 0.0001				
U. alata	a	0.75	0.03	27.8	< 0.0001
	b	736.2	69.4	10.6	< 0.0001
	n = 46, Adj. R^2 = 0.89, F = 390.2, P < 0.0001				
P. serotina	a	0.84	0.02	34.3	< 0.0001
	b	766.1	64.5	11.9	< 0.0001
	n = 54, Adj. R^2 = 0.90, F = 470.5, P < 0.0001				

Light curves were essentially equal in magnitude and curvature for *Q. rubra*, *Q. velutina* and *U. alata*. However, Amb2 light curves were slightly higher than Amb1 curves for *Q. alba*, *A. rubrum*, and *P.serotina*, but did exhibit similar profiles. Amb1 provided a more complete data sets than did the Amb2 sample method.

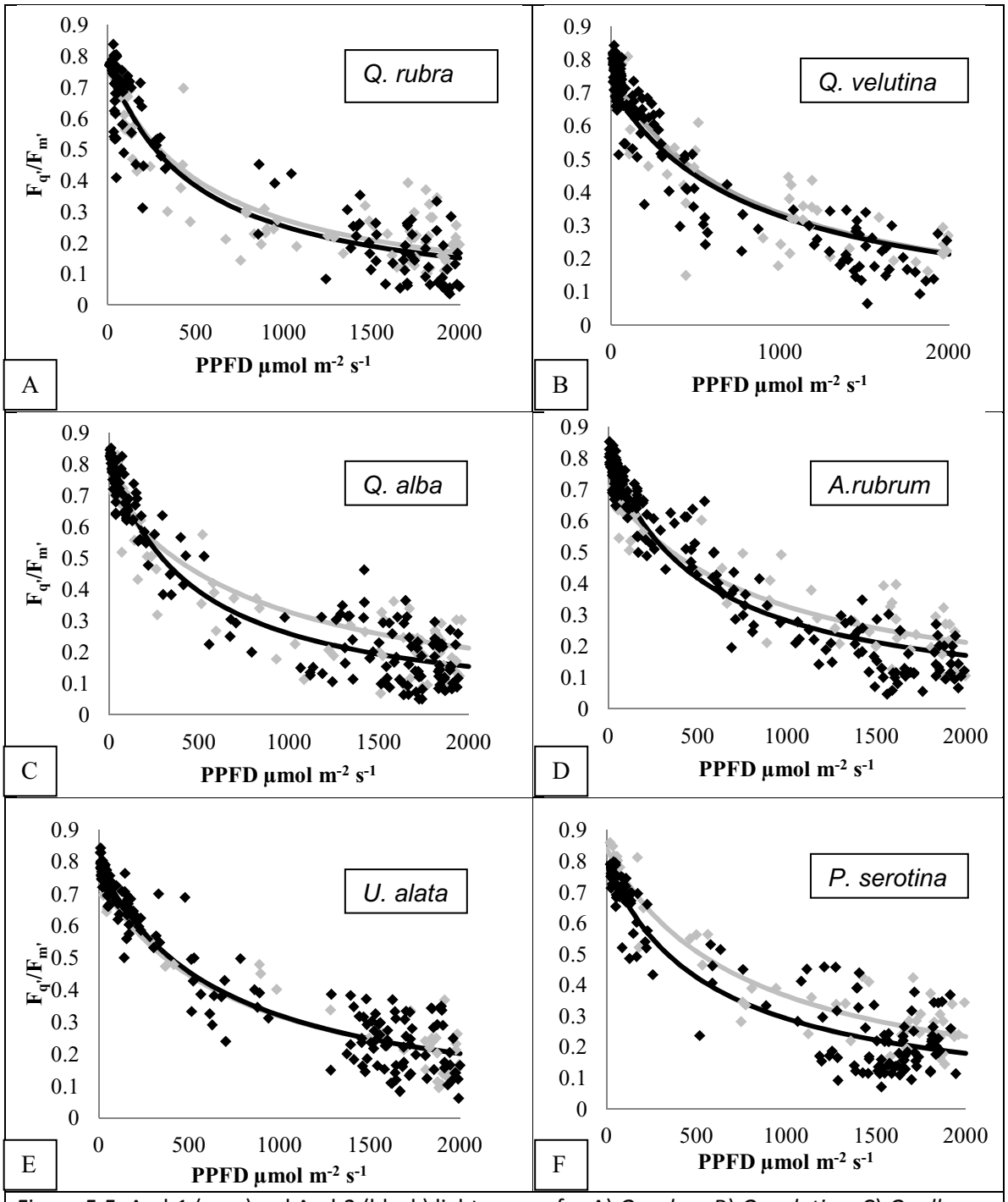

Figure 5.5. Amb1 (gray)and Amb2 (black) light curves for A) *Q. rubra*, B) *Q. velutina*, C) *Q. alba*, D) *A. rubrum*, E) *U. alata*, and F) *P. serotina*.

Discussion

CO_2 samples paired with DA samples correlated well for all six species. *Q. alba*, *A. rubrum*, and *P. serotina* exhibited linear relationships between paired samples. *Q. rubra*, *Q. velutina*, and *U. alata* expressed similar and linear relationships in light values above 300 µmol m^{-2} s^{-1}, and increased in spread at lower light levels below 300 µmol m^{-2} s^{-1}. The major divergence occurred at PPFD 50 µmol m^{-2} s^{-1}. At low light, effective quantum yield was lower for PSII than for CO_2 effective quantum yield for some samples (Figure 5.6A). The CO_2 effective quantum yield values at PPFD 50 µmol m^{-2} s^{-1} were more closely related to dark adapted CF yield (F_v/F_m).

The variations or gradients present in sample data at low light could be attributed to oxygenation of RuBP at the site of the dark reactions, instead of carboxylation. Photorespiration processes would result in a competing mechanism for ATP and NADPH generated in the light reactions, resulting in a sink for light reaction products. However, that was not what appeared to be the case in these sample data. With CF quantum efficiency being lower than CO_2 quantum efficiency, one would conclude that a process occurred that lowered demand for electrons from PSII. A plausible cause could be cyclical electron flow, where electrons are returning to plastoquinone from ferredoxin in place of them being used to reduce $NADP^+$ to NADPH. Photorespiratory processes may have been more evident in electron transfer rate discrepancies at very high sunlight (Figure 5.6B), where assimilatory photochemistry is CO_2 limited.

Additionally, one of the limitations to the study was that CF sampling and gas exchange sampling could not be performed simultaneously. They were performed sequentially. Therefore, it is possible some variation could be a product of environment or change in leaf status. Overall, electron flow in PSII correlated well with assimilation rate.

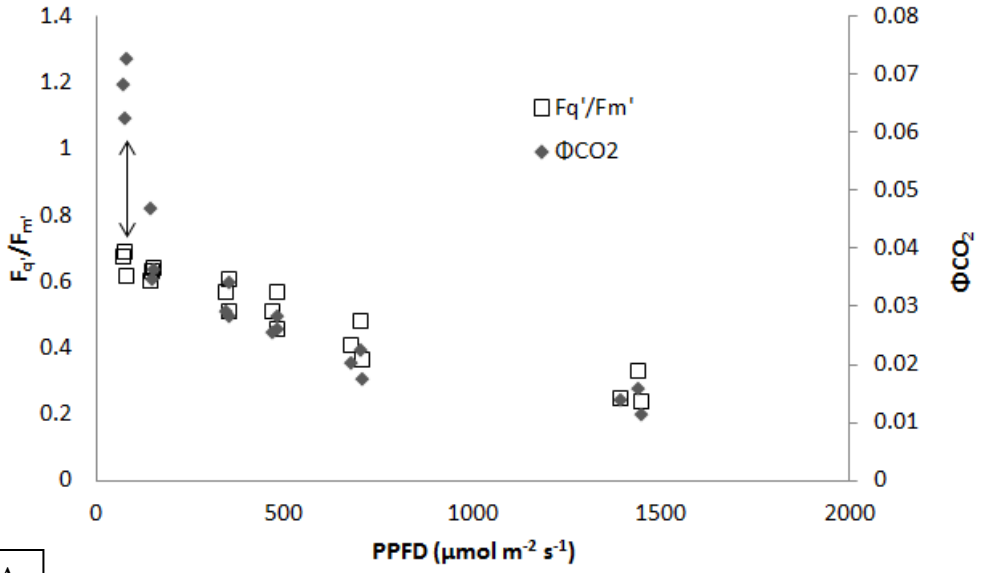

A

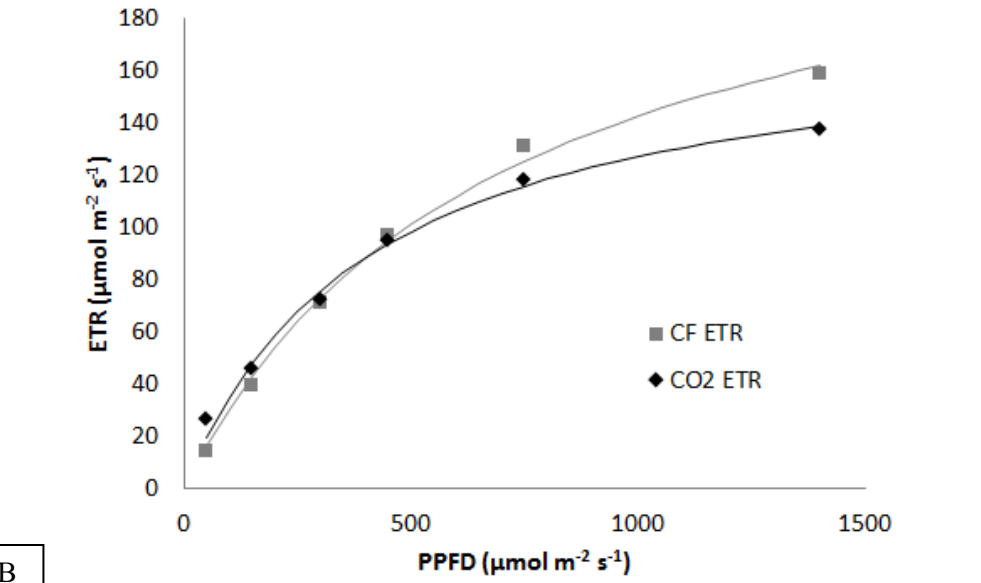

B

Figure 5.6. Illustration of low light variation present between $F_{q'}/F_{m'}$ and ΦCO2 for Q. velutina. A) Yield data points for both CF and gas exchange (ΦCO2 multiplied by a factor of 18 to put on similar scale as $F_{q'}/F_{m'}$). B) CF ETR and CO_2 ETR calculated values for Q. velutina.

CO_2 ETR = (A+Rd)/(ETR/A @I_i); I = irradiance i from Table 5.8

Light curves from dark adapted samples were either the same or shared similar profiles with light curves from Amb2 sample data (Figure 5.6). Other than *Q. rubra*, DA light curves were either the same or lower than light curves from Amb2 data. Differences could easily be corrected using a linear adjustment to DA sample curves, applying the overall mean difference between sample point values. This concept is illustrated in Figure 5.6.

The lower magnitude for DA curves was likely due to ambient curves better representing "steady state" photosynthesis conditions. DA curves were obtained from dark adapted seedlings, and were illuminated by the PAM light source in light steps that were 1 minute in duration. DA samples possibly do not represent complete "steady state" photosynthesis conditions. Furthermore, utilizing more than one leaf to obtain Amb2 samples could create some variation between methods.

Some studies rely solely on DA samples with 30 second widths in light steps and operate under the assumption that the relationships between non-steady state and steady state exist. This study examined both sample types with longer light step widths in DA samples. The results of this study suggest ambient samples would be a recommended component to any CF based study. The sample design in this study allowed the collection and use of ambient data. Ambient data collection may be more difficult to obtain based on different study designs.

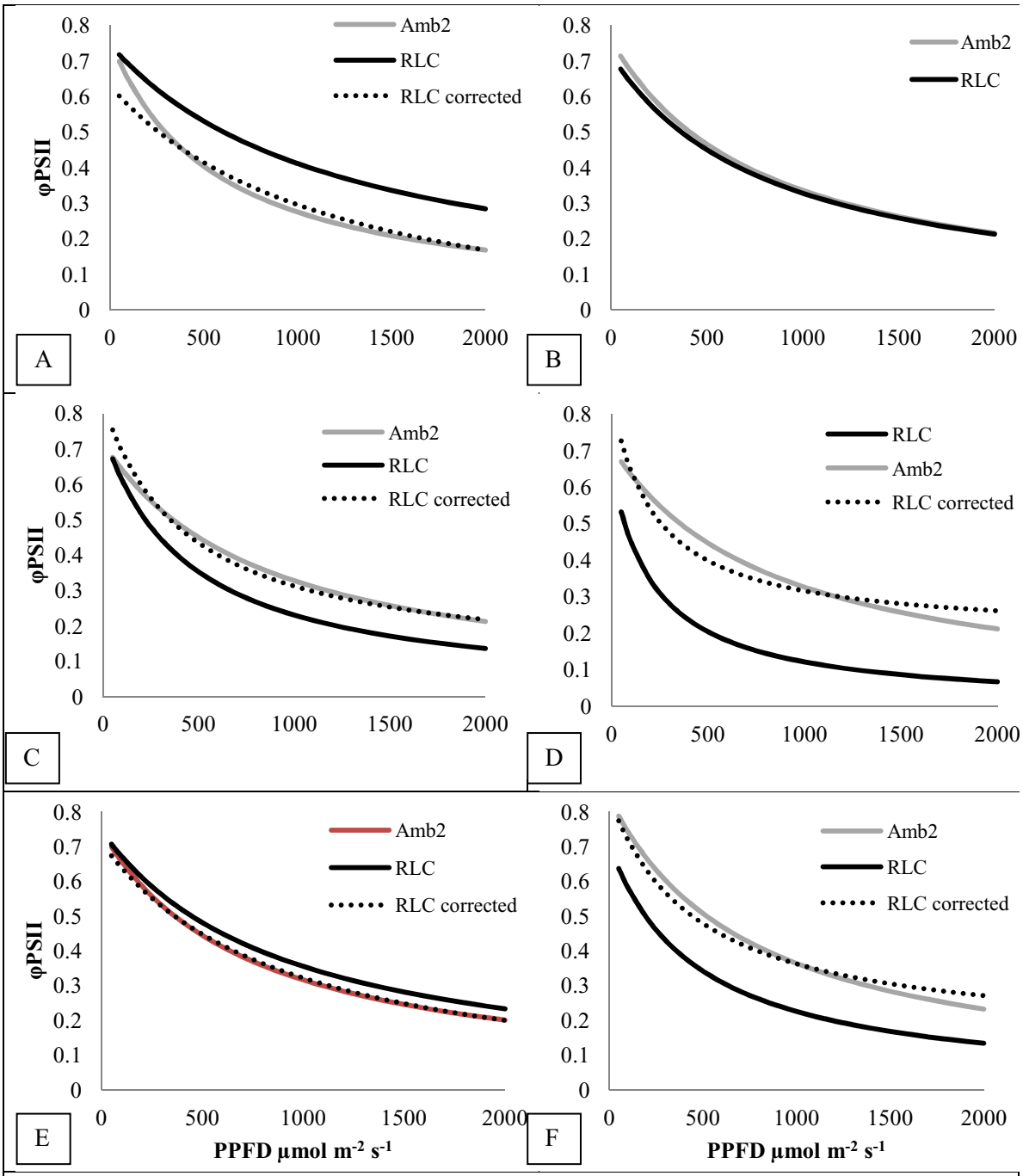

Figure 5.7. Linear correction of RLCs to ambient light curves for Amb2 samples A) Q. rubra, B) Q. velutina, C) Q. alba D) A. rubrum, E) U. alata,and F) P. serotina.

RLC corrected = ΔX + RLC value; where, ΔX = mean difference between sample points.

The good relationships between DA and CO_2 effective quantum efficiencies, the similar profiles between light curves from DA samples, and the similarity between Amb1 and Amb2 ALCs demonstrate that all of the CF based data provide useful and similar datasets. While each sampling method produced comparable results, some differences did occur across methods. If one were to only employ one sampling method, an understanding of these differences should be understood.

Based on the results of this study, the utilization of a large, homogeneous sample pool better accounts for variation across samples than would a sample pool of a few individual plants or a single individual. Therefore, the Amb1 samples should provide the most useful dataset for studies examining phenomena across a gradient of environmental variables, such as the effective quantum yield across varying sunlight environments.

The inability of being able to obtain measurements from a large sample pool over rough terrain with CO_2 exchange analysis and the ability to collect large sample datasets from a homogeneous pool, as in Amb1 sampling, made chlorophyll fluorescence a very useful technique for evaluating the photosynthesis physiology of different hardwood species within different light environments. CF sampling from a single seedling provided similar curves to those from a sample pool. However, similarities in seedling morphology were essential to uniformity in results.

The light curves used for comparisons between sampling methods involved effective quantum yields, which is the most direct measure provided by CF sampling. A large benefit to CF sampling is the ability to calculate an electron transfer rate (ETR) from effective quantum yield and absorbed sunlight (Formula 7.2). ETR values can serve as proxy measures to photosynthesis rates and allow comparisons relating to photosynthetic performance. Cardinal points (as described by Rascher et al. 2000) of ETR-based (or of CO_2 assimilation) light curves provide useful and uniform parameters for comparisons among sample units (Figure 5.8). The two parameter, single rectangular curve in Formula 5.3 establishes a physiologically relevant curve with parameter *a*

impacting magnitude or maximum ETR and parameter *b* impacting curvature or bending degree of the fitted line (correlating to quantum yield). Establishing ETR_{max}, $PPFD_{sat}$, and a corresponding $F_{q'}/F_{m'}$ from the fitted curves provide useful data points for comparisons between samples.

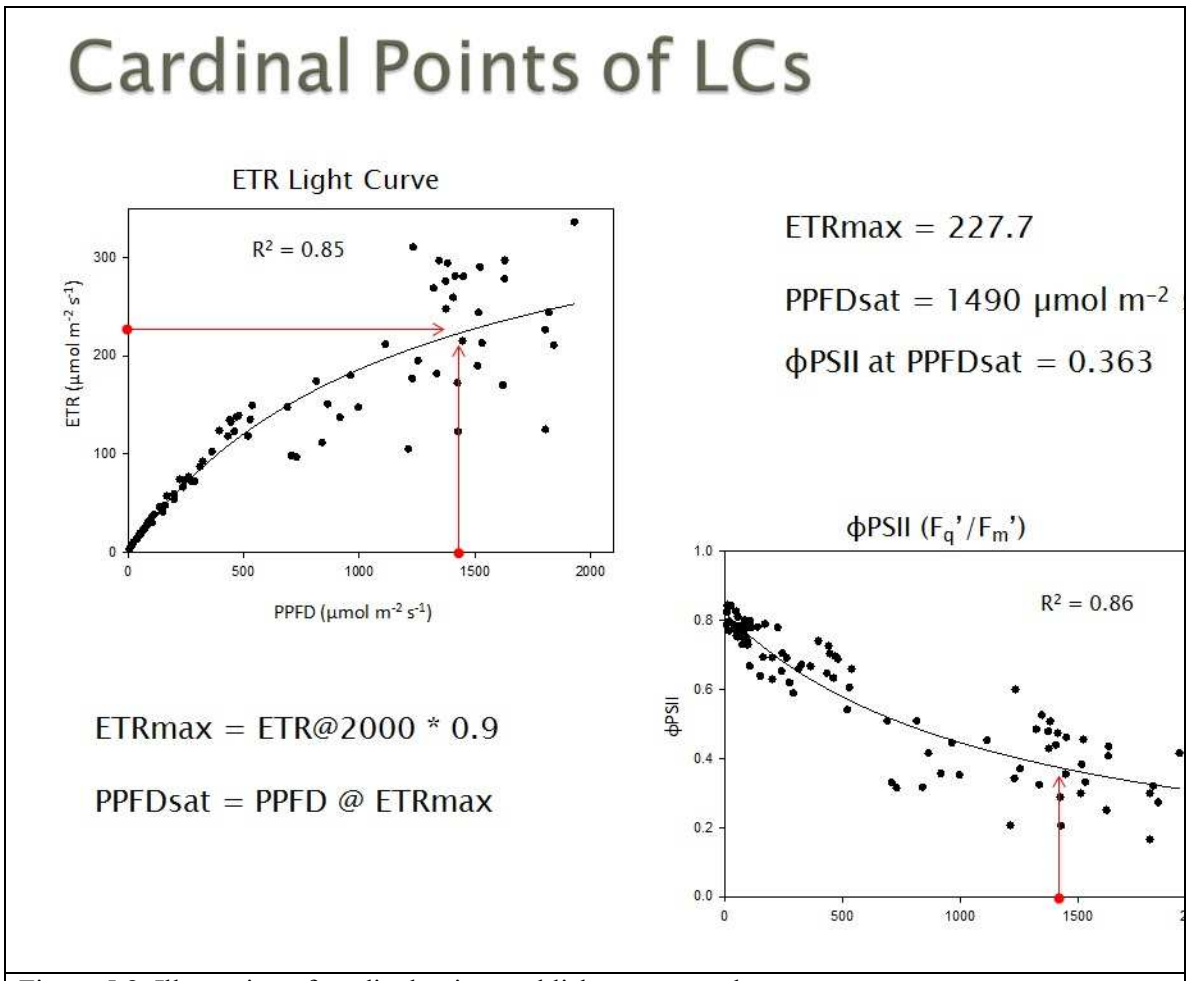

Figure 5.8. Illustration of cardinal point establishment procedures.

Data are from U. alata sampled in July 2011 (year 2 post treatment).

Table 5.6 provides an illustration of how cardinal point parameters can be compared among species for both ETR and CO_2 assimilation. A ranking of maximum ETR and maximum net assimilation rate exhibit similar relationships among species. Light saturation differences likely occurred due to a more rapid impact of CO_2 limitation on dark versus light reactions. The ability to attain similarities between ETR and CO_2 assimilation allows for CF sampling, and the

resulting ETR values, to be a highly useful comparative method in ecophysiological studies involving sunlight conditions. The primary factor is that ETR incorporates irradiance into its calculated value, making it a great complement to and potentially more informative than $F_{q'}/F_{m'}$ comparisons alone, in such settings.

Table 5.6. Example comparison between CF analysis and CO_2 analysis for six species.

Species	ETR_{max}	$PPFD_{sat}$ (ETR)	NAR_{max}	$PPFD_{sat}$ (NAR)	ETR_{max} rank	NAR_{max} rank
Q. rubra	102.7	1100	7.9	900	6	5
Q. velutina	126.8	1300	9.1	900	3	3
Q. alba	117.3	1300	9.1	700	4	3
A. rubrum	110.1	1100	6.5	500	5	6
U. alata	148.5	1300	10.6	550	1	1
P. serotina	134.5	1300	9.3	700	2	2

Data from May 2012. ETRmax and NARmaxValues equal 90% of 2,000 µmol m^{-2} s^{-1}.

The final question to be answered is how does ETR relate to gross photosynthesis rate? Table 5.7 illustrates the ETR/A ratios (µmol electrons m^{-2} s^{-1}/(µmol CO_2 m^{-2} s^{-1}+R_d)) for each species. The red oak group (*Q. rubra* and *Q. velutina*) expressed the highest ETR/A ratios, while *A. rubrum* had the lowest ratio. These results would suggest that *A. rubrum* was more efficient at total CO_2 assimilation than other species observed and suggests alternative electron sinks such as photorespiration are more active in oak species.

Table 5.7. ETR/A ratios for advanced reproduction of six hardwood species.

	PPFD (µmol m^{-2} s^{-1})						
Species	**300**	**500**	**800**	**1200**	**1800**	**Ave.**	**Std. Dev.**
Q. rubra	8.3*	7.4	8.9	10.7	12.9	9.6	2.2
Q. velutina	9.3	9.2	9.4	9.9	10.6	9.7	0.6
Q. alba	6.2	6.8	7.6	8.4	9.1	7.6	1.2
A. rubrum	3.5	4.5	5.1	5.7	6.1	5.0	1.0
U. alata	5.4	7.3	9.0	10.8	12.5	9.0	2.8
P. serotina	4.7	5.6	6.4	7.2	7.9	6.4	1.3
All Species	6.2	6.8	7.7	8.8	9.9	7.9	1.5

*ETR/A = (µmol photons m^{-2} s^{-1}/(µmol CO_2 m^{-2} s^{-1}+R_d)). Data from May 2012

Conclusions

Chlorophyll fluorescence sampling in the field proved to be a useful tool for evaluating photosynthesis of hardwood reproduction in the field. Chlorophyll fluorescence samples compared favorably with samples taken using CO_2 assimilation. Three methods of chlorophyll fluorescence sampling demonstrated the magnitude of light curves generated may exhibit variation, particularly between ambient samples and dark adapted samples run under an actinic light source. However, all three methods provided useful results. The ability to establish additional chlorophyll fluorescence parameters, such as electron transfer rate, adds to the importance of the method. This study supports the findings of many others regarding chlorophyll fluorescence in that the data is easy to obtain, but caution must be taken ensure the sampling method is valid and that the researcher understands the type of data being collected and the uses and limitations of that data. The ability to incorporate other measures, such as gas exchange, will remain important to increasing validity and depth of chlorophyll fluorescence studies.

Literature Cited

Logan, B.A., Adams, W.W., and B. Demmig-Adams. 2007. Avoiding common pitfalls of chlorophyll fluorescence analysis under field conditions. *Functional Plant Biology*, 34; 853-859.

Maxwell M. and Johnson G.N. (2000). Chlorophyll fluorescence—a practical guide *Journal of Experimental Botany* 51(345): 659-668.

Ögren, E., & Evans, J. R. (1993). Photosynthetic light-response curves. *Planta*,*189*(2), 182-190.

Rascher, U., Liebig, M., & Lüttge, U. (2000). Evaluation of instant light-response curves of chlorophyll fluorescence parameters obtained with a portable chlorophyll fluorometer on site in the field. *Plant, Cell & Environment*, *23*(12), 1397-1405.

Schreiber, U., & Bilger, W. (1993). Progress in chlorophyll fluorescence research: major developments during the past years in retrospect. *Progress in Botany/Fortschritte der Botanik* 151-173.

Schreiber, U., Bilger, W., & Neubauer, C. (1995). Chlorophyll fluorescence as a nonintrusive indicator for rapid assessment of in vivo photosynthesis. *Ecophysiology of photosynthesis* 49-70.

CHAPTER VI – A GROWING SEASON ANALYSIS OF PHOTOSYNTHESIS

Abstract

Photosynthesis analyses were performed on six upland hardwood species including: Quercus rubra, Quercus velutina, Quercus alba, Acer rubrum, Ulmus alata, and Prunus serotina. Gas exchange was measured using a LiCOR 6400xt photosynthesis system (LiCOR, Lincoln, NE). Seedlings were selected from a "sun" light environment and a "shade" light environment. Three light response curves (8 light steps each) were measured using three leaves of a seedling from each species in each sunlight environment. Photosynthesis measurements were obtained in May (early), July (mid), and September (late) to represent points in the growing season. Sun versus shade analyses were conducted on early season measurements. Light saturated values for photosynthesis parameters were evaluated (values above 750 µmol m^{-2} s^{-1}). A significant difference was detected between sun and shade adapted seedlings for all light saturated photosynthesis parameter values (Mann Whitney Rank Sum; α = 0.05). Point of growing season analysis was performed on the sun adapted seedlings. Significant differences were detected between points of growing season for several photosynthesis parameters under light saturated conditions (P <0.001 Kruskal Wallace method, α = 0.05). Mid-season values differed from early and late season values for several parameters (Dunn's method, α = 0.05).

List of Abbreviations: PPFD = photosynthetic photon flux density, $PPFD_{sat}$ = photosynthetic photon flux density at a saturated photosynthesis rate , SLA = specific leaf area, A_{gross} = total CO_2 assimilation rate, A_{net} = CO_2 assimilation rate – respiration rate, $A_{max.g}$ = CO_2 saturated maximum total assimiliation rate, $A_{max.n}$ = CO_2 saturated maximum total assimiliation rate - respiration, ΦCO_2 = effective quantum yield of CO_2 assimilation, ΦPSII = effective quantum yield of photosystem II, R_d = dark respiration rate.

Introduction

Gas exchange has long been an essential component of photosynthesis physiological analyses of photosynthesis. Photosynthesis is unique in that it is a sensitive indicator for limitations of physiological processes that can be continuously monitored (Long et al. 1996). Forty years ago, a publication by Sestak et al. (1971) provided a manual of methods for photosynthesis measurements. At that time, to obtain photosynthesis measurements in the field was difficult, tedious, and basically required a lab be set up on site. Today, an array of portable photosynthesis analyzers are available that allow one to obtain real-time measurements of leaf photosynthetic CO_2 uptake, transpiration, leaf conductance, and intercellular CO_2 mole fraction with little knowledge required of the system and calculations involved (Long et al. 1996). Because of portable photosynthesis systems, such as the LI-6400xt photosynthesis system (LI-COR, Inc., Lincoln, NE), obtaining photosynthesis information can be easily achieved in the field.

Forest ecophysiologists have utilized gas exchange for examining forest condition (e.g. Ogaya and Peñuelas 2003), impacts of elevated atmospheric CO_2 on forests (e.g. Curtis 1996 and Hamilton et al. 2002), tree seedling performance (e.g. Lockhart and Hodges 1994), and other aspects of forest function. Lockhart and Hodges 1994 utilized gas exchange to evaluate *Quercus pagoda* seedlings from different sources of seedling stock (planted vs. natural). Additional forest ecophysiology studies have utilized gas exchange to examine irradiance and edaphic factors influence on oak reproduction survival and growth (e.g. Gardiner and Krauss 2001). Furthermore, gas exchange has been used to evaluate carbon gain by northern red oak advanced reproduction in the presence or absence of competing competition (Nilsen et al. 2009).

A few studies have explored photosynthesis analysis in the Ozark region of field grown saplings for a portion of the species included herein (Hinckley et al. 1978, Chambers 1976, and Phelps et al. 1976). These studies established potential drought and shade tolerance rankings for

four upland species: *Quercus rubra, Quercus velutina, Quercus alba,* and *Acer saccharum*. Two studies, Chambers et al. (1985) and Phelps (1976), contained potentially confounding factors, including: 1) presence of an overstory, resulting in low sunlight conditions, 2) sample seedlings across plots, resulting in potential edaphic variation, and 3) differences in species rooting patterns. Hinckley (1978) attempted to resolve some of these issues by transplanting saplings to a greenhouse prior to analysis.

The present study was able to better address issues associated with field sampling of photosynthesis data in several ways. First, portable photosynthesis systems have made field data collection more feasible and provide measurement of many photosynthesis parameters simultaneously. Second, this study provided reproduction from both a sunlight acclimated environment and a shaded environment. Finally, the weather conditions during the growing season of measurement provided an "unstressed", "stressed", and "recovery" period for photosynthesis analysis. Therefore, this study attempted to supplement our understanding of photosynthesis rates for advanced reproduction of three *Quercus* species and three non-*Quercus* competitors in an upland hardwood stand in the Ozark highlands of Arkansas in differing sunlight environments and through a growing season.

Study Objectives:

- Determine differences in photosynthesis physiology between "sun" versus "shade" leaves of advanced hardwood reproduction.
- Determine differences between points of a growing season for sun adapted reproduction.
- Evaluate photosynthesis parameter differences between different hardwood species during a growing season.

Materials and Methods

Hardwood seedlings were selected from a reproduction pool within a partially harvested overstory (BA 11 m^{-2} h^{-1}; "Sun" seedlings) and from undisturbed closed canopy stand conditions (Non-Harvest Control, "Shade" seedlings). Advanced reproduction of six upland hardwood species were selected, including: *Quercus rubra*, *Quercus velutina*, *Quercus alba*, *Acer rubrum*, *Ulmus alata*, and *Prunus serotina*. Reproduction from both treatments had developed under closed canopy conditions for decades, Sun seedlings were released by a partial overstory harvest in 2009. Photosynthesis measurements were obtained in 2012 (year 3 post-harvest). Thus, Sun seedlings were adapted to a partial sun light environment for three growing seasons. Photosynthetic photon flux densities (PPFD) averaged 55 percent of full sunlight (Figure 6.1). Shade seedlings were obtained from a treatment plot with average PPFD near 5 percent of full sunlight.

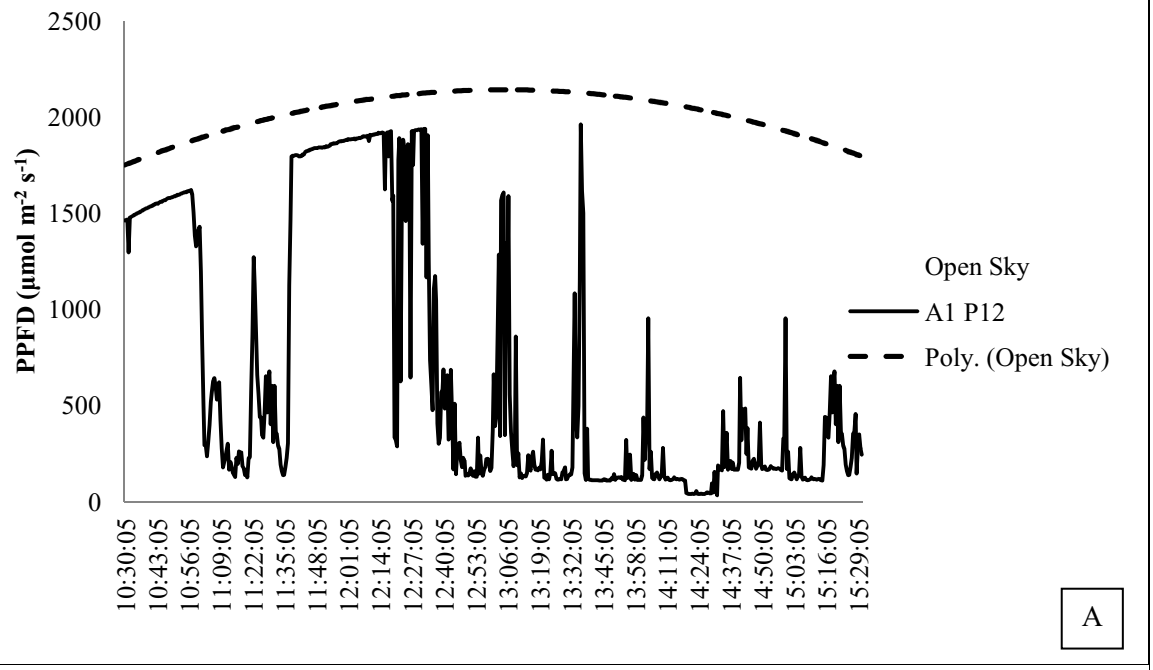

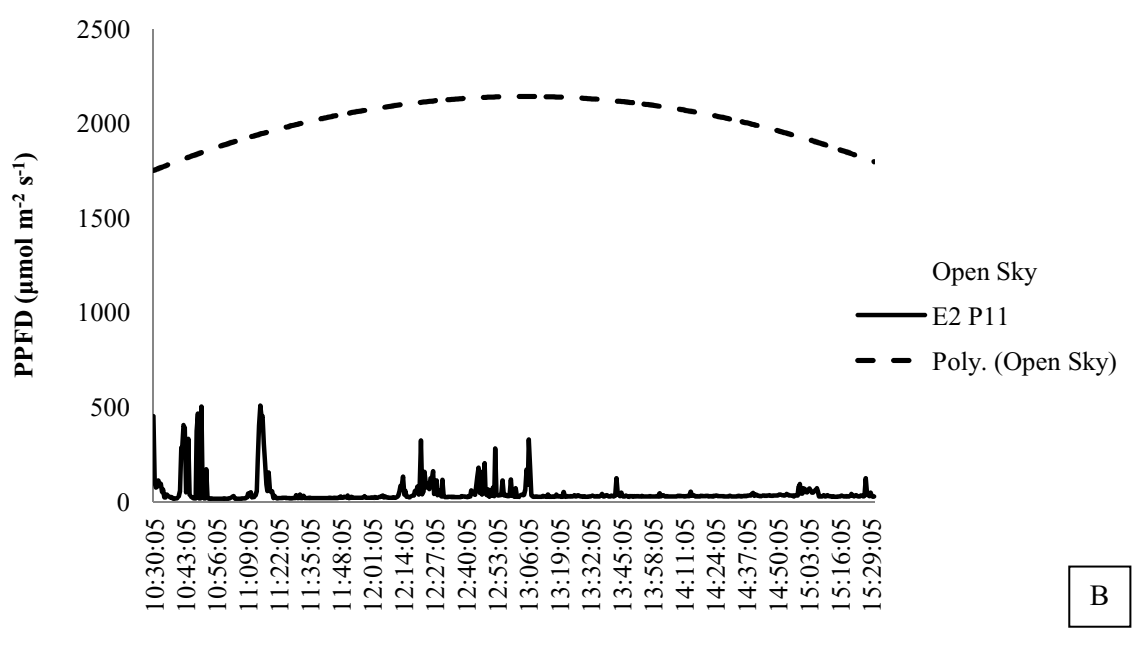

Figure 6.1. Sunlight course from 10:30 hrs to 15:30 hrs. A) Sun plot. B) Shade plot.

Gas exchange measurements were taken using a LiCor 6400xt portable photosynthesis system (LiCor, Inc., Lincoln, NE). The 6400xt was connected to a sensor head containing two infrared gas analyzers (IRGAs) to conduct photosynthesis measurements. The sensor head contained a sample and a reference IRGA. The sample IRGA was incorporated in a 2 x 3 cm^2 leaf chamber. During operation of the LiCor 6400xt system the CO2 concentration of gas entering the chamber was controlled by injecting CO_2 into air drawn through a gas scrubber. Reference CO_2 concentration was set at 400 µL L^{-1}, resulting in sample CO_2 concentrations at 390 uL $L^{-1.}$ The leaf chamber was illuminated with a LiCor 6400-02B light source utilizing red (peak spectral output = 670 nm) and blue (peak spectral output = 465 nm) light emitting diodes (LEDs). The leaf chamber was attached to a leaf and irradiance was increased in steps including 250, 750, 1250, and 1800 µmol m^{-2} s^{-1}. After photosynthesis rates stabilized at 1800 µmol m^{-2} s^{-1}, the light curve program was initiated. The light curve program recorded photosynthesis at decreasing light interval steps, including: 1800, 1250, 750, 450, 300, 150, and 50 µmol m^{-2} s^{-1}. The LED light source was turned off and dark respiration was recorded manually after photosynthesis rate stabilized. Air flow through the chamber was set at a constant value of 250 µmol s^{-1} during light curve sampling. Temperature and relative humidity were at ambient conditions. The LiCor 6400xt stability indicator option was activated and measurements were only recorded when the coefficients of variation of the measures CO_2 concentrations in the sample stream and photosynthetic rates over the preceding 10 s were less than 1% and the rate of change in values was less than 1% per minute. IRGA's were matched automatically by the 6400xt if needed. The 6400xt calculations of photosynthesis parameters follow those of von Caemmerer and Farquhar (1981).

PPFD was measured at each reproduction plot. PPFD was measured at plot center using a Delta OHM LP 471 (□400 to 700 nm). The sensor was mounted to a leveled tripod at each measurement plot. Sunlight observations were taken at mid-day (10:30 – 15:30 hrs) under mostly

clear to clear sky conditions in May of 2012. Open sky readings were taken in an open field near the study site. Open sky values were used to calculate percent of full sunlight values.

Average daily maximum temperatures and precipitation data were obtained from a National Oceanic and Atmospheric Administration (NOAA) weather station located approximately 1km from the study site. 2012 provided a season with a stress event for seedlings in the study. During the growing season, the study site experienced high maximum daily temperatures (MDTs), including a time period from mid-June to the end of July where MDTs were consecutively above 37^0 C. The period of time from June through July 2012 significantly impacted seedling physiology. A compounding factor during this time period was that it followed early season precipitation rates well below normal. The coupled impacts of high MDTs and low precipitation rates were evident in data collection during 2012 (Figure 6.2).

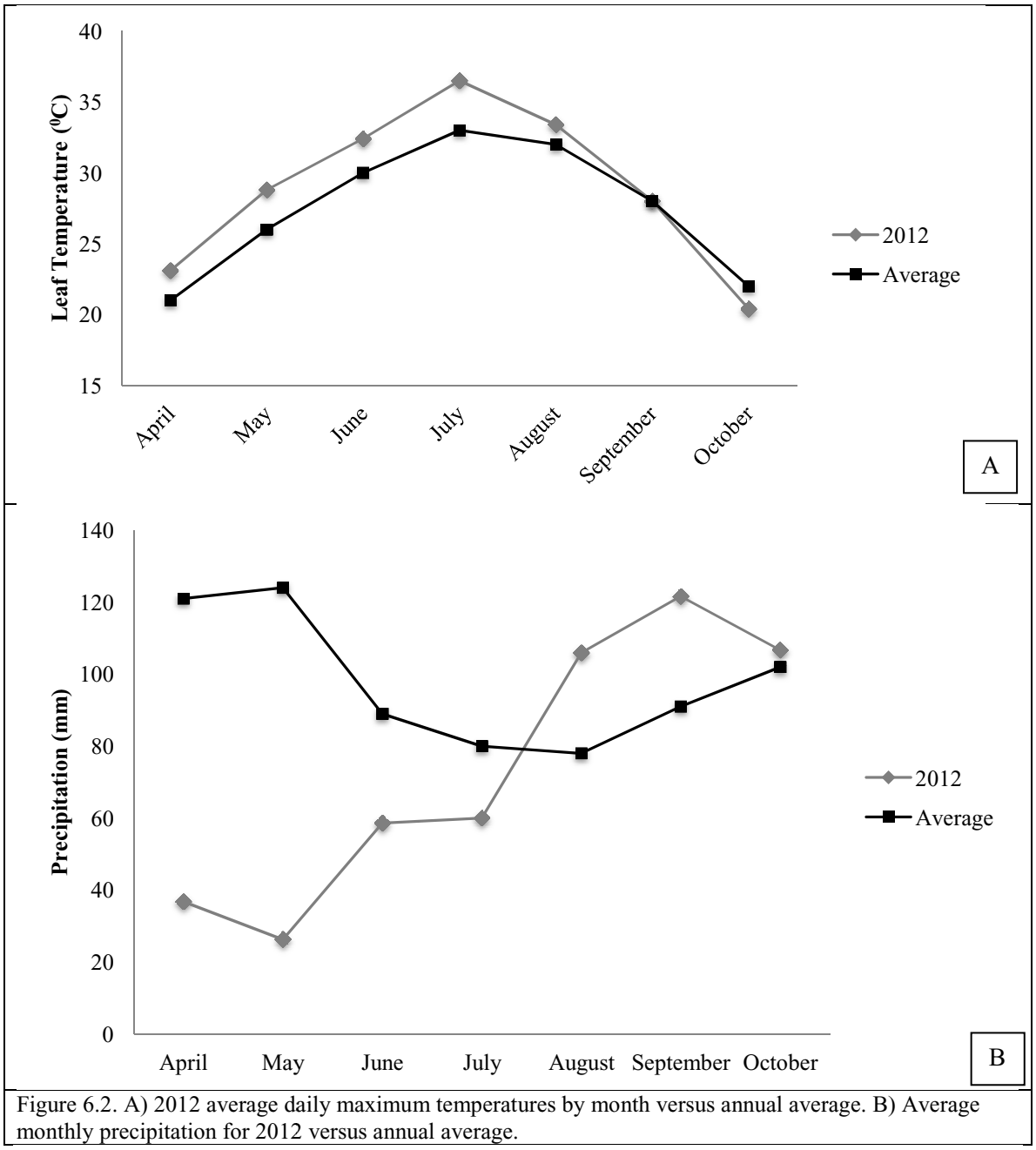

Figure 6.2. A) 2012 average daily maximum temperatures by month versus annual average. B) Average monthly precipitation for 2012 versus annual average.

Light curves for net CO_2 assimilation samples were fitted to a formula first described by Thornley (1976) and further developed by Ogren and Evans (1993). Formula 6.1 is the formula for assimilation rate based on effective quantum yield (Φ), bending degree (θ), irradiance (I), maximum assimilation rate (A_{max}). The equation was entered as a custom non-linear regression in Sigma Plot 11.0. The parameters Φ, θ, A_{max} were determined by a least squares solution. Gross assimilation rate was estimated by adding dark respiration (R_d) to the respective net assimilation rate.

$$A(I) = \frac{(\Phi \times I + A_{max} - \sqrt{(\Phi I + A_{max})^2 - 4\theta I A_{max}})}{2\theta}$$ Formula 6.1

All statistical analyses were performed in Sigma Plot 11.0. All data were tested for normality and equal variances. Due to the nature of the data, assumptions of normality and/or equal variances were not met. Thus, non-parametric analyses were conducted. Mann Whitney tests were performed between Sun and Shade average values. For point of growing season, a Kruskal Wallis ANOVA on ranks test was conducted for detection of overall median differences. Means (or medians) separation was conducted using Dunn's test. All statistical tests were performed at the alpha 0.05 level.

Results

Treatment level photosynthesis analysis

Significant differences were detected for every photosynthesis parameter under light saturated conditions (samples taken between 750 and 1800 µmol m^{-2} s^{-1}) between NHC (shade leaves) and harvested treatments (sun leaves in year three post-harvest) (Table 6.1). NHC seedlings were growing in an average of 5 percent of full sunlight and harvested treatment seedlings were growing in an average of 55 percent of full sunlight. Net assimilation, and other parameters, were significantly different between sun and shade leaves with mean assimilation rates of 9.7 and 5.4. Dark respiration was also notably different with an average R_d rate of 0.4 for shade leaves and 2.8 for sun adapted leaves.

Table 6.1. Light saturated photosynthesis parameters between NHC and harvested treatments for early summer year three postharvest.

	5%	55%		
	NHC	Harvest	U-value	P-value
Amax.g (µmol CO_2 m^{-2} s^{-1})	6	12.5	0	<0.001
Amax.n (µmol CO_2 m^{-2} s^{-1})	5.4	9.7	96	<0.001
ϕCO2 (µmol CO_2 m^{-2} s^{-1}/I_A)	0.006	0.01	296	<0.001
ϕPSII (F_q'/F_m')	0.15	0.29	130.5	<0.001
Cond. (mol H_2O m^{-2} s^{-1})	0.11	0.16	755	<0.001
VP Deficit-leaf (kPa)	1.8	2.8	150	<0.001
Transpiration (mmol H_2O m^{-2} s^{-1})	2.0	4.0	228	<0.001
Leaf temperature (C)	26.8	35.5	0	<0.001
Chlorophyll [SPAD(µg ml^{-1})]	34.2(17.7)	33.4(17.0)		

Mann Whitney Rank Sum, P-values below 0.05 were significantly different.
n = 54.
Note: Values represent light saturated means of measurements across all species.

Point of growing season analysis

Significant differences were detected between early, mid, and late growing season for every light saturated photosynthesis parameter in the 55 percent mean sunlight harvest treatment (Table 6.2). Individual means tests (Dunn's method) detected significant differences in points of growing season for all light saturated photosynthesis parameters in year 3 post-harvest. Significant differences were detected between early versus mid-season, and mid-season versus late season averages for $A_{max.g}$, $A_{max.n}$, ΦCO_2, ΦPSII, stomatal conductance, and chlorophyll index. No differences were detected in these parameters between early and late growing season averages. Significant differences were observed between all growing season points for vapor pressure deficit and leaf temperature. Furthermore, significant differences were observed between early versus mid-season and early versus late season for transpiration rate averages. Mid-season versus late season was determined to be similar for transpiration rate average.

Table 6.2. Points of growing season analysis of light saturated photosynthesis parameters in harvested treatments during year 3 post-harvest conditions.

	Early	Middle	Late	P-value
Amax.g (μmol CO_2 m^{-2} s^{-1} + R_d)	12.5 a	2.14 b	10.9 a	<0.001
Amax.n (μmol CO_2 m^{-2} s^{-1})	9.7 a	0.36 b	9.8 a	<0.001
ϕCO2 (Amax.g /I_A)	0.01 a	0.002 b	0.01 a	<0.001
ϕPSII (F_q'/F_m')	0.29 a	0.12 b	0.26 a	<0.001
Cond. (mol H_2O m^{-2} s^{-1})	0.16 a	0.02 b	0.19 a	<0.001
VP Deficit-leaf (kPa)	2.8 a	6.56 b	1.41 c	<0.001
Transpiration (mmol H_2O m^{-2} s^{-1})	4.0 a	2.0 b	2.0 b	<0.001
Leaf temperature(C)	35.5 a	44.3 b	27.5 a	<0.001
Chlorophyll [SPAD(μg ml^{-1})]	33.4 (17.0) a	32.4 (16.4)	31.5(15.5)	0.003

Kruskal Wallace Rank Sum. P-values below 0.05 were significantly different. n = 54. Means followed by the same letter do not significantly differ (Dunn's method, α = 0.05)

Table 6.3. illustrates non-light saturated photosynthesis parameters by species and point of growing season. Photosynthetic quantum yield (ΦCO_2) and bending degree (θ) represent fitted non-linear regression parameters for gross photosynthesis (Thornley et al. 1976 ,and Ogren and Evans 1993). Apparent quantum yield for CO_2 assimilation averaged 0.05 and 0.1 for early and late season respectively. Average curvature (θ) averaged 0.6 for early and late growing season. Curves could not be fit to mid-season data, since photosynthesis rates were at or below zero. Dark respiration was 2.8 in early season, 1.8 during mid-season, and 1.2 during late season measurements.

Table 6.3. Non-light saturated photosynthesis parameters by species and point of growing season.

	ϕCO_2			**θ**			**R_d**		
Species	**Early**	**Mid**	**Late**	**Early**	**Mid**	**Late**	**Early**	**Mid**	**Late**
Q.rubra	0.04	***	0.09	0.4	***	0.5	2.0	2.6	2.0
Q.velutina	0.04	***	0.09	0.4	***	0.6	3.1	1.7	0.4
Q.alba	0.05	***	0.07	0.6	***	0.9	2.4	2.2	0.1
A.rubrum	0.07	***	0.10	0.8	***	0.6	3.5	1.7	0.6
U.alata	0.06	***	0.11	0.8	***	0.4	1.8	1.7	1.8
P.serotina	0.06	***	0.12	0.8	***	0.5	4.0	1.1	2.0
Average	*0.05*	***	*0.10*	*0.6*	***	*0.6*	*2.8*	*1.8*	*1.2*
Std. dev.	*0.01*	***	*0.01*	*0.2*	***	*0.2*	*0.8*	*0.5*	*0.9*

Figure 6.3 illustrates light curves for the Shade plot in early season by species. Light saturation was determined as 90 percent of net assimilation at 2000 μmol m^{-2} s^{-1}. Mean $PPFD_{sat}$ for samples of *Quercus* species combined was 325 μmol m^{-2} s^{-1}. Mean $PPFD_{sat}$ values for *Q. rubra, Q. velutina,* and *Q. alba* were 250, 300, and 400 μmol m^{-2} s^{-1}, respectively. $PPFD_{sat}$ values for *A. rubrum*, *U. alata*, and *P. serotina* were 450, 350, and 150 μmol m^{-2} s^{-1}, respectively. $A_{max.n}$ values for *Q. rubra, Q. velutina,* and *Q. alba* were 6.2, 4.5, and 3.9 μmol CO_2 m^{-2} s^{-1}. $A_{max.n}$ values for *A. rubrum*, *U. alata*, and *P. serotina* were 6.6, 4.5, and 3.5 μmol CO_2 m^{-2} s^{-1}.

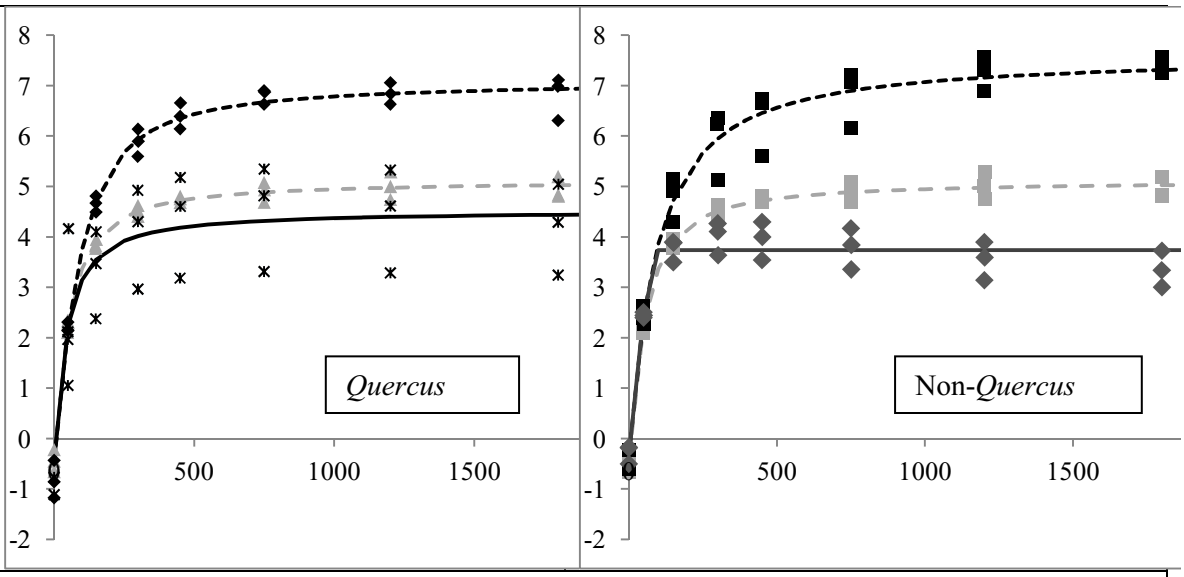

Figure 6.3. Shade light curves for *Quercus* and non-*Quercus* species.

Figure 6.4 illustrates light curves for the Sun plot during early, mid, and late points of growing season by species. In early season, mean $PPFD_{sat}$ values for *Q. rubra, Q. velutina,* and *Q. alba* were 900, 800, and 550 µmol m^{-2} s^{-1}, respectively. $PPFD_{sat}$ values for *A. rubrum*, *U. alata*, and *P. serotina* were 325, 450, and 550 µmol m^{-2} s^{-1}, respectively. $A_{max.n}$ values for *Q. rubra, Q. velutina,* and *Q. alba* were 9.0, 9.9, and 8.9 µmol CO_2 m^{-2} s^{-1}. $A_{max.n}$ values for *A. rubrum*, *U. alata*, and *P. serotina* were 6.3, 10.5, and 9.0 µmol CO_2 m^{-2} s^{-1}.

In mid-season, mean $PPFD_{sat}$ values for *Q. rubra, Q. velutina,* and *Q. alba* were less than 100 µmol m^{-2} s^{-1}. $PPFD_{sat}$ values for *A. rubrum*, *U. alata*, and *P. serotina* were also less than 100 µmol m^{-2} s^{-1}. $A_{max.n}$ values for *Quercus Spp.* were 0.1 µmol CO_2 m^{-2} s^{-1}. $A_{max.n}$ values for *A. rubrum*, *U. alata*, and *P. serotina* were -1.0, 1.0, and 0.5 µmol CO_2 m^{-2} s^{-1}.

In late-season, mean $PPFD_{sat}$ values for *Q. rubra, Q. velutina,* and *Q. alba* were 375, 375, 200, µmol m^{-2} s^{-1}. $PPFD_{sat}$ values for *A. rubrum*, *U. alata*, and *P. serotina* were 350, 550, and 500 µmol m^{-2} s^{-1}. $A_{max.n}$ values for *Quercus Spp.* were 5.5, 9.3, and 8.2 µmol CO_2 m^{-2} s^{-1}. $A_{max.n}$ values for *A. rubrum*, *U. alata*, and *P. serotina* were 8.9, 9.8, and 11.8 µmol CO_2 m^{-2} s^{-1}.

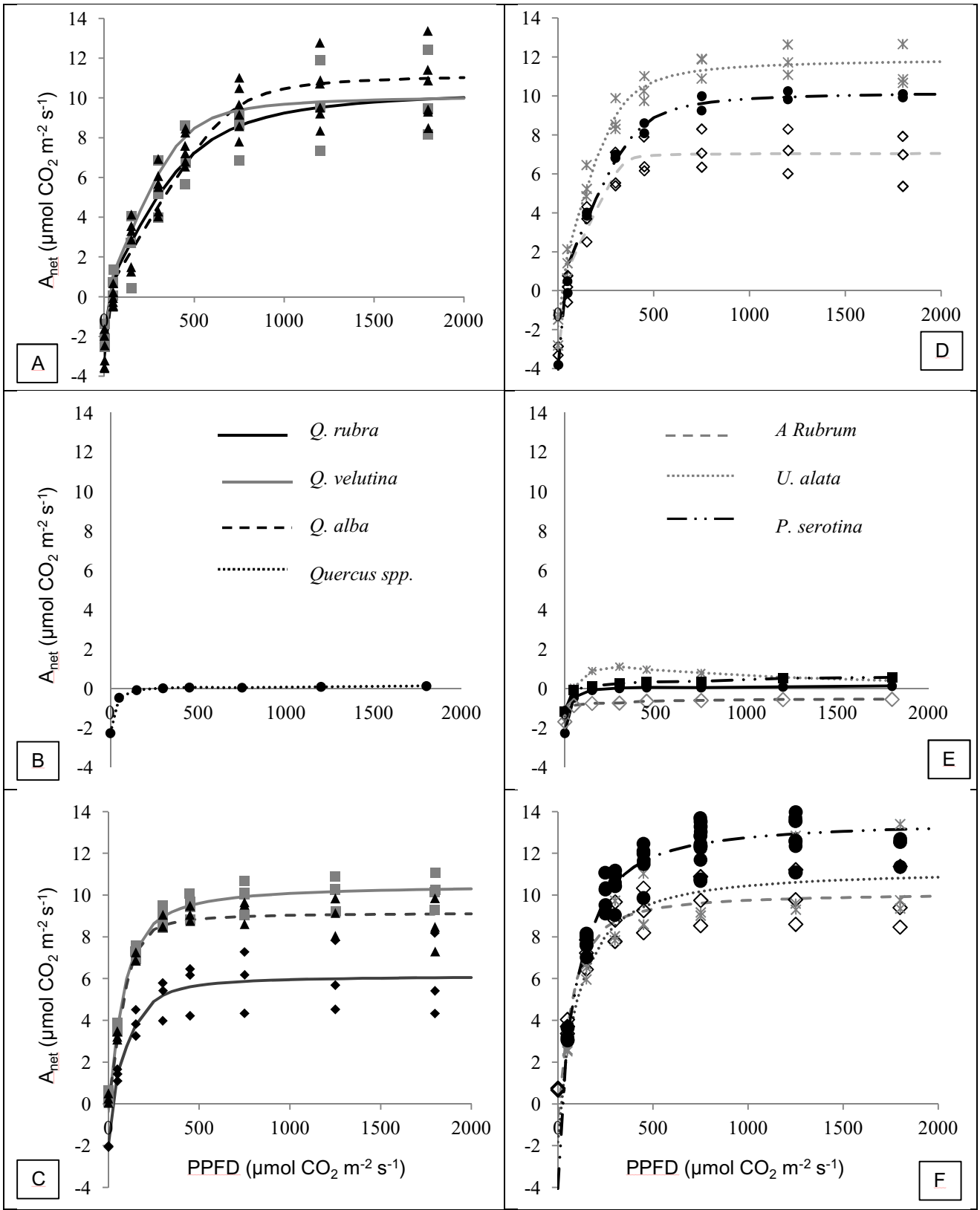

Figure 6.4. Net assimillation rate light curves for early (A,D), mid (B,E), and late (C,F) for *Quercus* (A, B, and C)and non-*Quercus* species (D, E, and F).

Discussion

Differences were evident between Sun and Shade samples for all photosynthesis parameters. Both gross and net maximum photosynthesis rates for Sun samples were two times that of Shade samples. Dark respiration rates were seven times higher in Sun samples versus Shade samples. Effective quantum yields for photosynthesis rate and electron transfer were double in Sun versus Shade samples. Stomatal conductance and transpiration rates were also appreciably higher in Sun versus Shade samples. Vapor pressure deficit (leaf) was significantly higher in Sun samples. A primary factor in generating these differences was leaf temperature. Leaf temperatures were approximately seven degrees (C) higher in Sun samples than in Shade samples (Table 6.1). As one would expect, the higher leaf temperature, conductance, transpiration rate, and other photosynthesis parameters resulted in appreciably different overall physiological activity and development of Sun samples versus Shade samples (Figure 6.3 and Figure 6.4).

Specific leaf area (SLA) was an additional physiological parameter was measured to supplement the results. SLA values were representative of expected results for corresponding available sunlight conditions (Figure 6.5). *Q. rubra* and *Q. velutina* (red oaks) exhibited the greatest differences between irradiance levels (Figure 6.6). The appreciable difference in SLA between treatments for the red oaks potentially illustrates the inability of the red oak group to grow well in low light conditions and the potential positive growth response in adequate to optimal sunlight conditions. Sun sample seedlings averaged 0.8 m height growth from year 1 to year 3 following overstory release. The Shade sample seedlings had essentially no growth over the same time period.

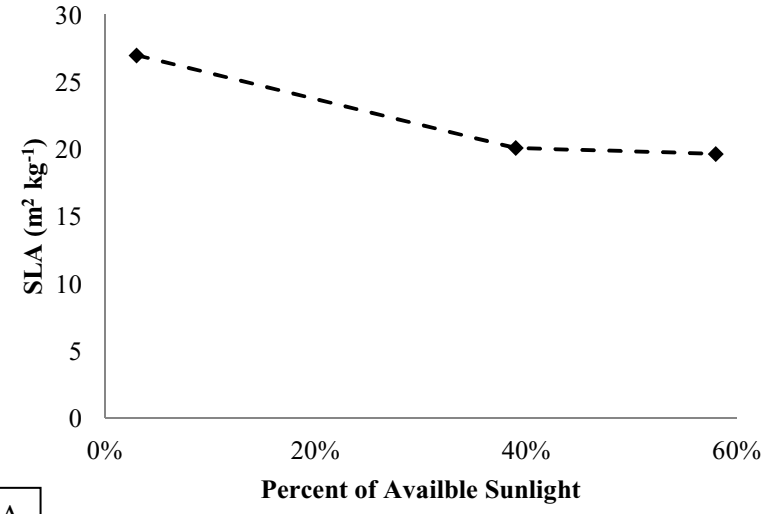

A

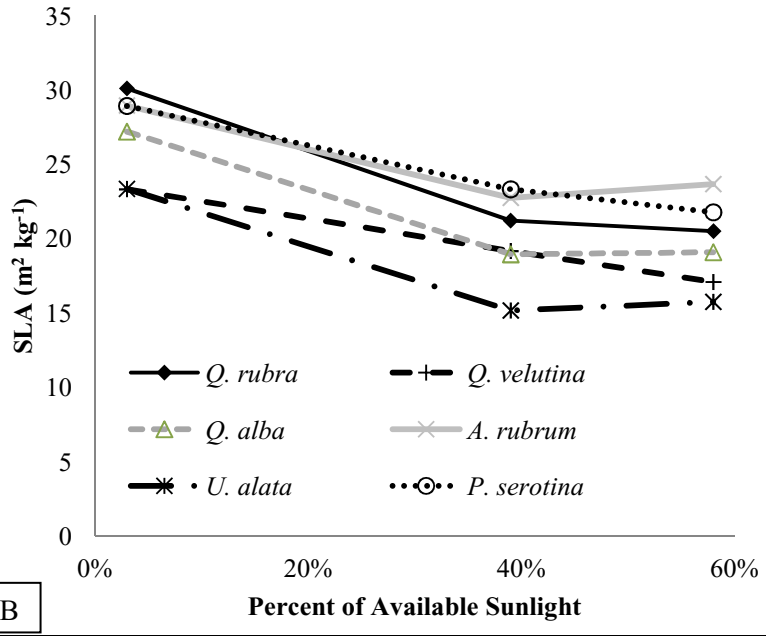

B

Figure 6.5. Mean specific leaf area (SLA) for all sample species combined in June 2011 (±1SE). The SLA values for 3 percent, 39 percent, and 55 percent total sunlight.

Nine samples were collected per species for each sunlight environment, each were dried and weighed.

A analysis of light saturated photosynthesis parameters provided insight into differences between points of growing season for hardwood reproduction. Significant differences were observed between points of growing season for all parameters. Maximum net assimilation rates observed were normal in early season around 10 μmol CO_2 m^{-2} s^{-1}. By mid-season, net assimilation rates were near zero and significantly different from both the pre-drought early season observations and the post drought, recovery period late season measurements. By late season, net assimilation rates had returned to early season levels. The return to normal levels coincided with a return of moisture availability, evident in vapor pressure deficits, and cooler leaf temperatures.

Both ΦCO_2 and ΦPSII followed similar patterns through the growing season. These parallels in assimilation rate and electron transfer suggested both the light reactions and dark reactions were similarly impacted by the drought conditions. Chlorophyll levels were significantly different between points of growing season. However, biologically, little impact would be expected from changes in chlorophyll levels due to the relatively small variations in mean SPAD indices between points.

Figure 6.6 illustrates species level values for early, mid, and late points of the growing season. Species level differences in photosynthesis rate were similar by point of growing season. The impact of stressing factors on sample seedlings was obvious for all species. Net photosynthesis rates in mid-season were near zero or negative for all species and were significantly lower for all species compared to early and late season values. *Q. alba* did exhibit the highest mid-season net photosynthesis rate.

Vapor pressure deficits in the early measurements were similar for all species ranging from 2.4 kPa (*U. alata*) to 3.2 kPa (*P. serotina*). Vapor pressure deficits in mid-season exhibited the stress of environmental conditions on all species. Vapor pressure deficit ranged from 5.4 kPa (*Q. rubra*) to 7.4 kPa (*A. rubrum*) in mid-season measurements. In late season measurements, vapor pressure deficits were low to normal ranging from 0.89 kPa for *A. rubrum* to 3.1 kPa for *Q.*

rubra. Early season measurements were within a normal range, mid-season measurements were high, late season measurements were back to more normal numbers for hardwood reproduction (Xu and Baldocchi 2003 and Hinkley et al. 1978).

Observation of conductance, transpiration, and ΦCO_2 at non-saturated light levels displayed trends between *Quercus* and non-*Quercus* species. *Non-Quercus* ΦCO_2 values were above the mean value for all species combined, while ΦCO_2 values for all Quercus species were below the mean for all species combined. The lower effective quantum yields were likely due to conductance and transpiration yielded by *Quercus* species (Figure 6.6). The higher quantum yield of non-*Quercus* species in both low and high sunlight conditions makes them strong competitors to *Quercus* species from a photosynthesis physiological standpoint.

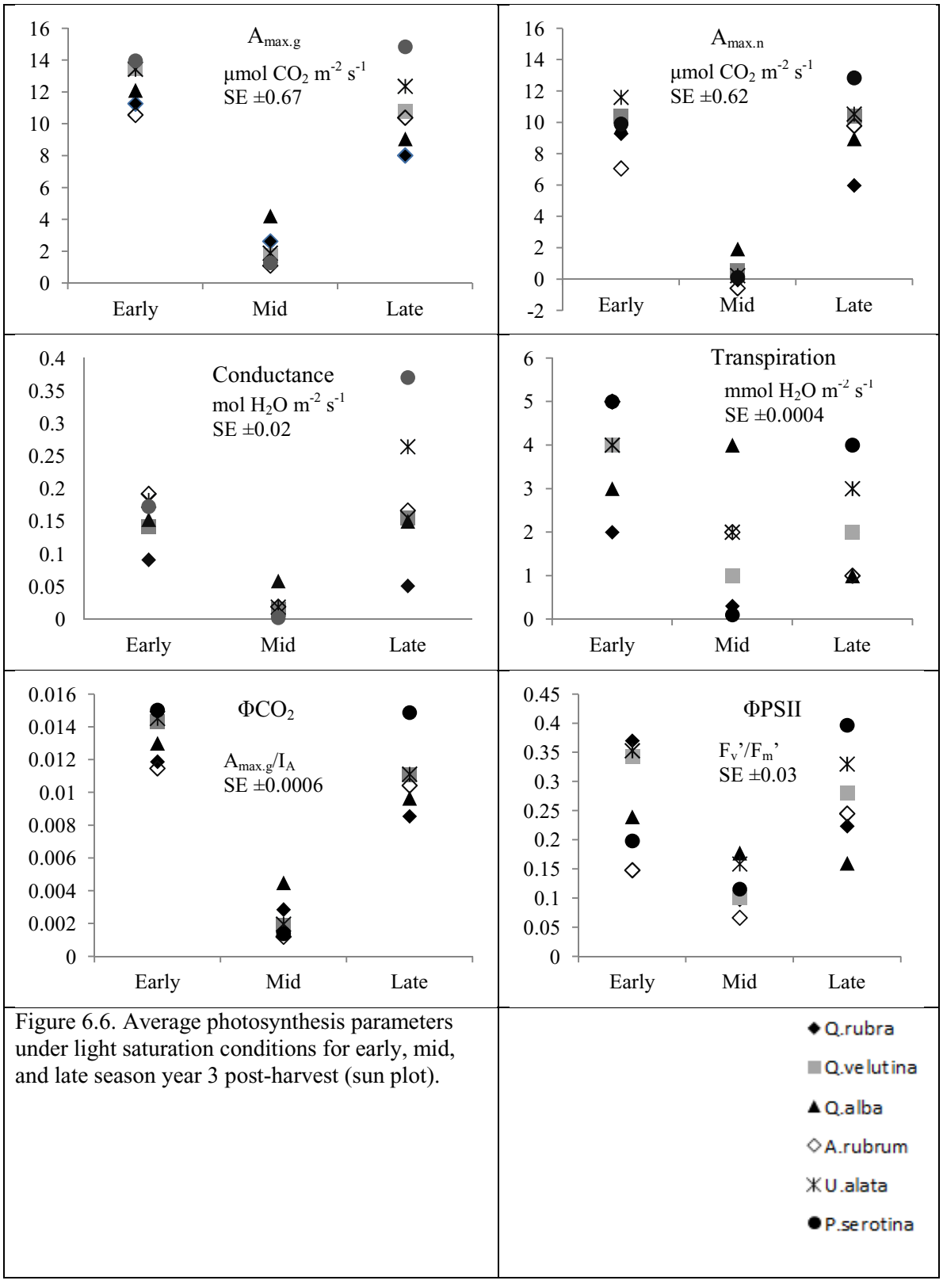

Figure 6.6. Average photosynthesis parameters under light saturation conditions for early, mid, and late season year 3 post-harvest (sun plot).

Conclusions

The six hardwood species observed in this study demonstrated the differences between sun and shade adaptation of advanced reproduction. Sunlight light levels in shaded conditions yielded photosynthesis parameters half the magnitude of sun adapted reproduction samples. The similar patterns of response in photosynthesis parameters to environmental conditions illustrated ecological filtering that has taken place over thousands of years in the upland hardwood region. *Quercus rubra* and *Acer rubrum* exhibited a lower level of photosynthesis physiological activity versus the other species observed across the growing season. This observation could lead one to believe they were less adapted to the study site environment than the other species observed.

Drought conditions had profound effects on photosynthesis physiology for all species observed. All photosynthesis related parameters were significantly impacted by the stressed conditions. However, each species demonstrated an ability to recover following a return to less stressful environmental conditions.

Non-*Quercus* species exhibited higher effective quantum yields than did *Quercus* species in both light saturated and non-light saturated environments. Therefore, non-*Quercus* species remain strong competitors in both high and low sunlight environments. The sun adapted *Quercus* samples in this study had adjusted to increased sunlight conditions for two growing seasons prior to measurement. Thus, discrepancies between the species groups may have been at a greater magnitude in years one and two following release.

Literature Cited

Chambers, J. L., Hinckley, T. M., Cox, G. S., Metcalf, C. L., & Aslin, R. G. (1985). Boundary-line analysis and models of leaf conductance for four oak-hickory forest species. *Forest Science*, *31*(2), 437-450.

Curtis, P.S. (1996) A Meta-analysis of Leaf Gas Exchange and Nitrogen in Trees Grown Under Elevated Carbon Dioxide. *Plant, Cell and Environment* 19, 127 -137.

Gardiner, E. S., & Krauss, K. W. (2001). Photosynthetic light response of flooded cherrybark oak (Quercus pagoda) seedlings grown in two light regimes. *Tree physiology*, *21*(15), 1103-1111.

Hamilton J.G., DeLucia,E.H., George, K., Naidu, S.L., Finzi, A.C., and Schlesinger W.H. (2002). Forest carbon balance under elevated CO_2. *Oecologia*. 131 (2), 250-260.

Hinckley, T.M., Aslin, R.G., Aubuchon, R.R., Metcalf, C.L., and J.E. Roberts. 1978. Leaf conductance and photosynthesis in four species of the oak-hickory forest type. *Forest Science* 24(1):73-82.

Lockhart, B.R., and J.D. Hodges, J.D. (1994) Comparitive gas-exchange in leaves of intact and clipped, natural and planted cherrybark oak (Quercus pagoda Raf.) seedlings. Proceedings of the Arkansas Academy of Science, Vol. 48.

Long, S. P., Farage, P. K., & Garcia, R. L. (1996). Measurement of leaf and canopy photosynthetic CO2 exchange in the field. *Journal of Experimental Botany*, *47*(11), 1629-1642.

Nilsen, E. T., Lei, T. T., & Semones, S. W. (2009). Presence of understory shrubs constrains carbon cain in sunflecks by Advance-Regeneration Seedlings: Evidence from *Quercus rubra* Seedlings Growing in Understory Forest Patches with or without Evergreen Shrubs Present. *International Journal of Plant Sciences*, *170*(6), 735-747.

Ogaya, R., & Peñuelas, J. (2003). Comparative field study of *Quercus ilex* and *Phillyrea latifolia:* photosynthetic response to experimental drought conditions. *Environmental and Experimental Botany*, *50*(2), 137-148.

Ögren, E., & Evans, J. R. (1993). Photosynthetic light-response curves. *Planta*,*189*(2), 182-190.

Phelps, J. E., Chambers, J., & Hinckley, T. M. (1976). Some morphological, ecological and physiological traits of four Ozark forest species. *In* Proc. First Central Hardwood Forest Conference. Eds. JS Fralish, GT Weaver and RC Schlesinger. South Illinois Univ., Carbondale 231-243.

Sestak, Z., Catský, J., & Jarvis, P. G. (1971). Plant photosynthetic production. Manual of methods. *Plant photosynthetic production. Manual of methods.*

Thornley, JHM. 1976. Mathematical models in plant physiology. Academic Press: New York

Von Caemmerer, S. and G.D. Farquhar. 1981. Some relationships between the biochemistry of photosynthesis and the gas exchange of leaves. *Planta* 153:376-387.

Xu, Liukang and D.D. Baldocchi. 2003. Seasonal trends in photosynthetic parameters and stomatal conductance of blue oak (Quercus douglassii) under prolonged summer drought and high temperature. *Tree Physiology* 23:865-877.

CHAPTER VII – CHLOROPHYLL FLUORESCENCE ANALYSIS

Abstract

Chlorophyll fluorescence (CF) was used to evaluate the photosynthetic response of advanced reproduction to varying sunlight conditions following a partial harvest in an upland hardwood stand. CF samples were taken from three Quercus species and three non-*Quercus competitors. Stand level treatments were post-harvest residual basal area 11.6 m^2 h^{-1} (BA11), BA11 plus midstory control (BA11+MR), and non-harvest control (NHC). Treatment analyses were conducted on leaf level irradiance, quantum yield of PSII ($F_{q'}/F_{m'}$), and electron transfer rate (ETR). Average leaf level irradiances for all years by treatment were 423.4 (SE=70.0), 677.4 (SE = 101), and 137.1 (SE=35) µmol m^{-2} s^{-1} for BA11, BA11+MR, and NHC, respectively. Average $F_{q'}/F_{m'}$ values were 0.581 (SE=0.042), 0.495 (SE=0.051), and 0.691 (SE=0.018) for BA11, BA11+MR, and NHC, respectively. Mean ETR values were 58 (SE= 14.1), 921.1 (SE= 20.1), and 23.1 (SE= 4.3) µmol m^{-2} s^{-1} for BA11, BA11+MR, and NHC, respectively. A one-way analysis of variance determined significant differences to exist ($P < 0.001$ for PPFD, ΦPSII, and ETR). SNK means separation determined all treatments to significantly differ for PPFD, ΦPSII, and ETR. At the species level, light response curves were established from ambient sunlight samples and sequential actinic lightsteps for dark adapted samples. Mid-season, ambient ETR_{max} of advanced reproduction adapted to two growing seasons of partial sun/partial shade ranged from 143.8 for Quercus rubra to 231.1 µmol m-2 s-1 for Ulmus alata. Year two ETR_{max} values were higher than mid-season, year one values for all species excluding Acer rubrum which was reduced in year 2. Year 3 light curve analyses provided insight into a season of drought stress conditions.*

Introduction

Chlorophyll fluorescence provides potentially valuable information on the status of PSII in a leaf. This assessment can provide insight into photosynthesis, nutrient availability, and plant stress levels. The development of miniaturized pulse amplitude modulation has allowed chlorophyll fluorescence measures to be obtained in the field and have become important components of ecophysiological plant research (Maxwell and Johnson 2000 and Bilger et al. 1995). These instruments, such as the MiniPAM 2000 (Walz, Inc., Germany), have made collecting non-destructive fluorescence sampling in the field possible.

Advances in instrumentation (e.g. Orgen and Baker, 1985; Schreiber et al. 1993, Schreiber, 1986; and Schreiber et al., 1986) and methodology (e.g. Bradbury and Baker, 1981; Krause et al., 1982; Bilger et al., 1989; and Genty, 1989) have linked basic and applied chlorophyll fluorescence ecophysiological research in recent decades (e.g. Kooten and Snel, 1990, and Maxwell and Johnson 2000). For field analysis, the Mini-PAM 2000 (Walz, Inc.) provides a rugged, non-destructive, portable instrument for obtaining chlorophyll fluorescence data *in situ*.

Chlorophyll fluorescence analysis has become one of the most powerful and widely used techniques available to plant physiologists and ecophysiologists (Maxwell and Johnson 2000). Perhaps the single greatest advantage of fluorescence is that it can be performed in the field using a portable chlorophyll fluoremeter. While chlorophyll fluorescence has been utilized extensively *in vivo* and in numerous plant physiological studies, it has been sparingly utilized in forest ecophysiology. The majority of forest ecophysiology studies have relied on gas exchange in leaves (Ball et al. 1994). There have been a limited number of studies in forest ecology and in urban forests (e.g., Epron et al. 1992 and Schindler and Lichtenthaler 1996). A need exists to explore methods for incorporating chlorophyll fluorescence into a forest ecophysiology context.

Study Objectives

- Generate varying sunlight levels for advanced reproduction analysis
- Evaluate response of PSII photochemistry to different sunlight conditions
    - Treatment level
    - Topographical position
    - Species level
    - Environmental conditions

Materials and Methods

Three treatments with four replicates were incorporated into a completely randomized design. Treatments included: 1. shelterwood harvest to BA 11 m^2/h (BA11), 2. shelterwood harvest to BA 11 m^2/h plus injection of non-oak stems between 2.5 and 12.7 cm DBH (BA11+MR) and 3. non-harvested control(NHC).

Advanced reproduction of six hardwood species were selected for chlorophyll fluorescence analysis of PSII: *Quercus rubra*, *Quercus velutina*, *Quercus alba*, *Acer rubrum*, *Ulmus alata,* and *Prunus serotina*. Sixteen individual seedlings from each treatment for *Quercus velutina*, *Quercus alba*, *Acer rubrum*, and *Ulmus alata* were selected. These four species occurred at every sampling location and provided equal representation of slope position and sample size. *Quercus rubra* and *Prunus serotina* did not occur at every sample point and are not included in treatment level analyses. They are included in species level results and discussion utilizing light curve parameters. Morphological data collected on these sample seedlings included: species, ground line diameter (GLD), height, and leaf area. Leaf level physiological data collected included: chlorophyll, specific leaf area, and chlorophyll fluorescence.

Chlorophyll fluorescence measurements were obtained using a Mini-PAM 2000 (WALZ, Inc.). Mini-PAM light readings were calibrated against an additional quantum light sensor (Delta OHM LP 471, □400 to 700 nm) for accuracy. Observations were taken at mid-day (10:30 – 15:30 hrs) under mostly clear to clear sky conditions during early, middle, and late growing season of 2010, 2011, and 2012 (year 1, 2, and 3 respectively). Open sky readings were taken prior to and after replicate light measurements were obtained. Open sky readingss were used to calculate percent of full sunlight values.

The instrument utilized initial and maximal fluorescence in the presence of ambient sunlight to determine apparent quantum yield ($F_{q'}/F_{m'}$), the most direct parameter provided by CF analysis (Formula 7.1). Utilizing $F_{q'}/F_{m'}$ and absorbed sunlight an electron transfer rate was calculated (Formula 7.2).

$$F_{q'}/F_{m'} = \frac{F_{m'} - F'}{F_{m'}} \qquad \text{Formula 7.1}$$

Where:

$F_{m'}$ = Maximum fluorescence under ambient light

F' = Minimal fluorescence under ambient light

Electron Transfer Rate or ETR is calculated using Formula 2, as recommended by Genty et al., 1989).

$$ETR = PPFD \times a \times 0.5 \times F_{q'}/F_{m'} \qquad \text{Formula 7.2}$$

Where:

ETR = Electron transfer rate

$F_{q'}/F_{m'}$ = Effective quantum yield

$PPFD$ = Photosynthetic Photon Flux Density

a = Constant for light utilization (0.84)

0.5 = Partitioning of absorbed light between PSII and PSI

All statistical analyses were performed in Sigma Plot 11.0. All data were tested for normality and equal variances. Two-way analyses of variance were performed for factors year and treatment. When necessary, non-parametric methods were utilized, using a Kruskal-Wallace analysis of variance on ranks and means separation using a SNK on ranks. All statistical tests were performed at the alpha 0.05 level.

Results

Figure 7.1A illustrates the maximal effective quantum yield ($F_{q'}/F_{m'}$) by point of growing season and year for all species combined. Figure 7.1B illustrates the maximal effective quantum yield ($F_{q'}/F_{m'}$) by point of growing season and year for each species. The highest ETR_{max} values were obtained in mid-season year 2 (ETR_{max} = 185.8 μmol m^{-2} s^{-1}). The lowest ETR_{max} values obtained in fall of year 1 post treatment (ETR_{max} = 74.5 μmol m^{-2} s^{-1}).

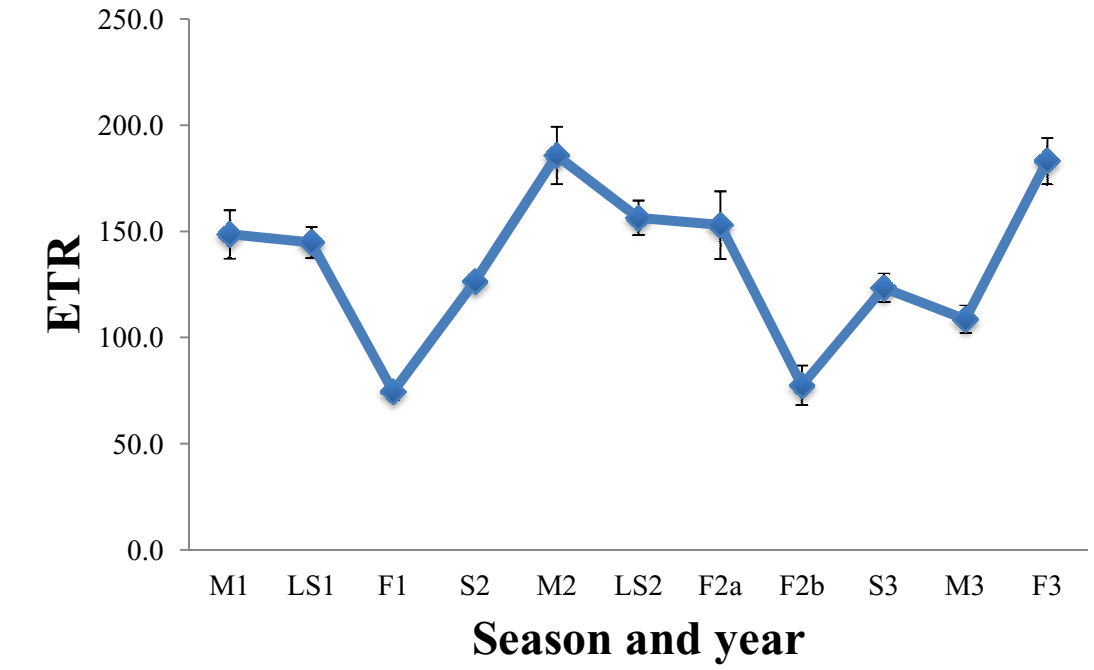

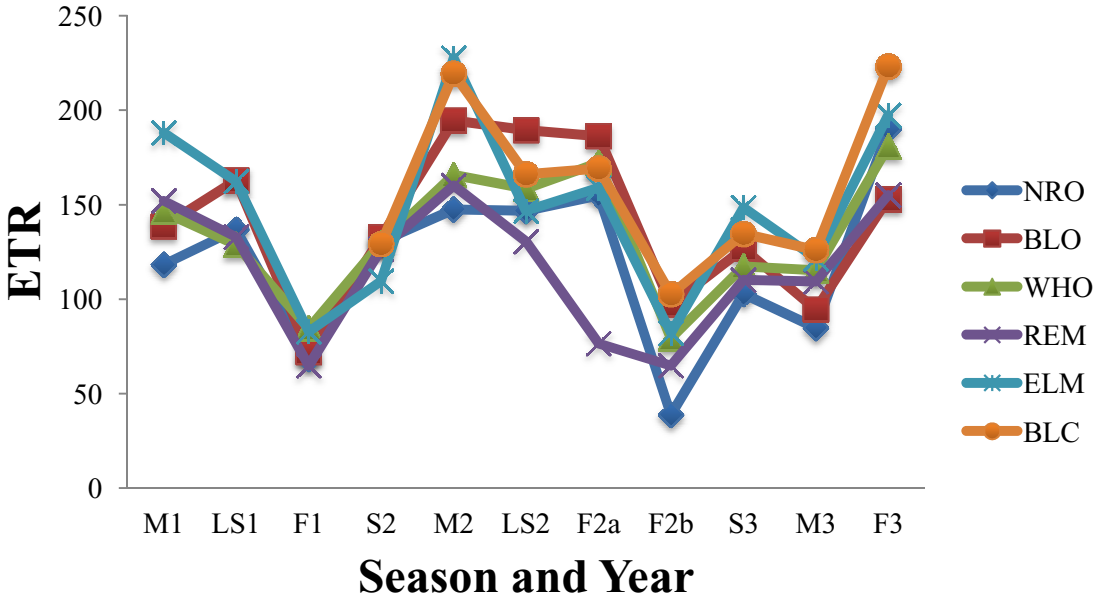

Figure 7.1. A) Mean seasonal ETR_{max} for all species by point of growing season and year. B) Seasonal ETR_{max} by point of growing season and year by species.

Data are from BA11 and BA11+MR pooled.

Figure 7.2A illustrates the impact precipitation had on ETR_{max} values. In year 1, precipitation was above average in mid-season at 103 percent above average for the growing season. Precipitation declined during late summer and early fall with cumulative growing season precipitation dipping to 32 percent above average and 52 percent below average for late summer and fall year 1. ETR_{max} exhibited a similar pattern. In year 2, cumulative growing season precipitation was above average for the entire growing season. Cumulative precipitation during spring was well above average (276 percent) and remained above average for the entire growing season. Year 2 exhibited the highest mid-season ETR_{max} values of any year measured with a mean of 185.8 µmol m^{-2} s^{-1}. Growing season cumulative precipitation was well below average for all points of the growing season in year 3. Cumulative growing season precipitation was 148, 208, and 134 percent below average for early, middle and late season measurement periods. Mid-season ETRmax values were the lowest in year 3 with a mean of 108.5 µmol m^{-2} s^{-1}.

Figure 7.2B illustrates the impact leaf temperature had on ETR_{max}. Similar patterns in leaf temperatures and ETR_{max} were observed. However, year 3 mid-season measurements exhibited a negative impact of leaf temperature paired with corresponding ETR_{max} values. Mid-season mean maximum daily leaf temperature was 36.2° C and ETR_{max} was 108.5 µmol m^{-2} s^{-1}. Year 3 fall average maximum daily temperature was 28.0 and the corresponding mean ETR_{max} was 183.2 µmol m^{-2} s^{-1}.

Figure 7.2C illustrates the interacting impact of leaf temperature and precipitation on ETR_{max} values. A leaf temperature and precipitation index (LTPI) was calculated using cummalitive depature from normal rainfall (± percent difference) for the growing season and mean maximum daily temperature for each month, scaled between -1 and +1. LPTI was highest in year 2 and lowest in year 3. Mid-season year 2 exhibited the highest LPTI and ETR_{max} (0.68 and 185.8 µmol m^{-2} s^{-1}). Mid-season year 3 exhibited the lowest LPTI and ETRmax (-0.75 and 108.5 µmol m^{-2} s^{-1}). LPTIs were near zero in year 1, strongly positive in year 2, and strongly negative in year 3. The corresponding ETRmax values illustrate the impacts of

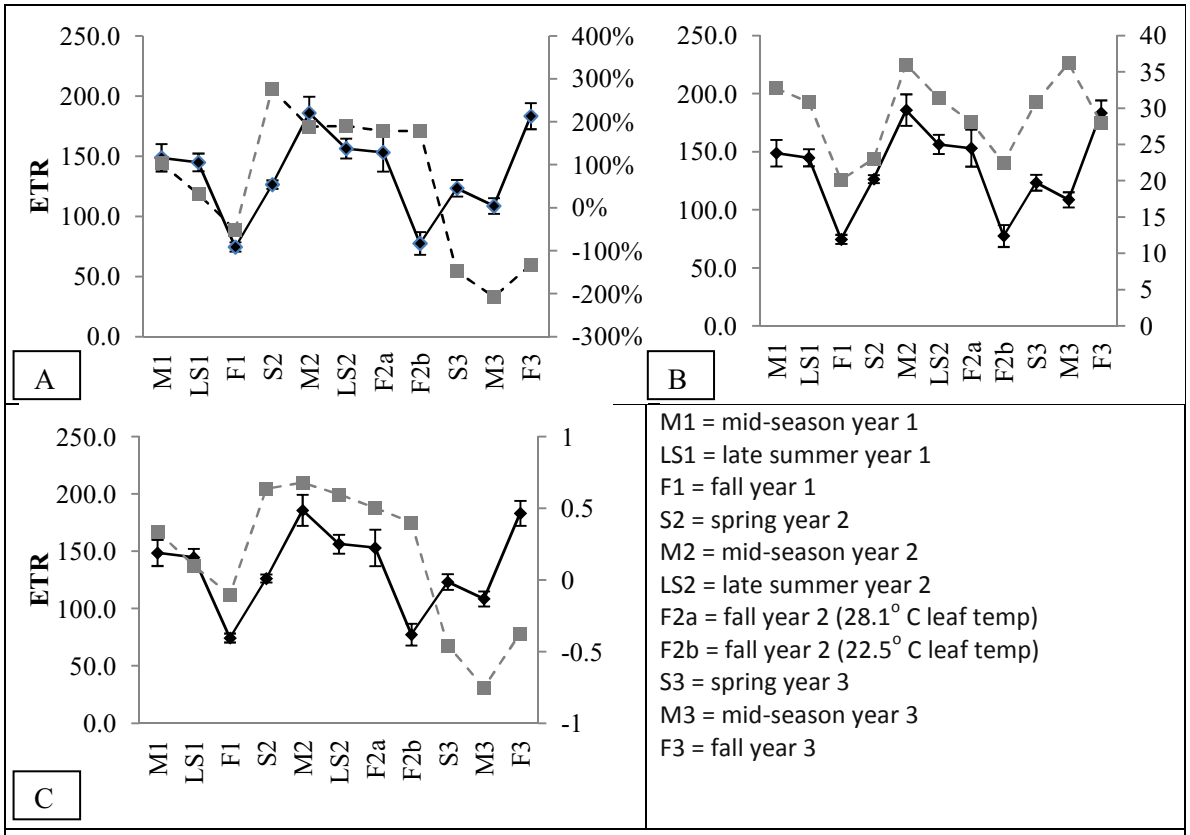

Figure 7.2 A) ETR_{max} and cumulative growing season rainfall percent departure from average versus point of growing season and year. B) ETR_{max} and average leaf temperature versus point of growing season and year. C) Leaf temp and precipitation index (LTPI) versus point of growing season and year (LTPI = LT x CP/100).

Mid-season Treatment Analysis by Year

SPAD chlorophyll measurements were similar for treatments across years. Figure 7.3A, B, and C illustrate SPAD chlorophyll ratings for each treatment year 1 through 3 post-harvest. Mean SPAD indices were 27.8, 28.7, and 34.4 for BA11, BA11+MR, and NHC in mid-season year 1. Mean SPAD indices were 31.3, 31.6, and 34.1 for BA11, BA11+MR, and NHC in mid-season year 2. Mean SPAD indices were 29.1, 29.9, and 34.2 for BA11, BA11+MR, and NHC in mid-season year 3. A one-way analysis of variance determined significant differences ($p = 0.002$, 0.012, 0.010) for all years. SNK means procedures detected significant differences between BA11 and BA11 + MR versus NHC for all three years.

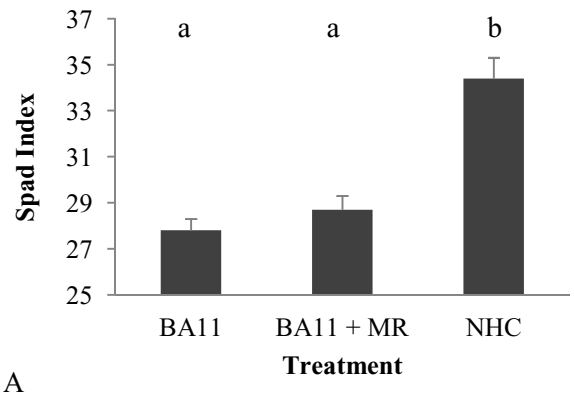

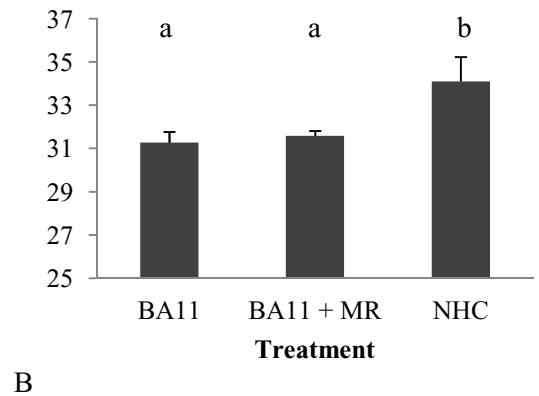

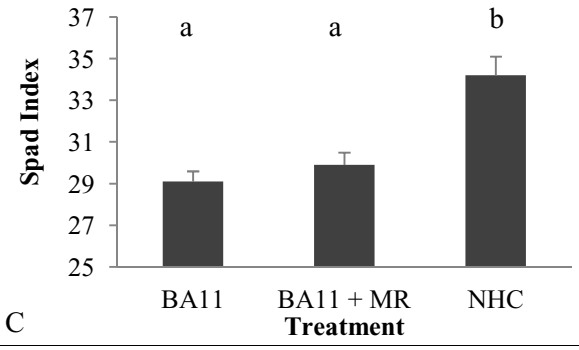

	Year 1	Year 2	Year3
BA11	12.8	15.3	13.7
BA11 + MR	13.4	15.5	14.2
NHC	17.9	17.7	17.8

D

Figure 7.3 SPAD chlorophyll indices for years 1 – 3 post-treatment. Letters followed by the same letter do not significantly differ (SNK method). A) year 1, B) year 2, and C) year 3. D) Predicted actual total chlorophyll in g/cm^2 (fit to model in Appendix IV for total chlorophyll).

Figure 7.4A, 7.4B, and 7.4C illustrate statistical analyses for photosynthetic photon flux density (PPFD), $F_{q'}/F_{m'}$, and ETR by year across all treatments. Mean PPFD values ranged from 300.9 for year 1 to 490.4 for year 2. Analysis of variance determined significant differences to exist ($p = 0.04$). A SNK method detected a significant difference between year 1 and year 2 (Figure 7.3A). Mean $F_{q'}/F_{m'}$ values by year were 0.626, 0.597, and 0.551 for years 1 through 3, respectively. Analysis of variance determined significant differences existed ($p = 0.02$). A SNK method detected a significant difference between year 1 and year 3 (Figure 7.4B). Mean ETR values by year were 46.8, 77.4, and 49.7 µmol m^{-2} s^{-1}. Analysis of variance determined significant differences to exist ($p < 0.001$). A SNK method detected significant differences between year 2 versus years 1 and 3.

Mean leaf temperatures were 32.3^0, 34.1^0, and 35.9^0 C for years 1 through 3, respectively. Analysis of variance detected a significant difference between years ($p < 0.001$). A significant interaction was detected between treatment and year for leaf temperatures ($p < 0.001$). Results are presented by year within treatment to account for treatment by year interaction. Mean leaf temperatures for BA11 were 31.9^0, 34.8^0, and 36.3^0 C in years 1, 2 and 3, respectively. A SNK method detected significant differences between year 1 versus year 2 and 3. Mean leaf temperatures for BA11+MR were 33.4^0, 37.5^0, and 36.1^0 C in years 1, 2 and 3, respectively. A SNK method detected significant differences between year 1 versus year 2 and 3. Mean leaf temperatures for NHC were 31.8^0, 30.1^0, and 35.6^0 C in years 1, 2 and 3, respectively. A SNK method detected significant differences between year 3 versus year 1 and 2.

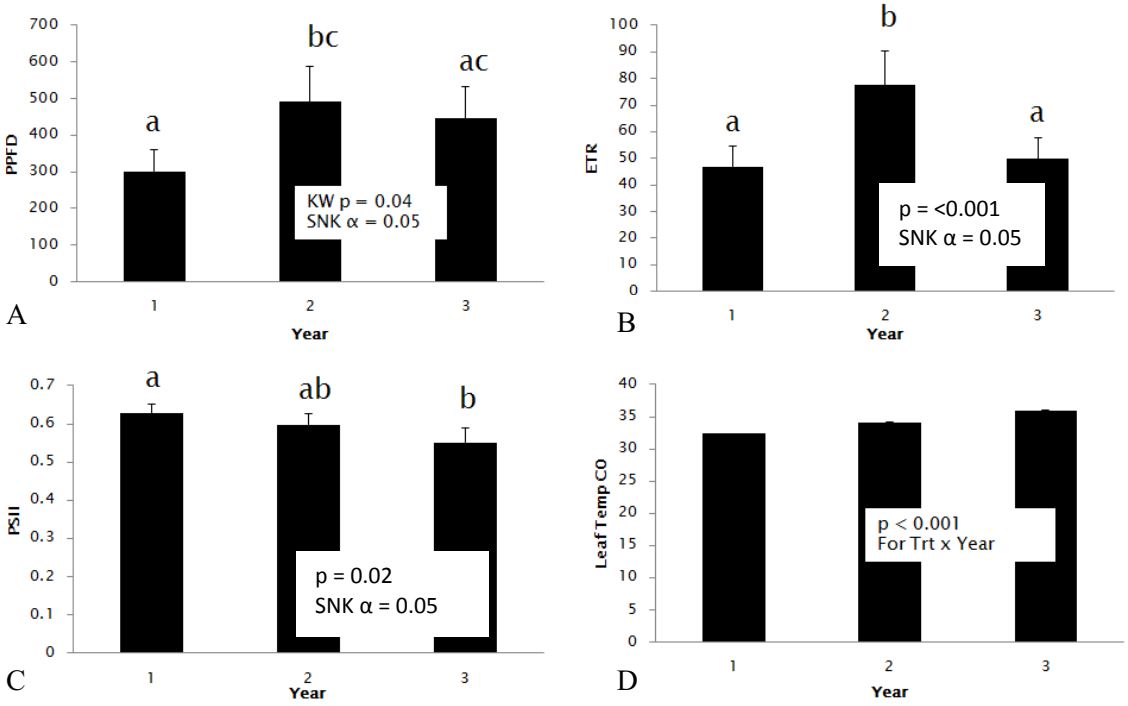

Figure 7.4. Year 1 through year 3 post treatment comparisons for A) PPFD, B) ETR, C) Fq'/Fm', and D) leaf temp. mean values.

Figure 7.5A, 7.5B, and 7.4D illustrate statistical analyses for photosynthetic photon flux density (PPFD), $F_{q'}/F_{m'}$, and ETR by treatment for all years. Mean PPFDs ranged from 137.1 for

NHC to 677.4 for BA11+MR. Analysis of variance detected a significant difference to exist ($p < 0.001$). A SNK method determined all three treatments to significantly differ. Mean $F_{q'}/F_{m'}$ values were 0.582, 0.495, and 0.698 for BA11, BA11+MR, and NHC, respectively. Analysis of variance procedure detected significant differences to exist ($P < 0.001$). A SNK method determined all treatments to significantly differ. Mean ETR values were 58.1, 92.1 and 49.7 $\mu mol\ m^{-2}\ s^{-1}$ for BA11, BA11+MR, and NHC, respectfully. An analysis of variance detected significant differences to exist ($p < 0.001$). A SNK method determined significant diffrences to exist between all treatments.

Three year average leaf temperatures were 34.3^0, 35.7^0 and 32.5^0 C for BA11, BA11+MR, and NHC, respectively. Analysis of variance detected a significant difference between treatments ($p < 0.001$). A significant interaction was detected between treatment and year for leaf temperatures ($p < 0.001$). Results are presented by treatment within year to account for treatment by year interaction. No significant differences were detected between treatments in year 1. A SNK method detected significant differences between all treatments within year 2. A SNK method detected no significant differences between treatments in year 3 mean leaf temperatures.

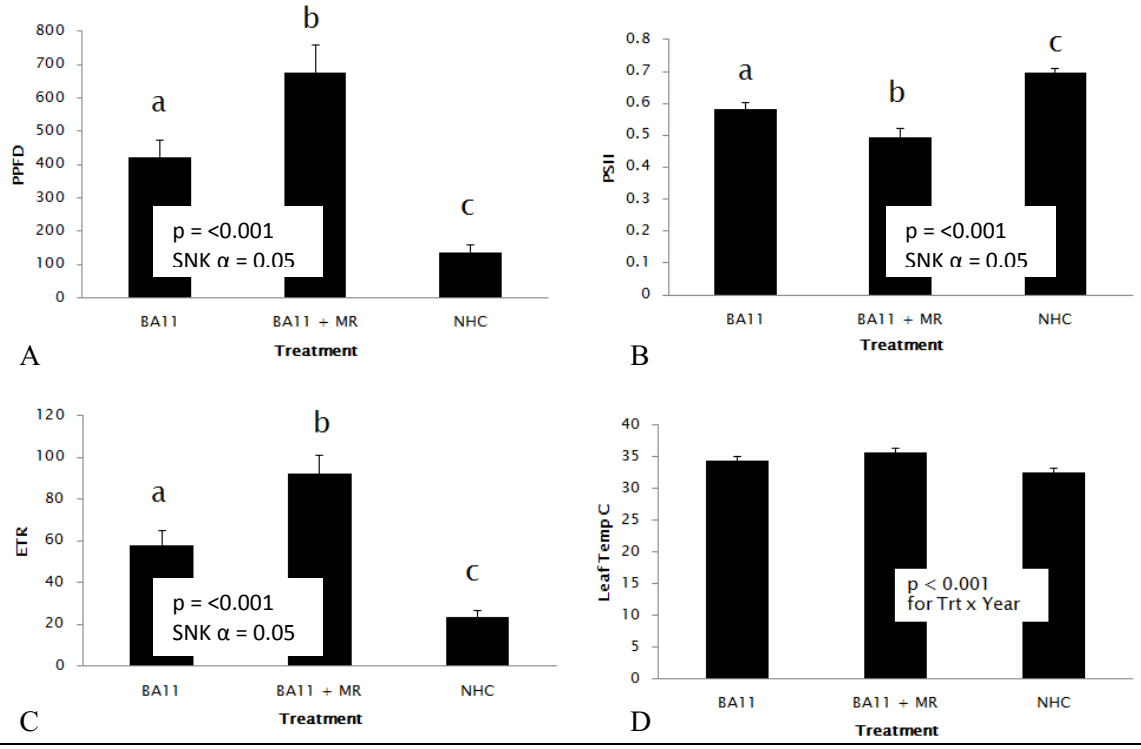

Figure 7.5. Mean three year treatment analysis for A) PPFD, B) $F_{q'}/F_{m'}$, C) ETR, and D) leaf temp.

Figure 7.6A and 7.6B illustrates an analysis of leaf temperature and PPFD by treatment and year. A one-way analysis of variance on ranks for year 1 detected significant differences between treatments ($p = 0.03$). A SNK method determined BA11+MR significantly differed from NHC. A one-way analysis of variance for year 2 detected significant differences to exist ($P < 0.001$). A SNK method determined significant differences existed all year 2 treatments for PPFD. A Kruskal-Wallace analysis of variance on ranks for year 3 detected no significant differences between treatments ($p = 0.78$).

A one-way analysis of variance for year 1 PPFD detected significant differences to exist ($P = 0.04$). A SNK on ranks method determined BA11+MR significantly differed from NHC. A Kruskal-Wallace analysis of variance on ranks for year 2 detected significant differences between treatments ($p = 0.003$). A SNK on ranks method determined BA11+MR significantly differed from NHC and BA11 significantly differed from NHC. One-way analysis of for year 3 detected

significant differences between treatments ($p < 0.001$). A SNK on ranks method determined all three treatments significantly differed.

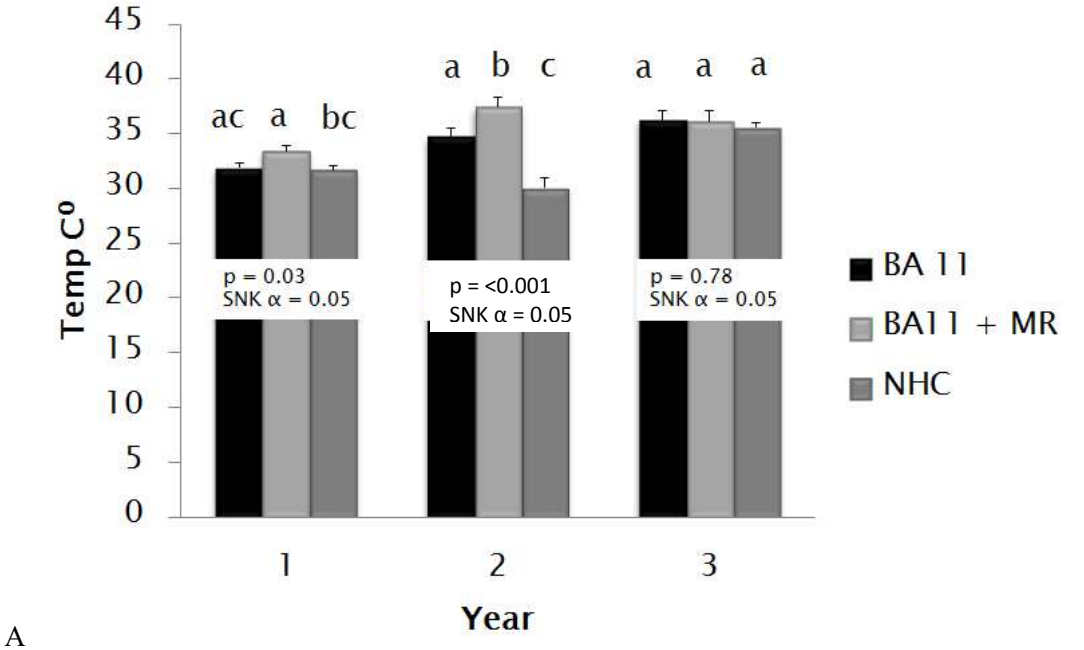

A

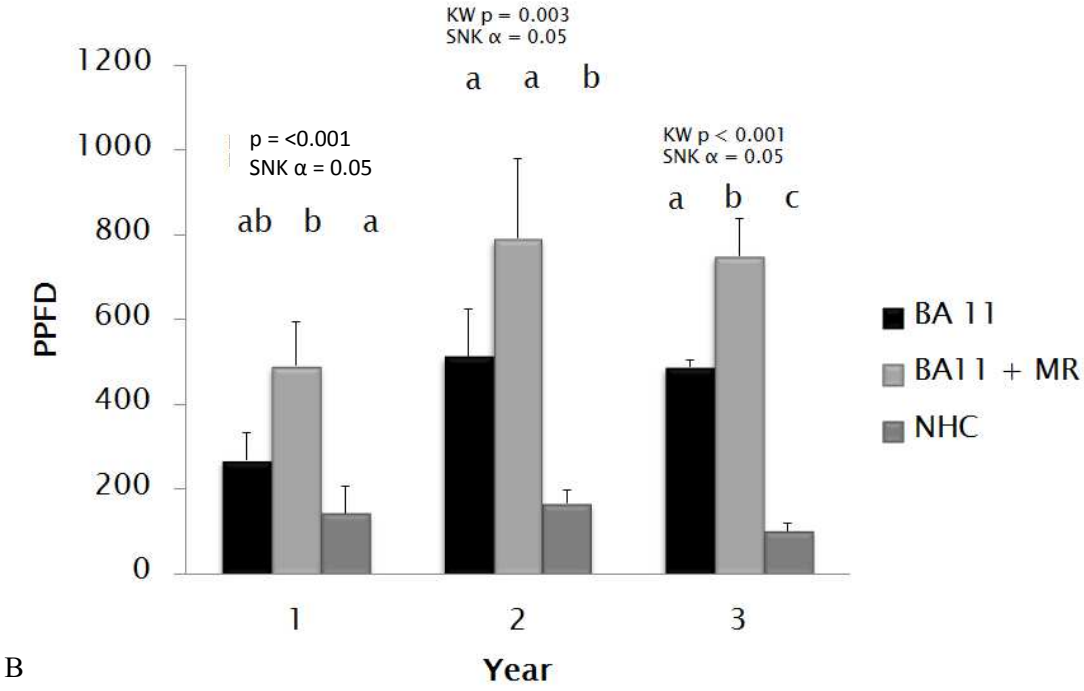

B

Figure 7.6. A) Leaf temperature by year and treatment. B) PPFD by year and treatment.

Figure 7.7A and 7.7B illustrates an analysis of $F_{q'}/F_{m'}$ and ETR by treatment and year. A one-way analysis of variance for year 1 detected significant differences between treatments for mean $F_{q'}/F_{m'}$ ($p = 0.02$). A SNK method determined BA11+MR significantly differed from NHC. A SNK on ranks method determined BA11+MR significantly differed from NHC. A one-way analysis of variance for year 2 detected significant differences between treatments ($p = 0.03$). A SNK on ranks method determined BA11+MR significantly differed from NHC. A One-way analysis of for year 3 detected significant differences between treatments ($p < 0.001$). A SNK on ranks method determined all three treatments significantly differed.

For ETR means, a one-way analysis of variance for year 1 ETR detected significant differences to exist ($P = 0.003$). A SNK method determined significant differences between BA11+MR versus BA11 and NHC. A one-way analysis of variance for year 2 detected significant differences to exist ($P < 0.001$). A SNK method determined significant differences for all year 2 treatments for ETR. A One-way analysis of variance for year 3 detected significant differences ($p < 0.001$). A SNK method determined all three treatments significantly differed.

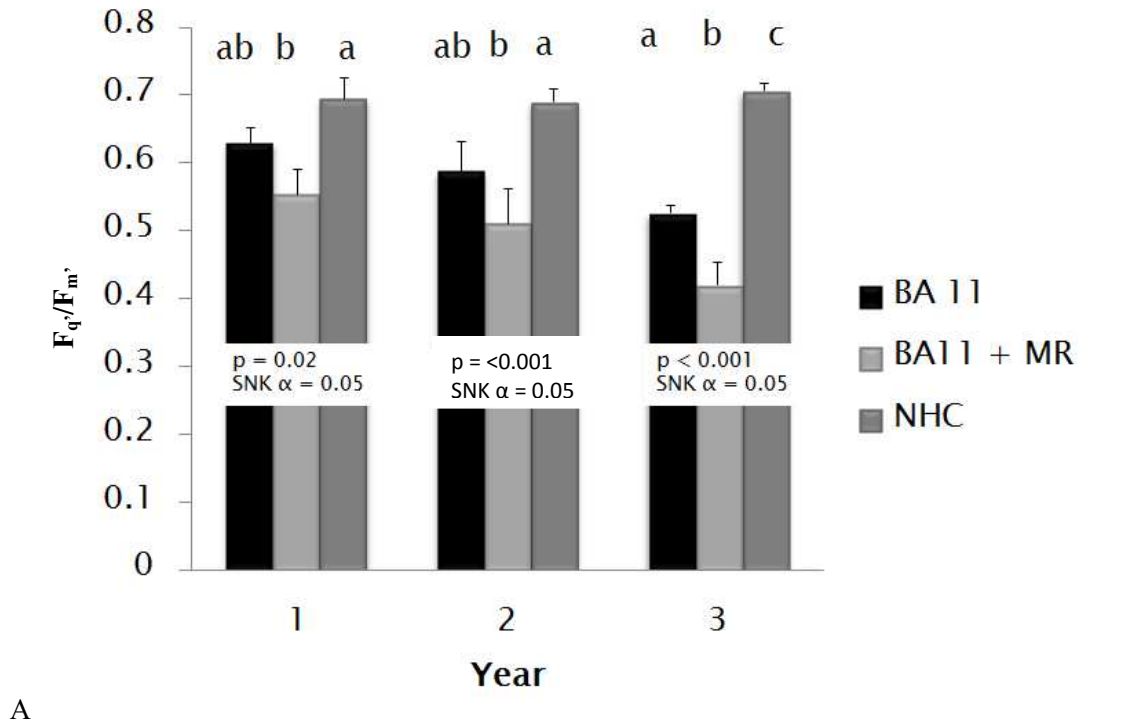

A

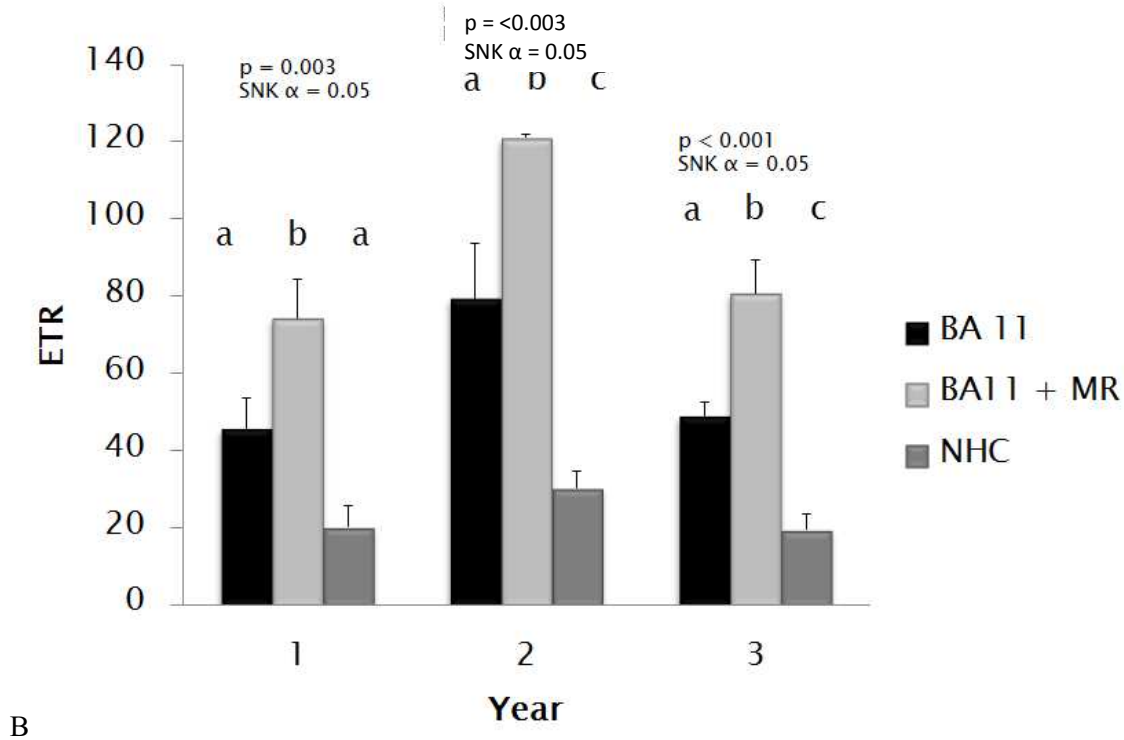

B

Figure 7.7. A) Mean F_q'/F_m' by year and treatment. B) Mean ETR by year and treatment.

Figure 7.8A illustrates average PPFD values for year 2 by treatment and slope position combinations. Mean leaf level PPFD ranged from 124.0 μmol m^{-2} s^{-1} for NHC lower slope to 882.1 μmol m^{-2} s^{-1} BA11+MR lower slope. A one-way analysis of variance detected significant differences between treatments by slope position combinations ($p = 0.004$). Pairwise multiple comparisons (SNK) determined differences existed between BA11+MR lower slope versus BA11 lower slope, NHC lower slope, and NHC upper slope. Also, differences were observed between NHC lower slope versus BA11 and BA11+MR upper slope positions.

Figure 7.8B illustrates average leaf temperatures (C) for year 2 by treatment and slope position combinations. Leaf temperatures ranged from 30.8^0 C in the NHC upper slope to 37.6^0 C in BA11+MR upper slope. A one-way analysis of variance detected significant differences to exist between treatments by slope combinations ($p < 0.001$). Pairwise multiple comparisons (SNK) determined BA11 upper slope, BA11+MR upper slope, and BA11+MR lower slope to be similar. Also, NHC upper slope, BA11 lower slope, and NHC lower slope were found to be similar.

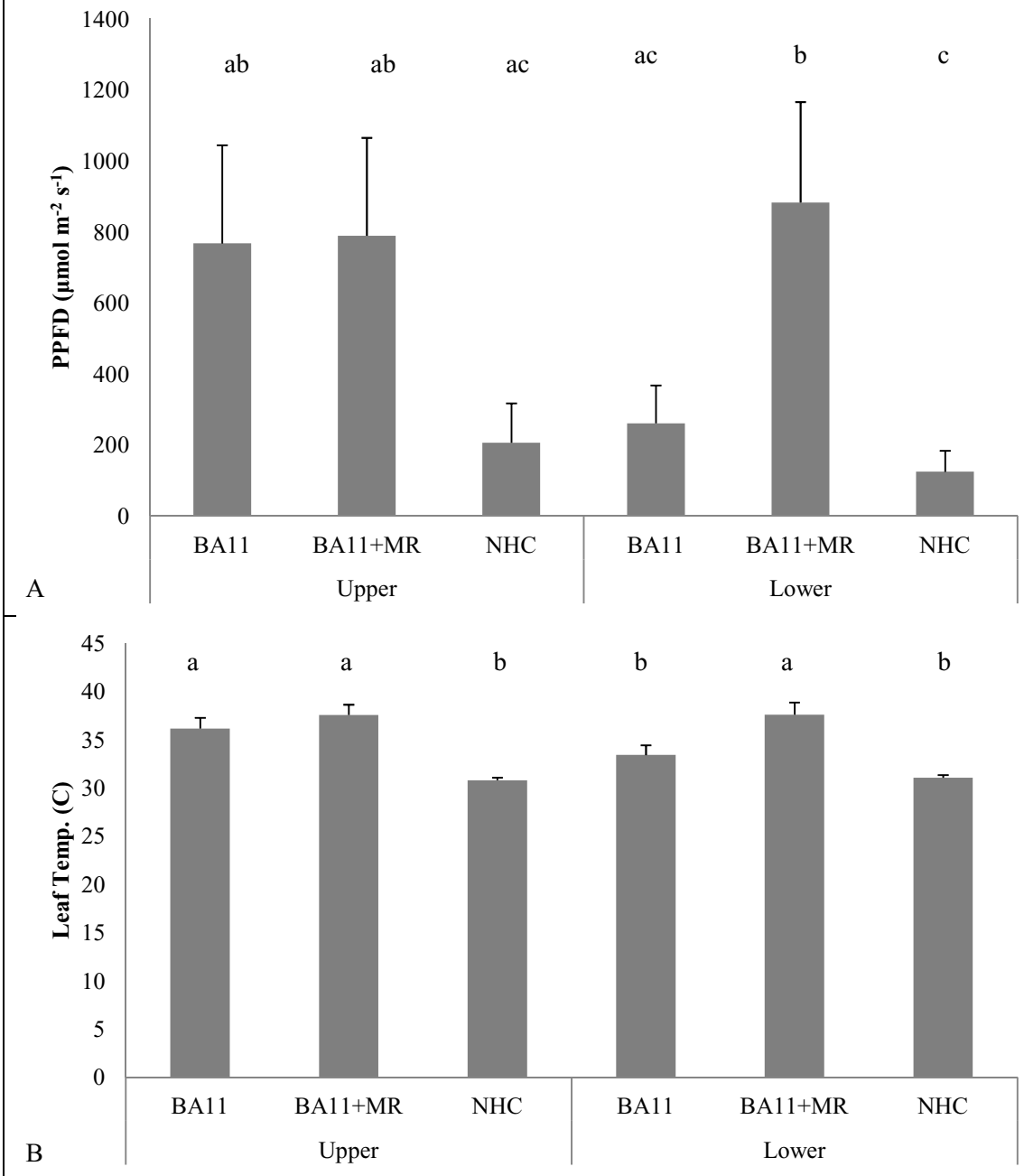

Figure 7.8 Slope position analysis by treatment in year 2 for A) mean PPFD and B) mean leaf temperature.

Data represent mid-season measurements.

Figure 7.9A illustrates $F_{q'}/F_{m'}$ and ETR mean values for lower and upper slope positions by treatment for year 2. Average $F_{q'}/F_{m'}$ ranged from 0.487 for BA11+MR lower slope to 0.706 for NHC lower slope. A one-way analysis of variance detected significant differences to exist ($p = 0.01$). However, a SNK method of pairwise multiple comparisons did not find significant differences. Also, significant differences were observed between BA11 lower slope versus BA11+MR and BA11 upper. Finally, significant differences were observed between NHC upper slope versus BA11+MR lower slope and BA11 upper slope.

Figure 7.9B illustrates ETR mean values for lower and upper slope positions by treatment for year 2. Average ETR ranged from 26.8 μmol m^{-2} s^{-1} for NHC lower slope to 127.9 for BA11+MR lower slope. A one-way analysis of variance detected significant differences to exist ($p < 0.001$). Pairwise multiple comparisons (SNK) determined BA11 upper slope, BA11+MR upper slope, and BA11+MR lower slope to be similar. Also, NHC upper slope, BA11 lower slope, and NHC lower slope were found to be similar.

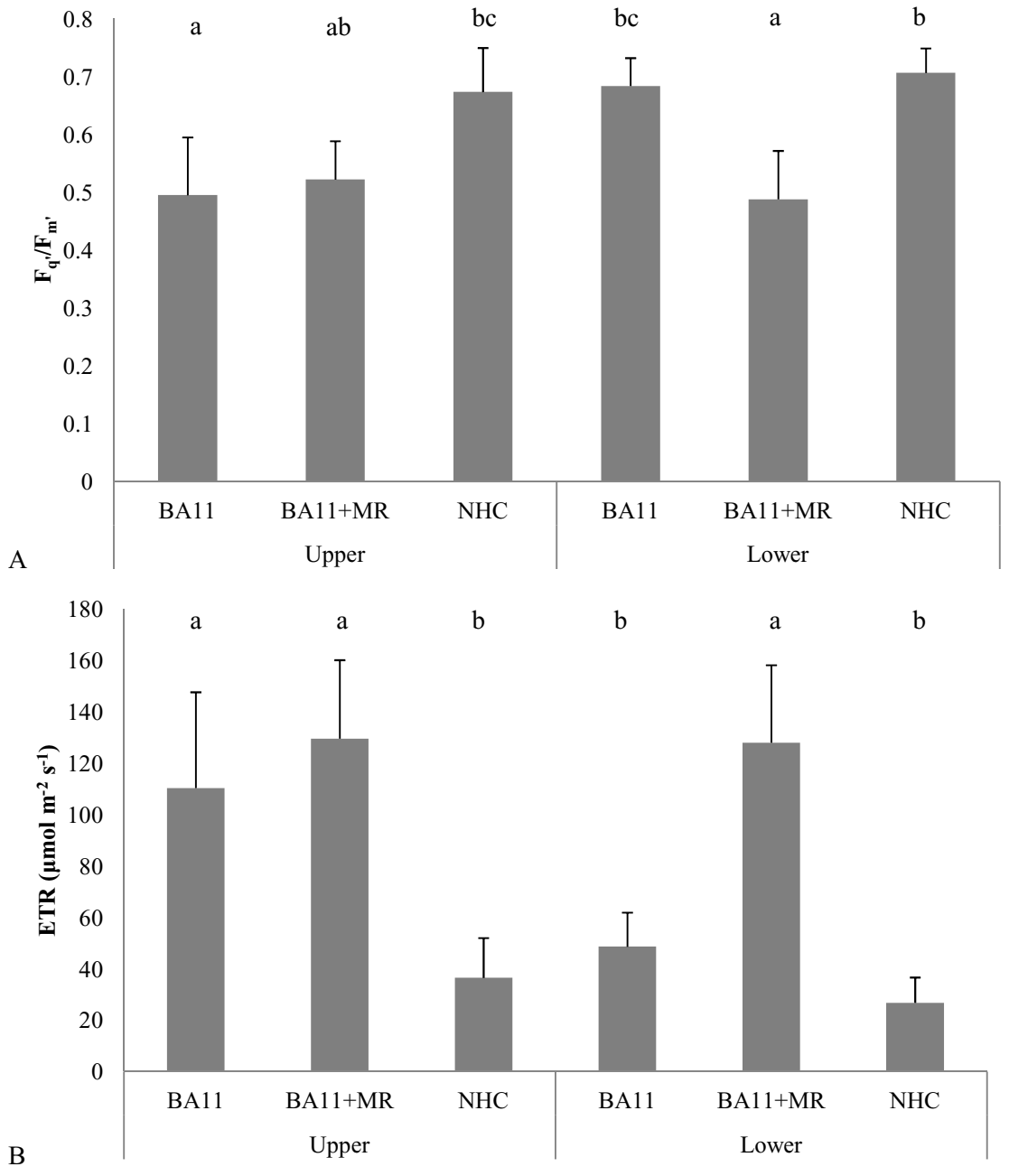

Figure 7.9. Slope position analysis by treatment in year 2 for A) mean Fq'/Fm' and B) mean ETR.

Data represent mid-season measurements.

Species Analysis

Table 7.1. Provides descriptive data for light saturated average CF parameter values by species. ETR data were square root transformed to meet the normalization assumption. A one-way analysis of variance detected significant differences to exist among species means for ETR under light saturated conditions ($p < 0.001$). A SNK method determined significant differences between *Q. velutina* versus *A. rubrum*, *P. serotina*, and *Q. rubra*. Significant differences were also observed between *U. alata* versus *A. rubrum* and *Q. rubra*. Finally, significant differences were observed between *Q. alba* and *A. rubrum* for light saturated ETR values.

A statistical analysis of $F_{q'}/F_{m'}$ produced similar, but not equivalent results as the ETR analysis. The assumption of normality could not be met. So, non-parametric analysis was performed. A Kruskal-Wallace analysis of variance on ranks detected significant differences ($p < 0.001$). A SNK on ranks method determined *A. rubrum* to significantly differ from all species. Also, *Q. velutina* was determined significantly different from *P. serotina*. One caveat, *P. serotina* leaf temperatures were significantly lower than *Q. alba*, *Q. rubra*, and *A. rubrum*. All other leaf temperatures were similar.

Table 7.1. Light saturated species level descriptive statistics in mid-seaon Year 2.				
Species	**PPFD**	**$F_{q'}/F_{m'}$**	**ETR**	**L. Temp.**
Q. rubra	1251.4 (294.8)	0.258 (0.09)	130.6 (51.7)	31.1 (4.7)
Q. velutina	1390.9 (331.8)	0.281 (0.11)	157.5 (59.9)	30.7 (4.9)
Q. alba	1346.1 (329.5)	0.268 (0.12)	144.2 (63.5)	31.6 (5.3)
A. rubrum	1404.0 (320.1)	0.216 (0.08)	124.3 (51.8)	32.1 (5.3)
U. alata	1388.5 (302.8)	0.266 (0.11)	151.2 (64.4)	30.5 (4.9)
P. serotina	1386.7 (333.7)	0.246 (0.11)	138.4 (58.8)	28.5 (5.7)

Table 7.2. provides species rankings for ETR_{max} at early, middle, and late points of growing season for year 2. *U. alata* and *P. serotina* were consistently ranked in the top two for ETR_{max}. *A. rubrum* and *Q. rubra* were consistently ranked lowest in ETR_{max} values. ETR_{max} values for U. alata were 50 µmol m^{-2} s^{-1} higher in mid-season than in early or late points of growing season.

Table 7.2. Species rankings for ETR_{max} for each point of growing season.						
Species	Early	Rank	Middle	Rank	Late	Rank
U. alata	129.0	3	179.1	1	130.3	2
P. serotina	131.9	1	172.7	2	165.0	1
Q. velutina	129.8	2	142.5	3	127.1	4
Q. alba	123.5	4	142.4	4	129.2	3
A. rubrum	118.3	5	140.6	5	90.3	6
Q. rubra	116.7	6	116.8	6	113.0	5

Discussion

Chlorophyll fluorescence provided very useful and informative data pertaining to the light response of photosystem II for the six hardwood species observed. Individual CF parameters, particularly ETR, provided useful data for treatment, topographic, and species level analyses. Statistically, CF data was most useful at the macro level, such as treatment analyses, but did provide insight into species level differences.

A seasonal analysis of maximum ETRs illustrated the impacts of both leaf temperature and moisture availability on PSII physiological activity (Figures 7.1 and 7.2). Seasonal trends were evident from spring through mid-summer and into fall, as maximum ETR trended upward from spring to mid-summer and downward as temperatures dropped in the fall. Annual differences were evident as well. These differences were a function of leaf temperature and available moisture. The differences between growing seasons were most evident in the mid-season growing points. Year 1 and year 2 had average to above average moisture availability and resulting ETRs ranged from around 125 to over 220 µmol m^{-2} s^{-1}. Year 3 experienced drought stress conditions at mid-season, with well above average temperatures and well below average moisture availability, resulting in ETR values between 90 and 130 µmol m^{-2} s^{-1}. The leaf temperature by precipitation index (LPTI) illustrated the interaction between temperature and precipitation and their cumulative effects on maximum ETRs (Figure 7.2).

Treatment Level Analysis

Significant differences in both $F_{q'}/F_{m'}$ and ETR were observed in mid-season, between year comparisons. However, two different environmental factors were impacting results. Year 1 exhibited lower average PPFDs than year 2 and year 3 (significantly different from year 2). The differences in PPFD were attributed to wind-throw of a couple overstory trees between year 1 and year 2 opening gaps for additional sunlight canopy penetration. Also, as seedlings developed more leaves were available to receive full sunlight in years 2 and 3 than in year 1. The impacts

from the difference in year 1 and year 2 PPFDs were evident in CF parameters, particularly ETR. The lower sunlight levels resulted in significant differences for average ETR values for the first two seasons. However, year 2 versus year 3 PPFDs were similar and yet differences still occurred in average ETR values. The primary factors creating year 2 versus year 3 differences were leaf temperature and available moisture. ETR values were basically the same in year 3 versus year 1 even with a higher PPFD. However, $F_{q'}/F_{m'}$ was significantly different between year 1 and year 3, with year 1 being higher. A lack of moisture negatively impacted PSII activity during year 3.

When observations were pooled for year by treatment, significant differences were evident across all treatments. Mean PPFDs, $F_{q'}/F_{m'}$, and ETR were significantly different for all treatments (Figure 7.5). PPFD values were highest in the BA11+MR treatment. The impact of mid-story trees present in BA11 was clear in the PPFD differences between it and BA11+MR. Mid-story trees present were the only difference between the two canopies, as both overstories were harvested similarly. Leaf level sunlight availability remained below adequate for development of *Quercus* reproduction in undisturbed stand conditions, adequate to inadequate for partial overstory removal, and adequate to optimal for partial overstory harvest coupled with mid-story removal.

Mean $F_{q'}/F_{m'}$ also differed across treatments, BA11+MR yielded the lowest $F_{q'}/F_{m'}$ values, as would be expected with the inverse relationship normally associated between sunlight and effective quantum yield. Undisturbed stand conditions yielded $F_{q'}/F_{m'}$ values near levels that would be expected from dark adapted leaves. BA11 differed from both of the other treatments and $F_{q'}/F_{m'}$ values fell between the two. Higher effective quantum yields would equal higher PSII activity under similar sunlight conditions. However, in this study they were due to sunlight differences across treatments for pooled three year treatment means.

Electron transfer rate yielded similar results to PPFDs, with significant differences across all treatments. Orders of magnitude were also similar between the differences across treatments for PPFD and ETR. ETR, combining both sunlight intensity and effective quantum yields,

provided a more complete analysis of PSII activity, than did $F_{q'}/F_{m'}$ alone. BA11+MR yielded the highest electron transfer rates. Average ETRs in BA11+MR were 34 and 42.4 μmol m^{-2} s^{-1} greater than BA11 and NHC, respectively. These results clearly demonstrate a difference in PSII physiological activity across treatments. Furthermore, these differences potentially equal a difference of 4.3 and 5.3 μmol CO_2 m^{-2} s^{-1} in CO_2 assimilation rate.

There was a significant interaction between treatment and year for the pooled three year leaf temperature data by treatment. The primary cause of the interaction was most likely due to a significant increase in leaf temperature for the non-harvest control between years 1 and 2 versus year 3. Conditions were so hot and dry in year 3 that no difference occurred between treatments, even under a closed canopy (Figure 7.5). Leaf temperature observations were different between BA11+MR versus BA11 and NHC for years 1 and 2. The difference could most likely be attributed to higher leaf level PPFDs in BA11+MR versus the other treatments during years 1 and 2.

BA11+MR leaf level PPFDs were significantly different than the NHC treatment in all three years. BA11+MR PPFDs were significantly different form BA11 in year 3. All three years would have likely differentiated with less variability in year 1 and 2 PPFD averages. As stated previously, BA11+MR maintained adequate to optimal sunlight conditions for development of *Quercus* reproduction. BA11 yielded inadequate conditions in year 1 to adequate conditions in years 2 and 3. The undisturbed stand conditions remained well below adequate sunlight levels.

Analysis of treatment by individual year illustrated differences across years for both $F_{q'}/F_{m'}$ and ETR. Average $F_{q'}/F_{m'}$ was lowest in BA11+MR for all three years, an effect of significantly higher PPFDs. The most important observation with BA11 and BA11+MR data for $F_{q'}/F_{m'}$ was the obvious impact a lack of moisture availability had on average values. PPFDs were similar in both years for the respective treatments: however, $F_{q'}/F_{m'}$ mean values were considerably lower. Under adequate moisture, one might have expected a slight increase in

effective quantum yield as a function of seedling development, but certainly not a significant decrease.

ETR average values significantly differed across all treatments for each individual year (Figure 7.5). BA11+MR exhibited profound differences in PSII physiological activity versus BA11 and NHC. During year 2, the differences were most evident in ETR values. Based on a ETR/A ratio of 8.0, CO_2 assimilation in BA11+MR would potentially operate at ~ 4μmol CO_2 m^{-2} s^{-1} higher than BA11 on average and ~ 10 μmol CO_2 m^{-2} s^{-1} higher than NHC on average.

An analysis of slope position was performed on year 2 observations. Year 2 precipitation was above normal for the entire growing season. Year 1 started normal then declined through the growing season. Year 3 precipitation was well below normal for early to mid-season and then increased during late season measurements. Therefore, year 2 provided the most consistent growing conditions to potentially minimize impacts of soil moisture on slope position analyses.

Analyses of sunlight, leaf temperature, effective quantum yield, and electron transfer rate yielded similar responses to treatment and slope positions. Sunlight levels essentially fell into two groups of higher and lower PPFD levels. BA11 upper slope and BA11 + MR lower and upper slope represented higher sunlight environments. BA11 lower slope and NHC lower and upper slope represented lower sunlight environments. Leaf level sunlight was most uniform between lower and upper slope positions in BA11+MR. Leaf level sunlight varied the greatest in BA11 lower and upper slope positions. The resulting leaf level sunlight conditions were consistent with the results for plot center sunlight analyses in Chapter 4. The primary difference between BA11 and BA11+MR lower and upper slope positions was the presence or absence of well developed mid-story trees. Virtually all non-oak mid-story trees were removed from BA11+MR. No mid-story trees were intentionally removed from BA11. However, during the partial-harvest operation, mid-story trees in the upper slope position were inadvertently removed by harvesting equipment

skidding logs from lower slope to ridge-top loading deck locations. Leaf level sunlight conditions in the undisturbed non-harvest control were minimal for both upper and lower slope positions.

Leaf temperature followed a similar pattern to sunlight levels for each treatment by slope combination. BA11 upper slope and BA11+MR lower and upper slope formed a high temperature group. Conversely, BA11 lower slope and NHC lower and upper slopes formed a lower temperature group. According to the analysis of ETR by leaf temperature in Figure 7.10, BA11 upper slope and BA11+MR lower and upper slope exhibited temperature ranges within the maximum for electron transport in the light reactions. The maximized electron transport potentially leads to higher carbon fixation particularly in the presence of adequate soil moisture, such as conditions present in year 2.

Figure 7.10 illustrates year 3 values for slope position by treatment combinations, to provide a contrast in environmental conditions regarding moisture availability and leaf temperature. Overall, patterns in PPFD, $F_{q'}/F_{m'}$ and ETR were similar to the slope by treatment combinations observed in year 2. Again, two groups could be established equivalent to year 2 results, with similar statistical differences. BA11 upper and BA11+MR lower and upper slope maintained higher average values. BA11 lower and NHC lower and upper slope maintained lower average values. The largest difference was the order of magnitude of average PPFD and CF values, with year 2 values being consistently higher than year 3. The take home is that there did not appear to be a moisture gradient effect by slope position in any year.

Leaf temperature, however, was similar across all treatments in year 3 mid-season and was notably higher than most all leaf temperatures for treatment by slope combinations for year 2 mid-season observations. The range in year 3 mid-season leaf temperatures was from 35.3^0 to 36.8^0 C. This was drastically different than the range from year 2 (30.8^0 to 37.6^0 C). The higher temperatures were associated with well below average precipitation for middle growing season (chapter 3), another difference in environmental conditions compared to mid-season year 2.

BA11+MR upper slope provided the best example for the impacts of low moisture availability. Mean PPFD was 788 μmol m^{-2} s^{-1} in year 2 and 925 μmol m^{-2} s^{-1} in year 3, both saturating sunlight levels. Mean leaf temperature was 37.5 in year 2 and 36.8^0 in year 3, both in the optimal range for electron transport. A Student's t-test confirmed no significant differences between year 2 and year 2 PPFDs or leaf temperatures (P = 0.56 and 0.54). However, effective quantum yield and electron transport rate were notably different between the two years. Mean $F_{q'}/F_{m'}$ was 0.521 in year 2 and 0.356 in year 3. Mean electron transfer rates were 128.3 in year 2 and 96.1 in year 3. A Student's t-test confirmed significant difference in effective quantum yield (p = 0.04), but not in electron transport rate (P = 0.17).

Year 2 mid-growing season provided significantly higher mean effective quantum yield, with a lower PPFD average. This effect contradicts the inverse relationship between PPFD and effective quantum yield one would expect. With sunlight levels and leaf temperatures being relatively constant, the variation in moisture availability most likely impact effective quantum yield and electron transport in the light reactions of PSII.

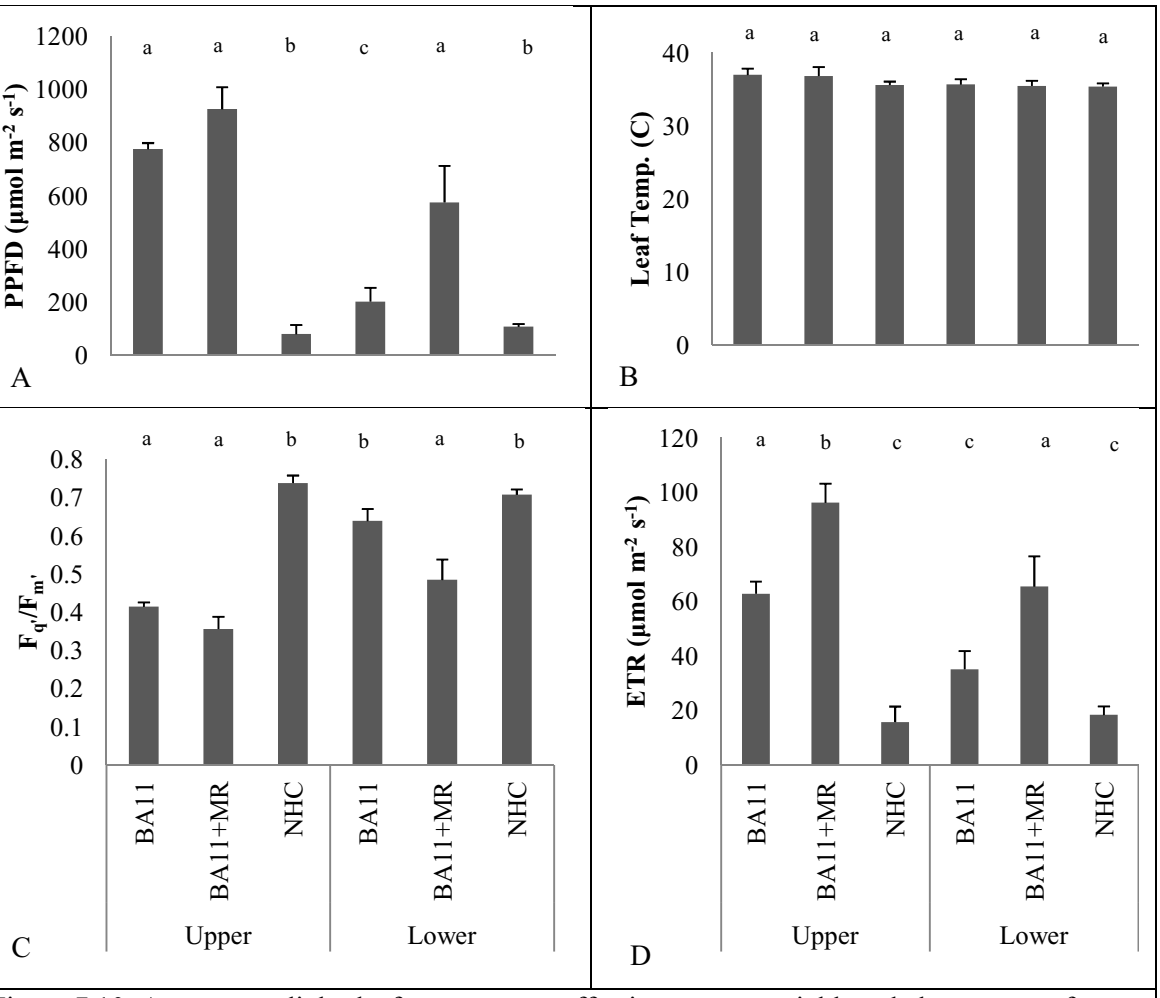

Figure 7.10. Average sunlight, leaf temperature, effective quantum yield, and electron transfer rate for treatment by slope combinations in mid-season year 3.

PPFD overall effects determined by Kruskal-Wallace ANOVA on ranks ($P = 0.001$). Analysis of variance detected differences for $F_{q'}/F_{m'}$ and ETR ($P < 0.001$). Means followed by same letter do not significantly differ (SNK method, $\alpha = 0.05$).

Leaf Temperature

Leaf temperature, along with and as a function of PPFD, can significantly impact PSII activity. Figure 7.11 illustrates the relationship between light saturated ETR and leaf temperature for combined data from all six hardwood species during the year 2 growing season. Light saturated electron transfer increased from 10^0 C to around 37^0 C, and then sharply declined as leaf temperatures moved above 40^0 C. Figure 7.12 illustrates light saturated ETR for each species. *Q. velutina, Q. alba, U. alata,* and *P. serotina* all expressed high light saturated ETRs in the 300s, with peaks occurring near 37^0 C. *Q. rubra* and *A. rubrum* did not respond similarly to leaf temperature. Peaks were not as clearly definable, with plateaus in light saturated maximums occurring between 25^0 and 40^0 C for *A. rubrum* and at 25^0 to 35^0 C for *Q. rubra*. *A. rubrum* and *Q. rubra* also exhibited lower light saturated ETR rates (~ 250 μmol m^{-2} s^{-1}).

Ecologically, the responses of each species to leaf temperature would fit into an expected pattern of adaptability for dryer sites. This study site would be considered between mesic and xeric, but more on the xeric side. On such sites, one would expect species such as *Q. velutina*, *Q. alba* to perform better at higher temperatures than some other species, which they did in PSII activity. Particularly, they outperformed *Q. rubra*. An outcome that would be expected, *Q. rubra* would certainly be better adapted to more mesic sites.

On a true xeric site, one would expect adapted Quercus species to have a competitive advantage over almost any species. This site being moderately productive (SIs ~70+ for upland *Quercus* species), demonstrated that PSII activity for *U. alata* and *P. serotina* performed comparably or slightly better at higher temperatures. A. rubrum responded similarly to *Q. rubra* in leaf temperature.

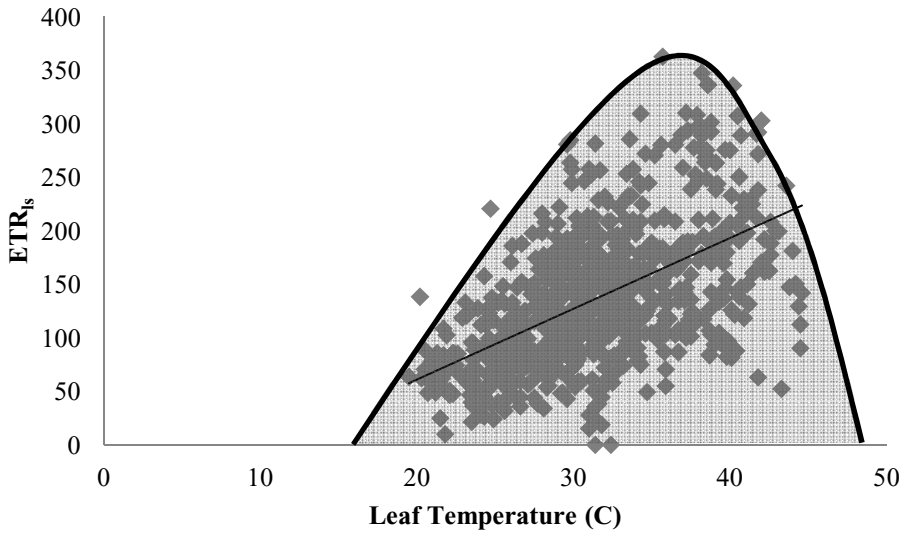

Figure 7.11. Light saturated (PPFD > 750 µmol m^{-2} s^{-1}) ETR values for year2, illustrating leaf temperature impacts on light reactions of PSII.

Note: Curve was hand drawn to illustrate peak ETR by leaf temperature combination.

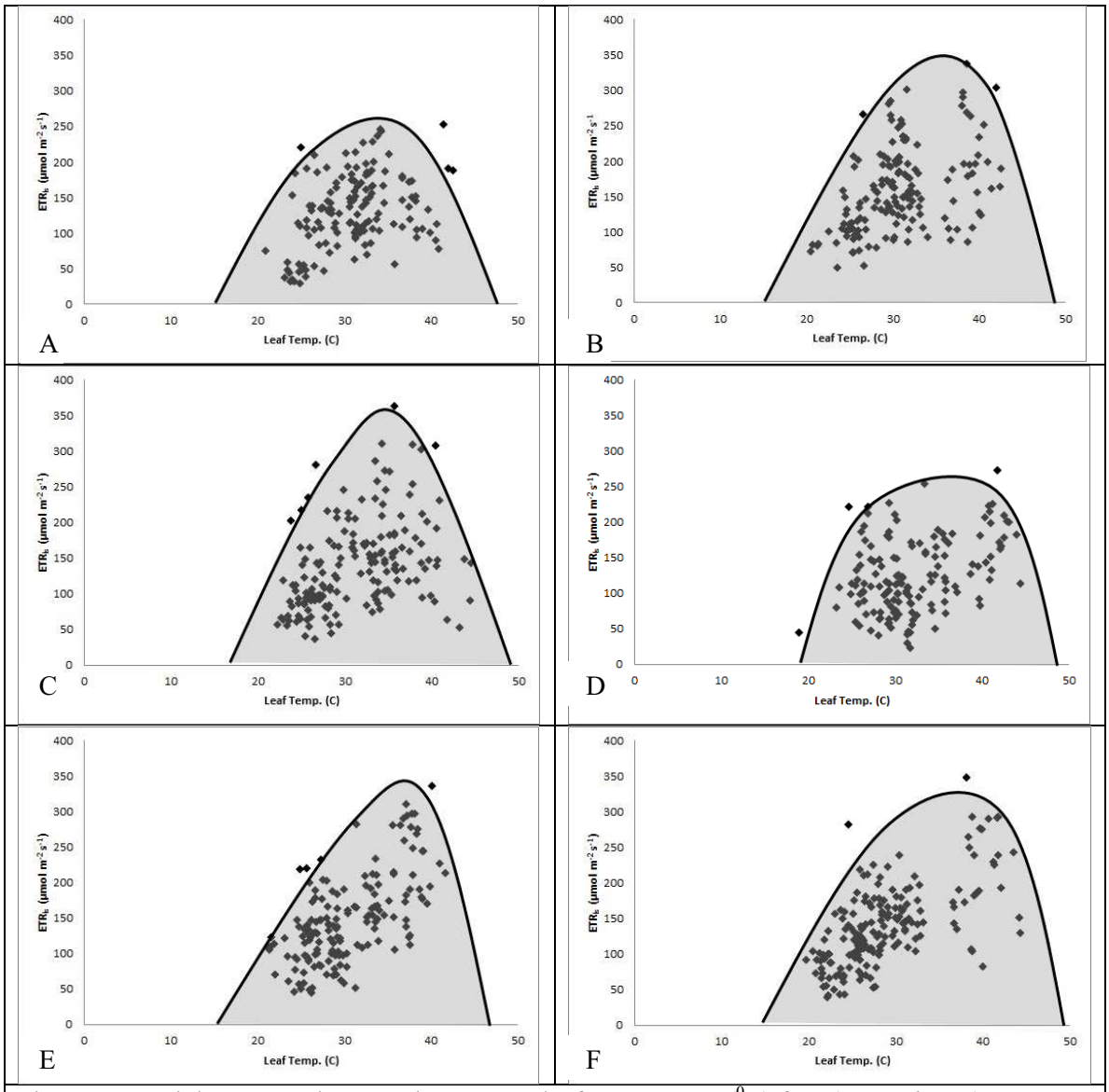

Figure 7.12. Light saturated ETR values versus leaf temperature (^{0}C) for A) *Q. rubra* B) *Q. velutina* C) *Q. alba* D) *A. rubrum* E) *U. alata* and F) *P. serotina*.

Note: curves were hand drawn to illustrate peaks of data.

A look at maximum ETR by species reveals similar patterns to those associated with leaf temperature (Tables 7.1and 7.2). U. alata and P.serotina were consistently 1 or 2 in ETR_{max} ranking. Those species were followed by *Q. velutina* and *Q. alba*., *A. rubrum*, and *Q. rubra* maintained the lowest ETR_{max} values. Again, from an ecological context these rankings are similar to what would be expected on this type of site. However, with the most efficient ETR/A ratio (Table 5.8) *A. rubrum* may remain comparable in PSII activity competitiveness, even with lower ETR values.

Conclusions

Chlorophyll fluorescence proved to be a useful tool for analyzing the light response of photosystem II to varying leaf level sunlight environments for the six hardwood species observed. Chlorophyll fluorescence provided sound data for treatment and treatment/topographical statistical analyses. Furthermore, chlorophyll fluorescence based light curves provided detailed analysis of species level differences.

Chlorophyll fluorescence parameters, effective quantum yield and electron transfer rate, proved to be sensitive indicators of photosystem II activity in response to sunlight availability. Cardinal points of light curves, such as ETR_{max}, clearly demonstrated seasonal impacts of leaf temperature and moisture availability, both across years and within points of a growing season. Mid-season (July) observations were determined to provide the most useful fluorescence data for comparisons.

Fluorescence analyses demonstrated that the light reactions of photosystem II responded in unison with corresponding leaf level irradiance for both treatment and treatment/slope combinations. Partial harvests combined with mid-story removal provided the highest and most uniform leaf level sunlight availability of any treatment. Partial harvesting alone provided comparable responses in photosystem II activity in upper slope positions, but was more similar to

undisturbed stand conditions in the lower slope positions. Undisturbed stand conditions generated minimal leaf level sunlight availability and corresponding photosystem II activity.

Quercus species demonstrated a comparatively slow, but positive response in photosystem II activity to multiple growing seasons in a partial shade/partial sun environment. Non-*quercus* species exhibited varying responses to increased sunlight. *Ulmus alata* and *Prunus serotina* exhibited higher initial responses to increased sunlight availability. However, *Acer rubrum* photosystem II activity did not demonstrate similar responses to sunlight. The sunlight conditions generated from the partial harvest operation plus mid-story control generate good light conditions for *Quercus* species photosystem II activity, particularly over a period of seasons. However, non-*Quercus* competitors collectively remain strong competitors for sunlight in naturally regenerated hardwood stands.

Literature Cited

Ball, M.C., Butterworth, J.A., Roden, J.S. Christian, R. and Egerton, J.G. (1994). Applications of chlorophyll fluorescence to forest ecophysiology. *Australian Journal of Plant Physiology* 22:311-319.

Bilger W. and Bjorkman, O. (1989) Light-induced spectral absorbance changes in relation to photosynthesis and the epoxidation state of the xanthophyll cycle components in cotton leaves. *Plant Physiology* 91: 542

Bilger, W., Schreiber, U., & Bock, M. (1995). Determination of the quantum efficiency of photosystem II and of non-photochemical quenching of chlorophyll fluorescence in the field. *Oecologia*, *102*(4), 425-432.

Bradbury, M. and Baker, N.R. (1981) Analysis of the slow phases of the in vivo chlorophyll fluorescence induction curve. Changes in the redox state of Photosystem II electron acceptors and fluorescence emission from Photosystems I and II. *Biochimica et Biophysica Acta*635:542-551.

Epron, D., Dreyer, E. and Breda, N. (1992). Photosynthesis of oak trees [*Quercus petraea* (Matt.) Liebl.] during drought under field conditions: diurnal course of net CO_2 assimilation and photochemical efficiency of photosystem II. *Plant, Cell and Environment* 15:809-820.

Genty, B., Briantais, J., and N.R. Baker, N.R. (1989) The relationship between the quantum yield of photosynthetic electron transport and quenching of chlorophyll fluorescence. *Biochimica et Biophysica Acta (BBA) - General Subjects* 990(1) 87-92.

Krause G.H., Briantais J.M. and C. Vernotte. 1982. Photo-induced quenching of chlorophyll fluorescence in intact chloroplasts and algae. Resolution into two components. Biochim. Biophys. Acta. 679: 116-124.

Maxwell M. and Johnson G.N. (2000). Chlorophyll fluorescence—a practical guide *Journal of Experimental Botany* 51(345): 659-668.

Orgen E. and Baker N.R. (1985). Evaluation of a technique for the measurement of chlorophyll Fluorescence from leaves exposed to white light. *Plant Cell and Environment* 8: 539-547.

Schreiber U. (1986) Detection of rapid induction kinetics with a new type of high frequency modulated chlorophyll fluoremeter. *Photosynthesis Resource* 10: 51-62.

Schreiber, U., Schliwa, U. and Bilger, W. (1986) Continuous recording of photochemical and non -photochemical chlorophyll fluorescence quenching with a new type of modulation fluoremeter. *Photosynthesis Research* 10: 51-62.

Schreiber, U., Neubauer, C. and Schilwa, U. (1993) PAM fluorometer based on medium-frequency pulsed Xe-flash measuring light: A highly sensitive new tool in basic and applied photosynthesis research. *Photosynthesis Research* 36(1):65-72.

Schindler, C. and H.K. Lichtenthaler, H.K. (1996) Photosynthetic CO_2 assimilation, chlorophyll fluorescence and zeaxanthin accumulation in field grown maple trees in the course of a sunny and a cloudy day. *Journal of Plant Physiology* 148:399-412.

Van Kooten, O., & Snell, J. F. H. (1990). Progress in fluorescence research and nomenclature for quenching analysis. *Photosynth Res*, *25*, 147-150.

CHAPTER VIII – COMPREHENSIVE DISCUSSION

Bringing the study results together in a complete ecophysiological context is important to linking key mechanistic photosynthesis responses to a broader ecological and silvicultural framework. The light reactions of photosystem II clearly demonstrated that sunlight availability is a driving force behind hardwood reproduction leaf level physiological activity. Additionally, the activity in the light reactions was demonstrated to correlate with photosynthetic rates for each for each sunlight environment and species observed. Figure 8.1 illustrates the relationship between maximum electron transfer rate and gross photosynthesis rate for all species combined in year 3 post-treatment. Early and late season data represented pre-drought and drought recovery periods. Mid-season data represent drought conditions. LPTIs for early and late season were -4.6 and -3.7. LPTIs for midseason were -7.5. Mean leaf temperatures were 30^0 and 33^0 C for early and late season measurements. Leaf temperatures in midseason averaged 40^0 C. There were strong relationships between ETRmax and gross assimilation. However, environmental conditions had a large influence on the scale of the relationships.

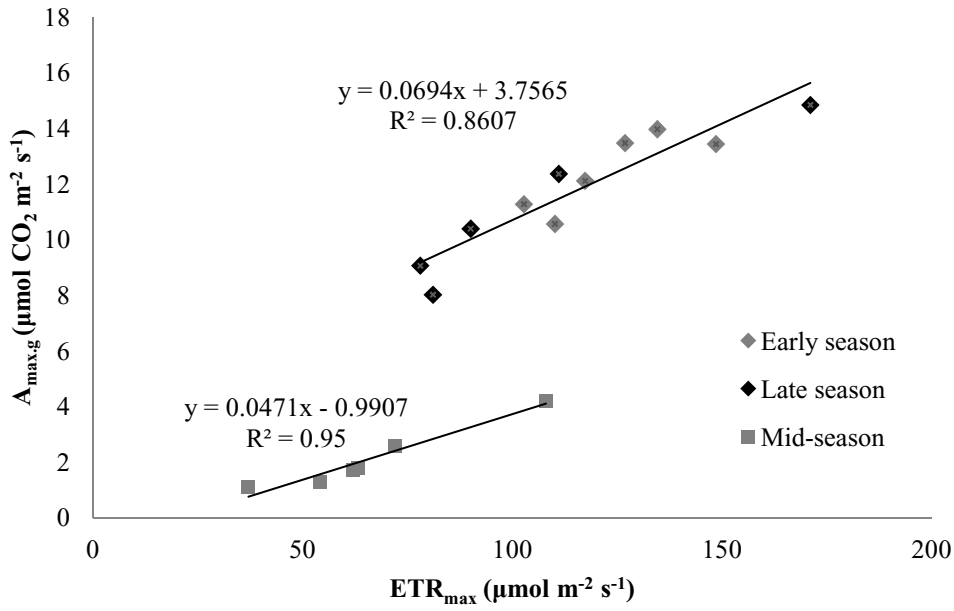

Figure 8.1. Early, mid, and late season relationships between ETR_{max} and $A_{max.g}$ for year 3.

Figure 8.2 illustrates the maximum electron transfer rates for the shaded sample pool, and year 1, year 2, and year 3 sun adapted sample pools. Figure 8.1A illustrates the progression from a shaded environment through each of the three growing season in an increased sunlight environment. A definite upward trend occurred in electron transfer rate in each respective season. The author feels mid-season year 3 would have shown an additional increase, as sun adapted seedlings continued to develop, in electron transfer had the severe drought conditions occurred in mid-season. The late season values (drought recovery period) used for year 3 were equivalent to year 2 and remained higher than year 1.

Figure 8.1B illustrates the progression of seedling from a shade adapted environment through three seasons of light adaptation. *Quercus velutina* demonstrated the most rapid response to increased sunlight over time than other *Quercus* species. *Quercus rubra* lagged in years 1 and 2 post-treatment, but did begin to increase appreciably in year 3. This was not an expected result as *Quercus rubra* would be considered the least drought hardy among the *Quercus* species

sampled. *Acer rubrum* had the highest shaded maximum electron transfer rate, but demonstrated only a slight increase following a sun adaptation period. *Prunus serotina* was not present in the shaded sample pool. Once prevalent, *Prunus serotina* demonstrated high electron transfer rates. *Ulmus alata* demonstrated the largest response and highest maximum electron transfer rates in mid-season measurements.

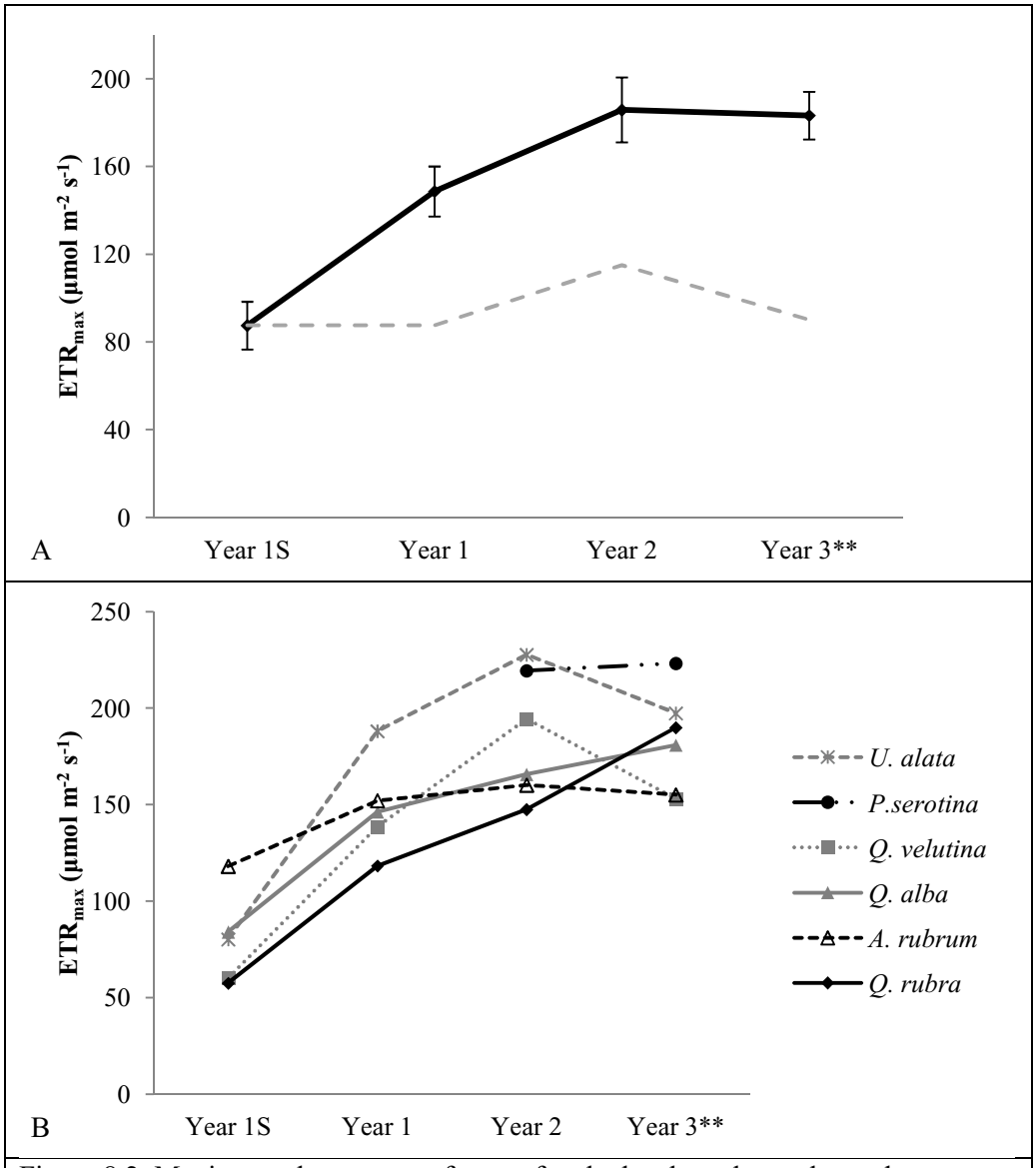

Figure 8.2. Maximum electron transfer rate for shade adapted samples and sun adapted samples years 1 through 3. A) All samples combined, and B) ETR max by species.

The dashed line in 8.2A is the maximum ETR of shade adapted seedlings for the respective season. Year 3 data are late season readings.

A question arises as to how these leaf level responses relate to plant or seedling level responses. An analysis of the reproduction pool for each species by size class was conducted in Chapter 4. The treatment level results clearly illustrated the growth response of each species group to the sunlight levels generated by each treatment. With increased sunlight levels, *Quercus* species responded well in both abundance and height growth. Removing a portion of the overstory combined with removal of mid-story non-*Quercus* competition had the most positive impacts on sunlight availability and development of the *Quercus* reproduction pool.

A look at the sample seedlings selected for chlorophyll fluorescence sampling provide more detail in linking leaf level to plant or seedling level responses. Figure 8.3 illustrates the size of samples seedlings at the beginning of year 1 post-treatment and their development by species in years 2 and 3 post-treatment. The first point to be made is the larger initial size of the two non-*Quercus* species compared to *Quercus* species in year 1. These size discrepancies relate the shade tolerance of each species group and the resulting ability of *U. alata* and *A. rubrum* to develop in a closed canopy shaded environment. *Quercus* seedlings are known to persist for a period of time, die-back and sometimes resprout in a cyclical manner. The other side of the equation pertains to the ability of these non-*Quercus* species and others to quickly respond in height growth. Conversely, *Quercus* species do not demonstrate such a response. Instead, *Quercus* seedlings respond slowly in year 1 then begin a greater response in subsequent growing seasons, assuming sunlight availability remains adequate for *Quercus* species.

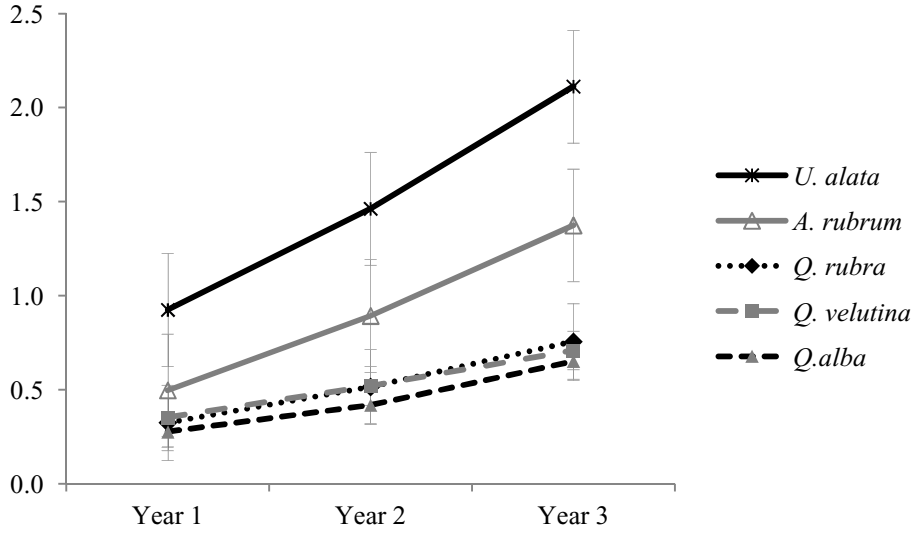

Figure 8.3. Average CF sample seedling heights (m) by species and year post-treatment application.

Applied natural regeneration studies have quantified that *Quercus* species survive and develop poorly in low sunlight environments (i.e. < 10 percent of full sunlight). The poor development of *Quercus* reproduction in low light environments combined with the ability of shade tolerant species, such as *Acer rubrum* and *Ulmus alata*, to persist in shaded sunlight conditions puts smaller-sized *Quercus* reproduction at a disadvantage when sunlight availability increases. Silvicultural treatments such as partial overstory and mid-story removal can gradually increase sunlight to the reproduction pool at the forest floor. This gradual increase allows *Quercus* reproduction time to increase in size and abundance, which increases its competitiveness in high sunlight conditions. Examining the mechanistic photosynthetic responses to increased sunlight demonstrated that an often desired partial sun/shade environment does not establish a physiological advantage for *Quercus* versus non-*Quercus* species. However, the partial sunlight environment does reduce competing species ability to outperform *Quercus* reproduction in photosynthesis rates and shoot growth as compared to what would be expected in a high sunlight environment. Thus, small *Quercus* reproduction is provided a window to develop and become a stronger competitor in newly developing hardwood stands.

APPENDICES

APPENDIX I – Treatment Layout

Treatment Layout

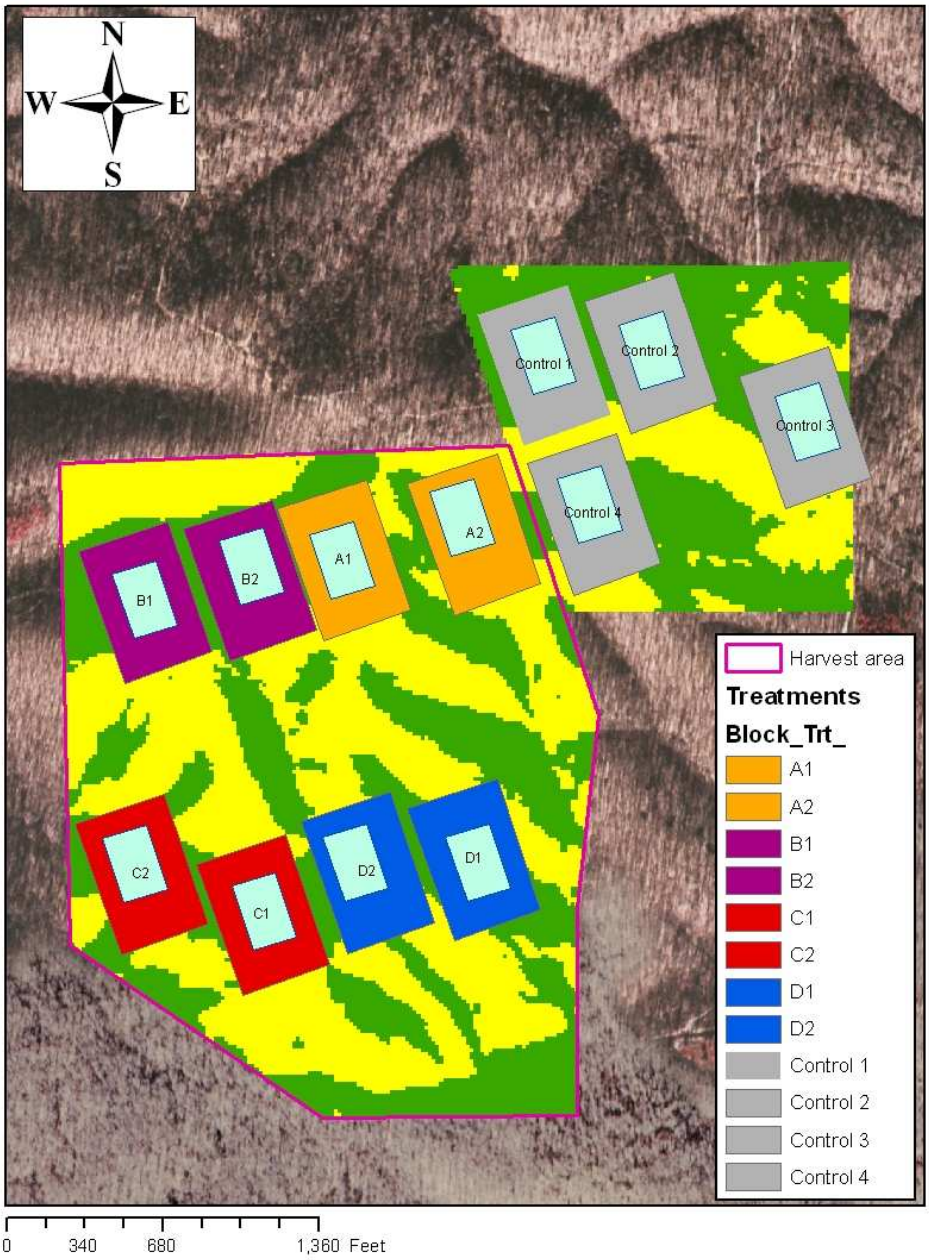

APPENDIX II – Sample Plots Layout

Sample Plots

- Two, fifth acre overstory plots
  - DBH > 5 inches
- Two twentieth acre midstory plots
  - DBH 1 to 5 in.

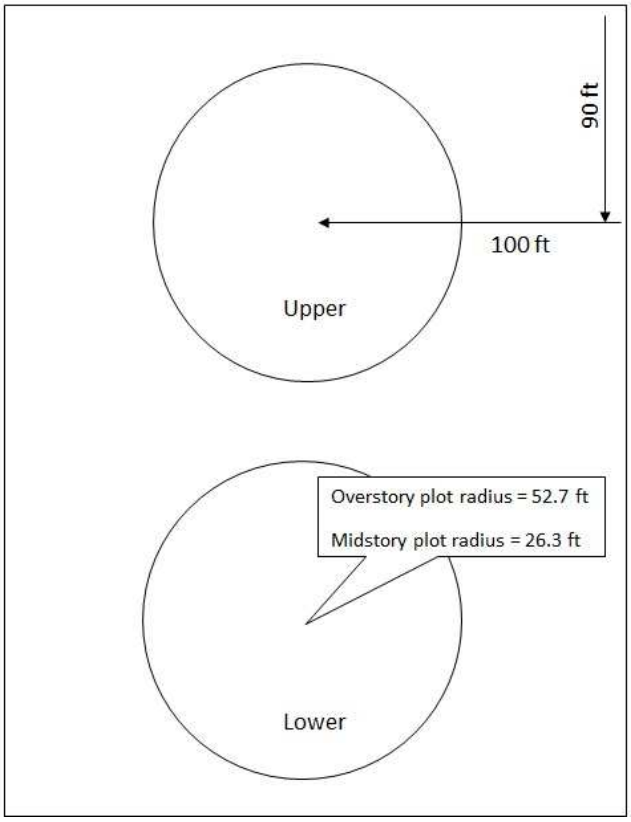

Sample Plots

- Twelve, hundredth acre regeneration plots
  - Regeneration = all trees less than 1 inch DBH
- Three plots per slope position
- Record species and height class

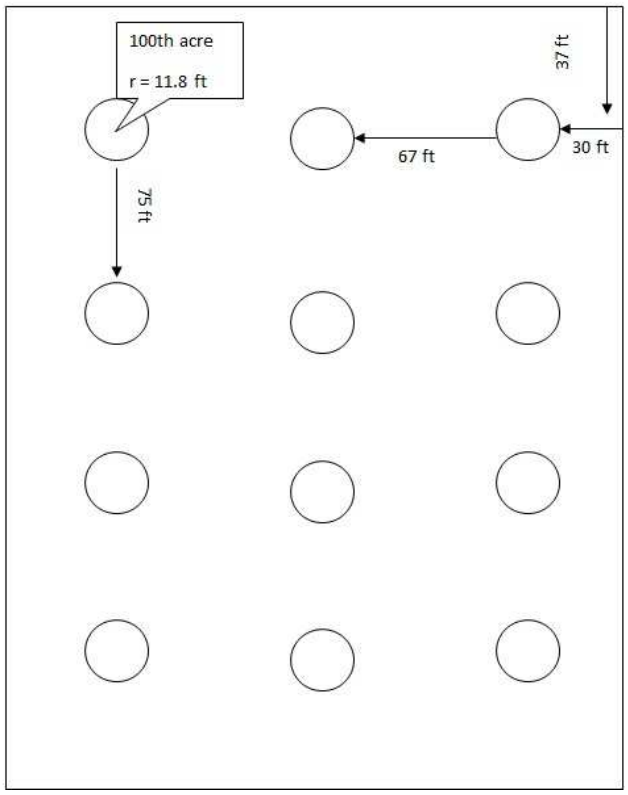

APPENDIX III – Reproduction Abundance

Table A3.1. Average *Quercus* SPH by treatment and replicate for initial through year 3 post treatment application.					
Treatment	**Replicate**	**Initial**	**Year 1**	**Year 2**	**Year 3**
BA11	A	1112.0	906.1	2409.2	3418.2
BA11	B	659.8	370.7	1029.7	4921.4
BA11	C	536.2	761.8	1256.0	2141.5
BA11	D	741.3	782.6	1441.3	6301.1
BA11+MR	A	1502.4	1606.2	4890.9	8442.6
BA11+MR	B	1482.6	1070.7	2965.2	5250.9
BA11+MR	C	783.3	898.7	1687.7	3819.8
BA11+MR	D	2285.7	3171.0	5065.6	12828.6
NHC	A	1420.8	1378.8	3622.5	15402.6
NHC	B	1317.0	1359.1	1359.1	4344.8
NHC	C	906.9	926.6	1161.4	6290.8
NHC	D	1771.7	1791.5	2263.4	6980.6
Means					
BA11		762.3	705.3	1534.1	4195.6
BA11+MR		1513.5	1686.6	3652.3	7585.5
NHC		1354.1	1364.0	2101.6	8254.7
Standard Error					
BA11		123.9	116.0	303.6	902.9
BA11+MR		306.9	517.2	809.5	1997.0
NHC		178.0	176.6	560.9	2447.1

APPENDIX IV – SPAD Index vs. Spectrophotometry

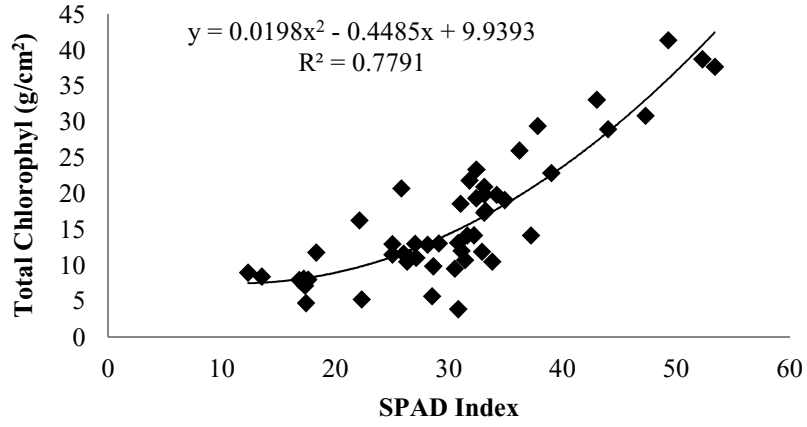

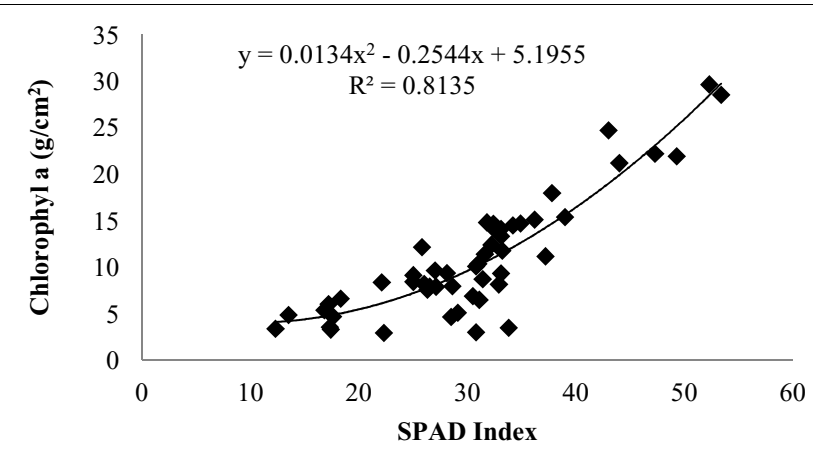

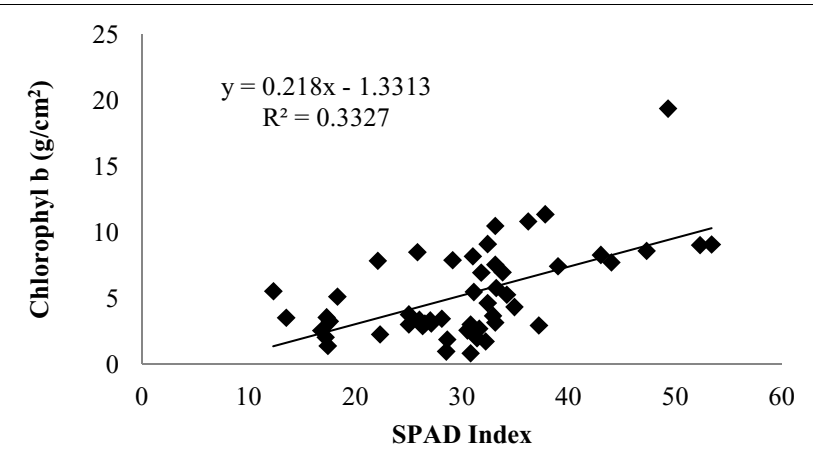

Figure 4A.1. Relationship between measured absorbance and SPAD indices for A) total chlorophyll, B) chlorophyll a and C) chlorophyll b.

Leaf samples were collected from each species and transported in LN_2, then stored at -80^0 C. Quantification was obtained measuring absorbance at 663, 645, and 480 nm in a spectrophotometer after extraction (85:15 acetone tris) using a 80:20 v/v aqueous acetone. Total chlorophyll, chlorophyll a, and chlorophyll b were calculated using the equation of Lichtenhaler and Welburn (1983).

APPENDIX V – CF Samples, Fitted Curves and Cardinal Points

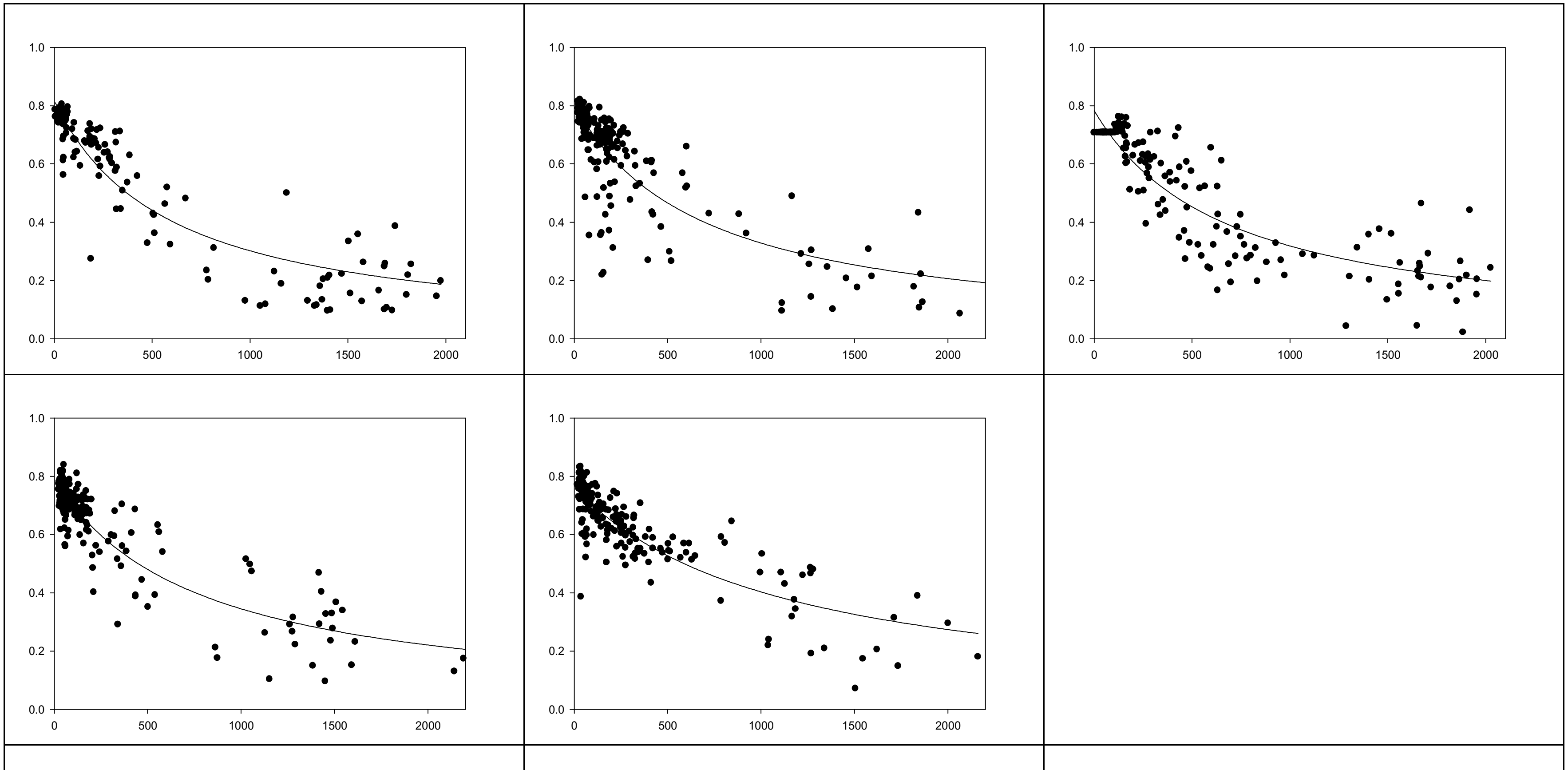

Figure A5.1 . $F_{q'}/F_{m'}$ light curves for July 2010. A) Q. rubra (hyperbolic decay), B) Q. velutina, C) Q. alba, D) A. rubrum E) U. alata. Curves were fit to a line by Formula (5.2), YLD = (*a***b*)/(*b*+x). Where *a* sets magnitude (*a* = F_v/F_m @ 0 ppfd) and *b* sets bending degree.

*

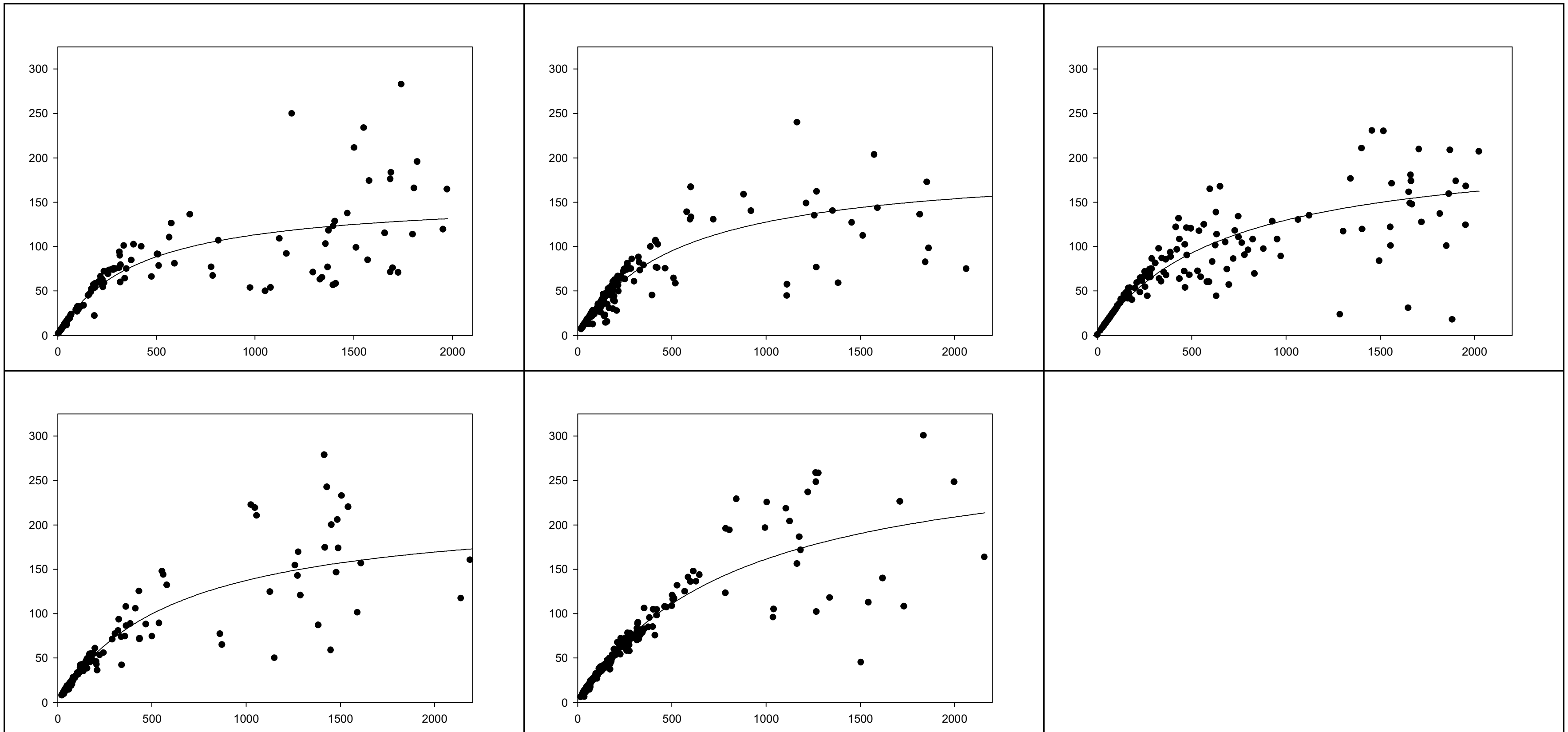

Figure A5.2. ETR light curves for July 2010. A) Q. rubra, B) Q. velutina, C) Q. alba, D) A. rubrum E) U. alata. Curves were fit to a line by Formula (5.3), ETR = (*a**x)/(*b*+x). Where *a* sets magnitude and *b* sets bending degree.

Table A5.1. Calculated cardinal points for July 2010.

Species	PPFDmax	ETRmax	Rank	Fv/Fm	Rank
Q. rubra	1177	118.3	5	0.242	5
Q. velutina	1266	138.6	4	0.284	3
Q. alba	1393	146.3	3	0.258	4
A. rubrum	1341	152.1	2	0.289	2
U. alata	1451	188.1	1	0.333	1

ETRmax = ETR @ 2000 mol * 0.9

Table A5.2. Cardinal points for PPFD 83.9 µmol m^{-2} s^{-1}.

Species	PPFD	ETR	Rank	Fv/Fm	Rank
Q. rubra	83.9	28	1	0.714	1
Q. velutina	83.9	27.3	3	0.713	2
Q. alba	83.9	24.9	5	0.700	5
A. rubrum	83.9	27.1	4	0.710	3
U. alata	83.9	27.4	2	0.710	3

Table A5.3. Cardinal points for PPFD 746 µmol m^{-2} s^{-1}.

Species	PPFD	ETR	Rank	Fv/Fm	Rank
Q. rubra	746	103.5	5	0.374	4
Q. velutina	746	114.3	3	0.384	3
Q. alba	746	114.4	3	0.374	4
A. rubrum	746	121.8	2	0.403	2
U. alata	746	139.9	1	0.458	1

Table ____. Cardinal points for PPFD 466 mean in BA11.

Species	PPFD	ETR	Rank	Fv/Fm	Rank
Q. rubra	466				
Q. velutina	466				
Q. alba	466				
A. rubrum	466				
U. alata	466				

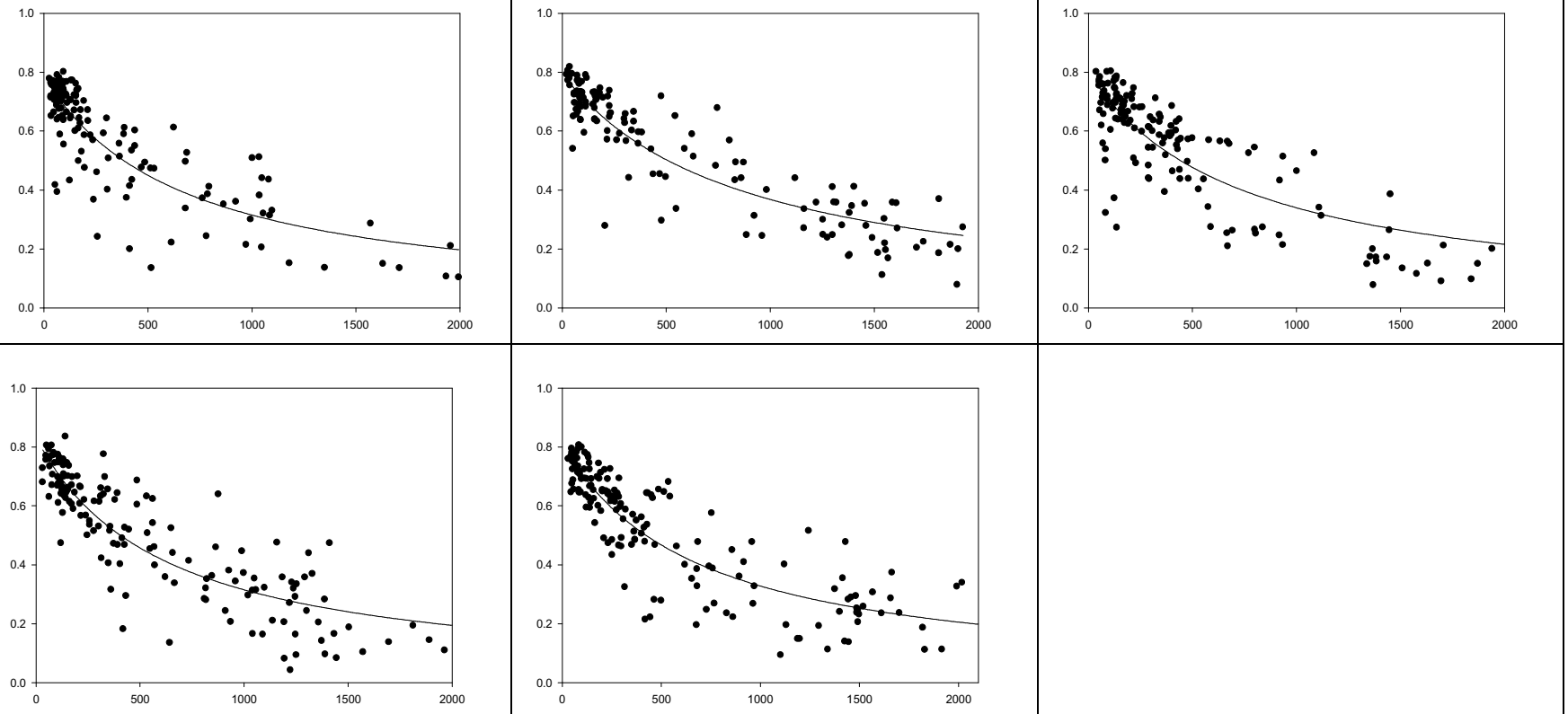

Figure A5.3 . $F_{q'}/F_{m'}$ light curves for September 2010. A) Q. rubra, B) Q. velutina, C) Q. alba, D) A. rubrum E) U. alata. Curves were fit to a line by Formula (5.2), YLD = (*a***b*)/(*b*+x). Where *a* sets magnitude (*a* = F_v/F_m @ 0 ppfd) and *b* sets bending degree.

*

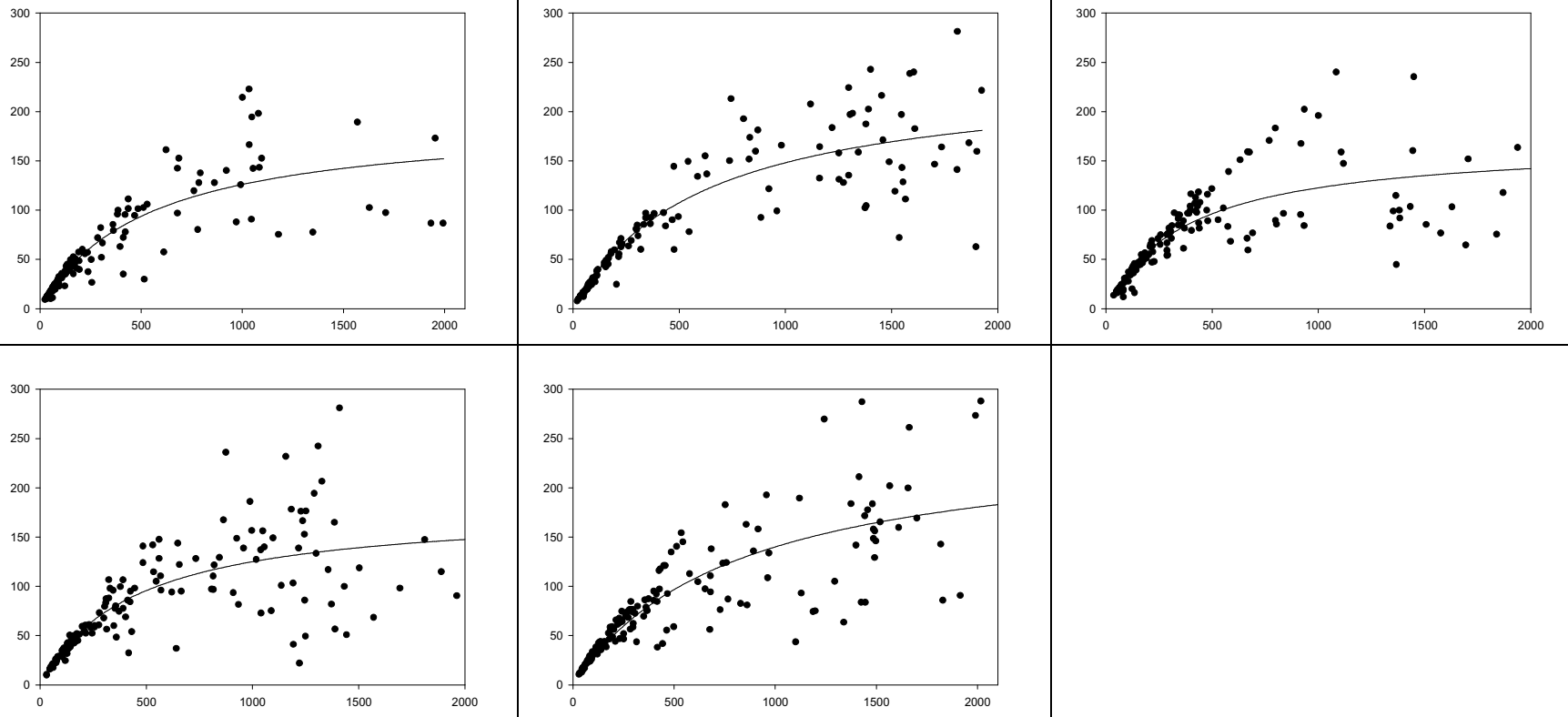

Figure A5.4. ETR light curves for September 2010. A) Q. rubra, B) Q. velutina, C) Q. alba, D) A. rubrum E) U. alata. Curves were fit to a line by Formula (5.3), ETR = (a*x)/(b+x). Where a sets magnitude and b sets bending degree.

Table A5.5. Calculated cardinal points for September 2010.

Species	PPFDmax	ETRmax	Rank	Fv/Fm	Rank
Q. rubra	1295	136.8	3	0.267	4
Q. velutina	1316	162.8	1	0.314	1
Q. alba	1215	128.9	5	0.302	2
A. rubrum	1238	132.9	4	0.274	3
U. alata	1443	162.4	2	0.259	5

ETRmax = ETR @ 2000 mol * 0.9

Table A5.6. Cardinal points for PPFD 83.9 µmol m^{-2} s^{-1}.

Species	PPFD	ETR	Rank	Fv/Fm	Rank
Q. rubra	83.9	26.4	4	0.700	5
Q. velutina	83.9	29.3	2	0.724	2
Q. alba	83.9	31.2	1	0.718	4
A. rubrum	83.9	28.4	3	0.730	1
U. alata	83.9	23.8	5	0.721	3

Table A5.7. Cardinal points for PPFD 746 µmol m^{-2} s^{-1}.

Species	PPFD	ETR	Rank	Fv/Fm	Rank
Q. rubra	746	112.7	4	0.371	5
Q. velutina	746	131.3	1	0.426	1
Q. alba	746	112.2	5	0.397	2
A. rubrum	746	113.0	3	0.374	4
U. alata	746	121.3	2	0.387	3

Table A5.8. Cardinal points for PPFD 466 µmol m^{-2} s^{-1}.

Species	PPFD	ETR	Rank	Fv/Fm	Rank
Q. rubra	466	90.5	5	0.463	5
Q. velutina	466	103.3	1	0.516	1
Q. alba	466	93.4	2	0.490	2
A. rubrum	466	92.5	4	0.471	4
U. alata	466	92.6	3	0.481	3

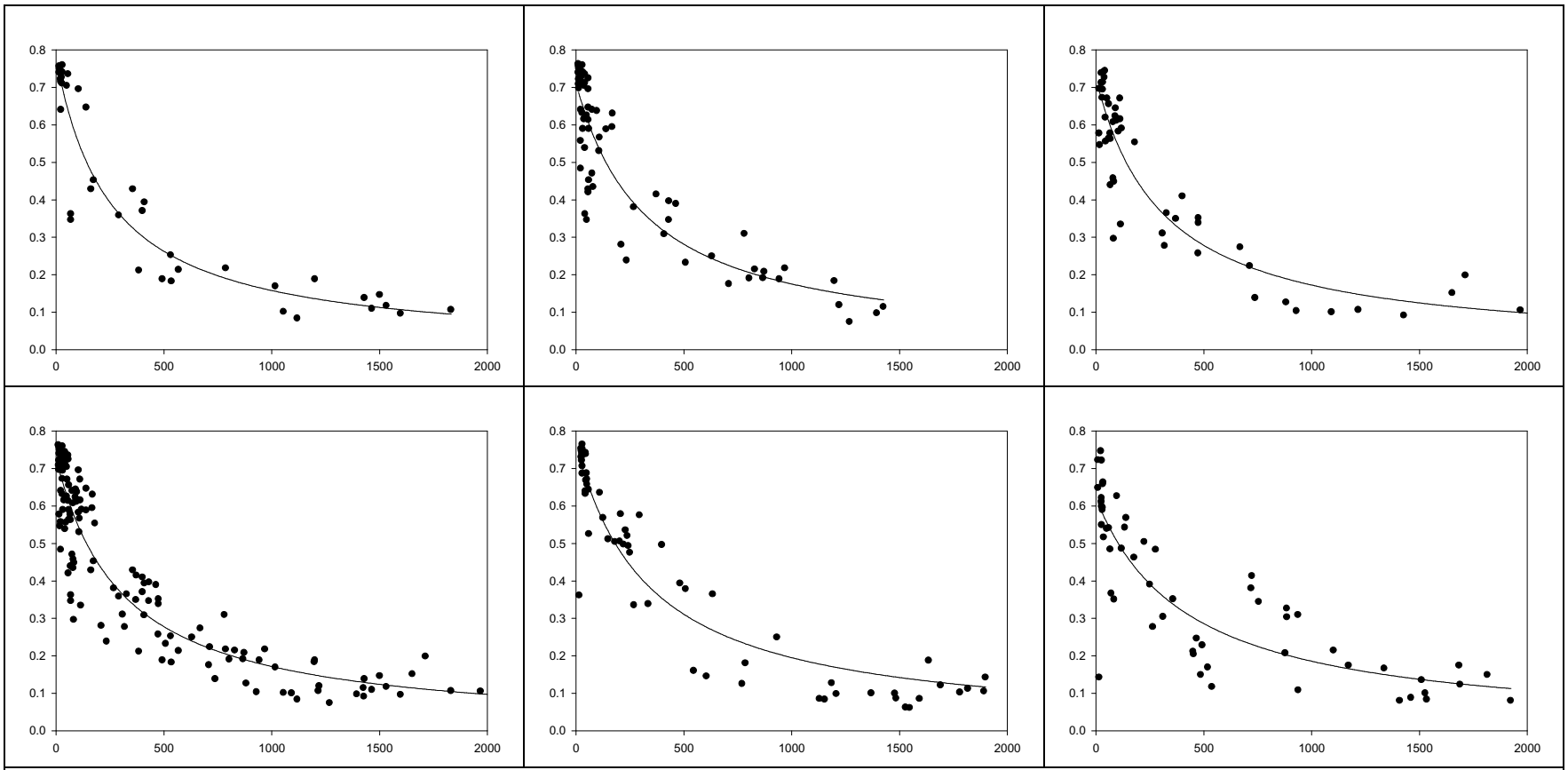

Figure A5.5. F_q'/F_m' light curves for October 2010. A) Q. rubra, B) Q. velutina, C) Q. alba, D) A. rubrum E) U. alata. Curves were fit to a line by Formula (5.2), YLD = (*a***b*)/(*b*+x). Where *a* sets magnitude (*a* = F_v/F_m @ 0 ppfd) and *b* sets bending degree.

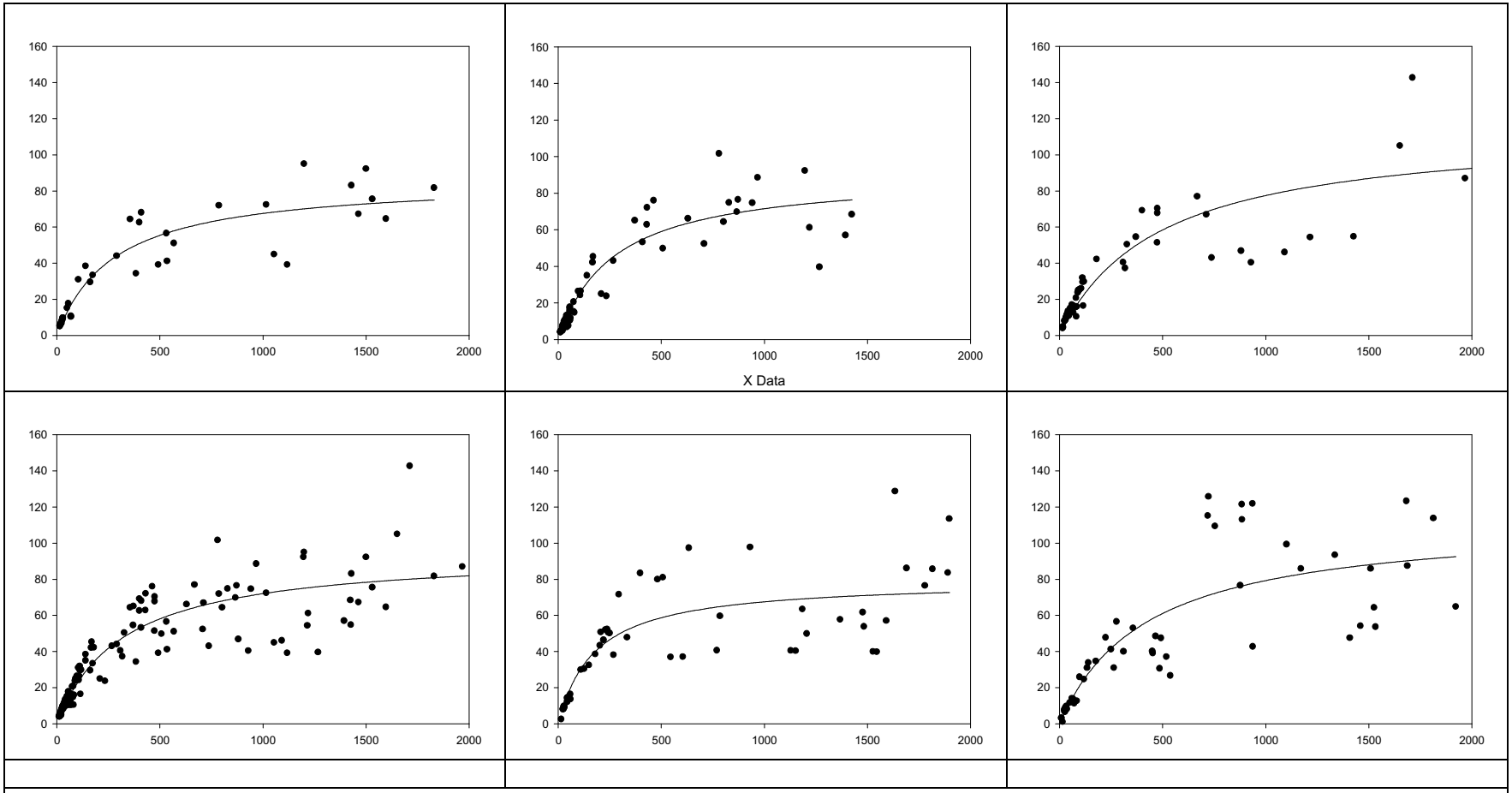

Figure A5.6. ETR light curves for October 2010. A) Q. rubra, B) Q. velutina, C) Q. alba, D) A. rubrum E) U. alata, and F) P. serotina. Curves were fit to a line by Formula (5.3), ETR = (*a**x)/(*b*+x). Where *a* sets magnitude and *b* sets bending degree.

Table A5.9. Calculated cardinal points for October 2010.

Species	PPFDmax	ETRmax	Rank	Fv/Fm	Rank
Q. rubra	1058	68.3	4	0.15	4
Q. velutina	1034	72.0	3	0.17	2
Q. alba	1341	84.5	2	0.14	5
A. rubrum	781	64.8	5	0.23	1
U. alata	1169	82.8	1	0.17	2

ETRmax = ETR @ 2000 mol * 0.9

Table A5.10. Cardinal points for PPFD 83.9 µmol m^{-2} s^{-1}.

Species	PPFD	ETR	Rank	Fv/Fm	Rank
Q. rubra	83.9	20.0	3	0.58	2
Q. velutina	83.9	21.5	2	0.57	3
Q. alba	83.9	16.8	5	0.57	3
A. rubrum	83.9	25.3	1	0.62	1
U. alata	83.9	19.1	4	0.52	5

Table A5.11. Cardinal points for PPFD 746 µmol m^{-2} s^{-1}.

Species	PPFD	ETR	Rank	Fv/Fm	Rank
Q. rubra	746	62.9	5	0.198	5
Q. velutina	746	66.7	3	0.217	3
Q. alba	746	69.2	2	0.215	4
A. rubrum	746	64.3	4	0.241	1
U. alata	746	72.0	1	0.226	2

Table A5.12. Cardinal points for PPFD 466 µmol m^{-2} s^{-1}.

Species	PPFD	ETR	Rank	Fv/Fm	Rank
Q. rubra	466	54.0	5	0.276	5
Q. velutina	466	57.5	3	0.294	3
Q. alba	466	56.3	4	0.287	4
A. rubrum	466	57.6	2	0.325	1
U. alata	466	59.1	1	0.298	2

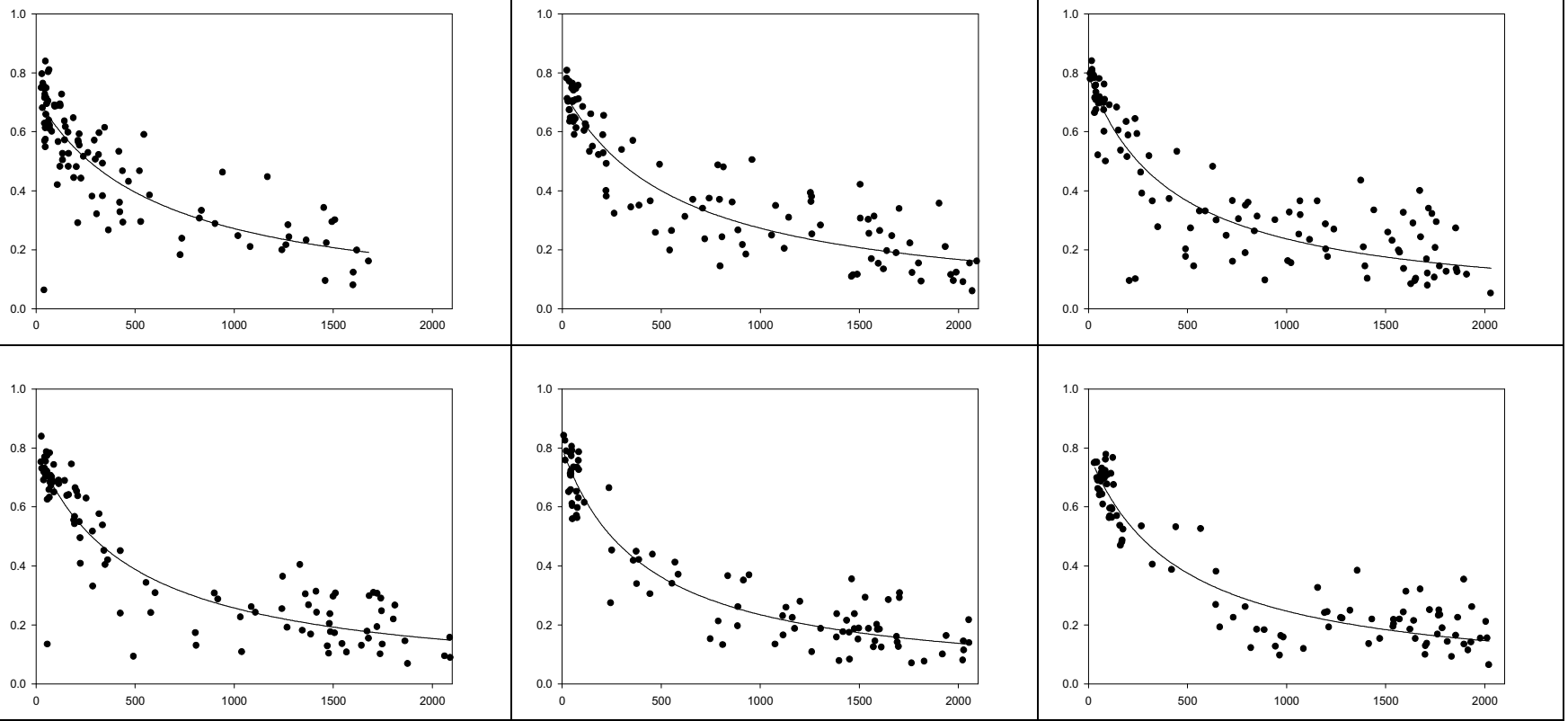

Figure A5.7. F_q'/F_m' light curves for April/May 2011. A) Q. rubra, B) Q. velutina, C) Q. alba, D) A. rubrum E) U. alata. Curves were fit to a line by Formula (5.2), YLD = (*a***b*)/(*b*+x). Where *a* sets magnitude (*a* = F_v/F_m @ 0 ppfd) and *b* sets bending degree.

*

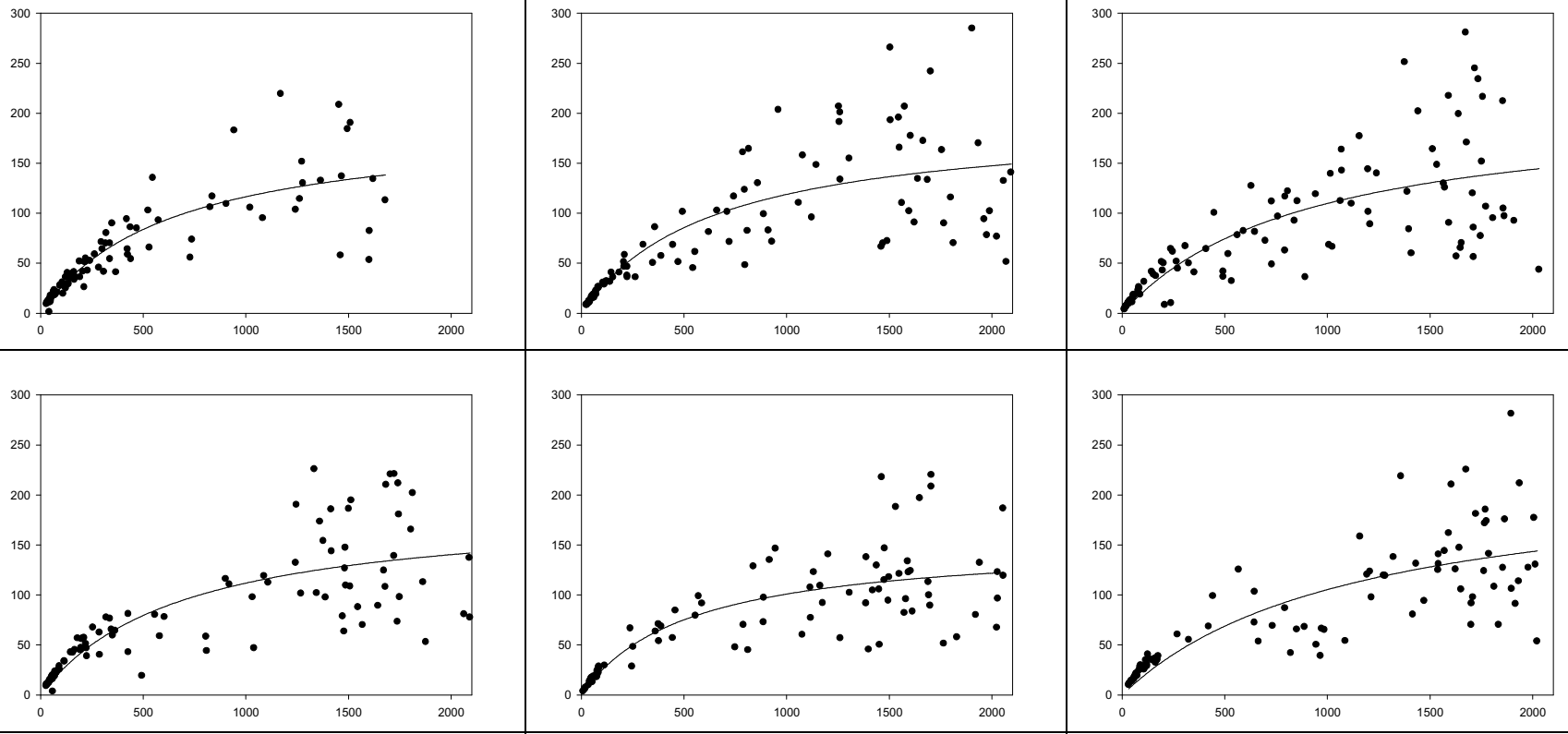

Figure A5.8. ETR light curves for April/May 2011. A) Q. rubra, B) Q. velutina, C) Q. alba, D) A. rubrum E) U. alata, and F) P. serotina. Curves were fit to a line by Formula (5.3), ETR = (a*x)/(b+x). Where a sets magnitude and b sets bending degree.

Table A5.13. Calculated cardinal points for April/May 2011.

Species	PPFDmax	ETRmax	Rank	Fv/Fm	Rank
Q. rubra	1383.4	130.6	2	0.219	2
Q. velutina	1368.1	132.8	1	0.221	1
Q. alba	1478.1	129.6	4	0.177	6
A. rubrum	1398.6	126.4	5	0.203	3
U. alata	1297.2	109.5	6	0.194	4
P. serotina	1532.5	129.2	3	0.181	5

ETRmax = ETR @ 2000 mol * 0.9

Table A5.14. Cardinal points for PPFD 83.9 µmol m^{-2} s^{-1}.

Species	PPFD	ETR	Rank	Fv/Fm	Rank
Q. rubra	83.9	22.0	2	0.634	6
Q. velutina	83.9	23.1	1	0.653	5
Q. alba	83.9	17.8	5	0.658	4
A. rubrum	83.9	20.7	4	0.674	1
U. alata	83.9	21.7	3	0.661	3
P. serotina	83.9	15.8	6	0.662	2

Table A5.15. Cardinal points for PPFD 746 µmol m^{-2} s^{-1}.

Species	PPFD	ETR	Rank	Fv/Fm	Rank
Q. rubra	746	102.8	2	0.322	2
Q. velutina	746	105.1	1	0.324	1
Q. alba	746	94.5	4	0.288	5
A. rubrum	746	98.2	3	0.311	3
U. alata	746	90.4	5	0.286	6
P. serotina	746	89.1	6	0.299	4

Table 5.16. Cardinal points for PPFD 466 µmol m^{-2} s^{-1}.

Species	PPFD	ETR	Rank	Fv/Fm	Rank
Q. rubra	466	80.7	2	0.407	2
Q. velutina	466	82.3	1	0.413	1
Q. alba	466	71.1	5	0.379	5
A. rubrum	466	76.4	3	0.401	3
U. alata	466	72.4	4	0.377	6
P. serotina	466	65.7	6	0.389	4

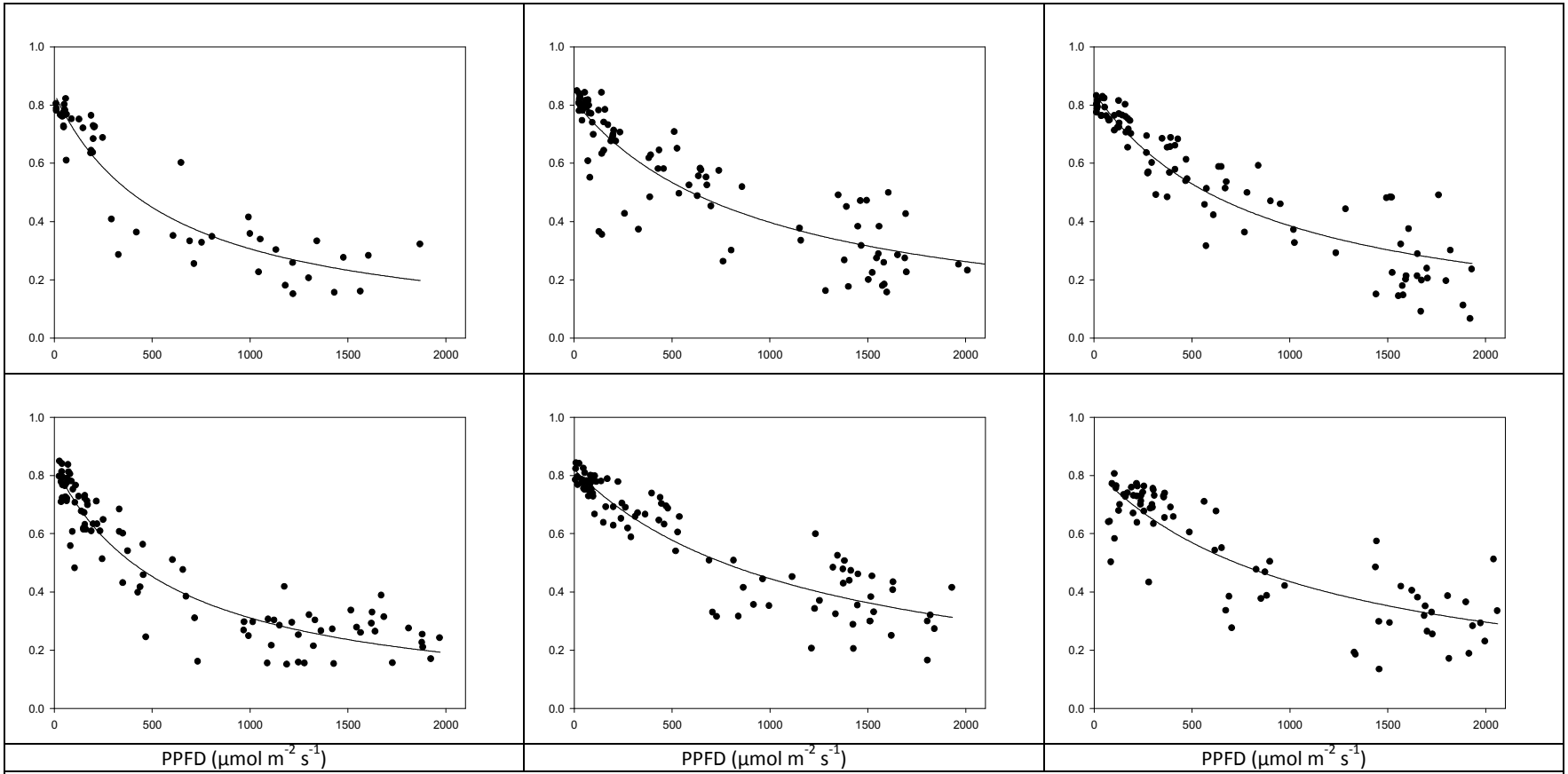

Figure A5.9. $F_{q'}/F_{m'}$ light curves for July 2011. A) Q. rubra, B) Q. velutina, C) Q. alba, D) A. rubrum E) U. alata. Curves were fit to a line by Formula (5.2), YLD = (*a***b*)/(*b*+x). Where *a* sets magnitude (*a* = F_v/F_m @ 0 ppfd) and *b* sets bending degree.

*

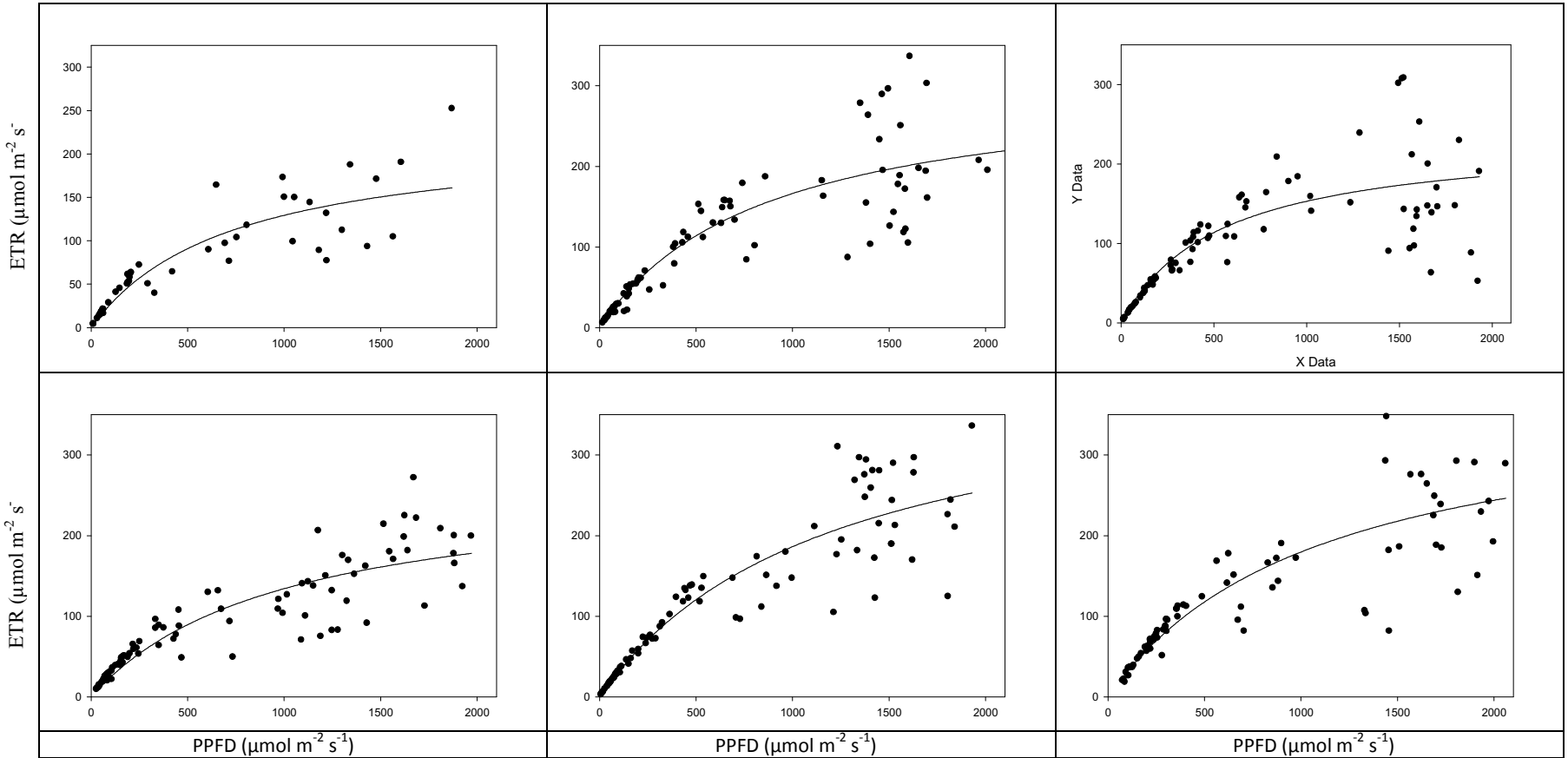

Figure A5.8. ETR light curves for July 2011. A) Q. rubra, B) Q. velutina, C) Q. alba, D) A. rubrum E) U. alata, and F) P. serotina. Curves were fit to a line by Formula (5.3), ETR = (*a**x)/(*b*+x). Where *a* sets magnitude and *b* sets bending degree.

Table A5.17. Calculated cardinal points for July 2011.

Species	PPFDmax	ETRmax	Rank	Fv/Fm	Rank
Q. rubra	1412.8	147.5	6	0.243	5
Q. velutina	1457.1	194.5	3	0.321	4
Q. alba	1279.8	165.7	4	0.334	3
A. rubrum	1477.1	160.2	5	0.239	6
U. alata	1495.7	227.7	1	0.363	1
P. serotina	1518.4	219.4	2	0.350	2

ETRmax = ETR @ 2000 mol * 0.9

Table A5.18. Cardinal points for PPFD 83.9 µmol m^{-2} s^{-1}.

Species	PPFD	ETR	Rank	Fv/Fm	Rank
Q. rubra	83.9	23.2	5	0.732	5
Q. velutina	83.9	27.7	2	0.748	4
Q. alba	83.9	32.3	1	0.768	2
A. rubrum	83.9	21.1	6	0.730	6
U. alata	83.9	26.6	4	0.763	3
P. serotina	83.9	26.7	3	0.770	1

Table A5.19. Cardinal points for PPFD 746 µmol m^{-2} s^{-1}

Species	PPFD	ETR	Rank	Fv/Fm	Rank
Q. rubra	746	113.1	6	0.364	5
Q. velutina	746	143.9	3	0.456	3
Q. alba	746	138.5	4	0.441	4
A. rubrum	746	116.5	5	0.364	5
U. alata	746	157.1	1	0.503	1
P. serotina	746	152.3	2	0.494	2

Table A5.20. Cardinal points for PPFD 466 µmol m^{-2} s^{-1}.

Species	PPFD	ETR	Rank	Fv/Fm	Rank
Q. rubra	466	87.1	5	0.463	5
Q. velutina	466	108.9	4	0.447	6
Q. alba	466	109.8	3	0.543	3
A. rubrum	466	85.3	6	0.468	4
U. alata	466	114.7	1	0.590	1
P. serotina	466	112.2	2	0.580	2

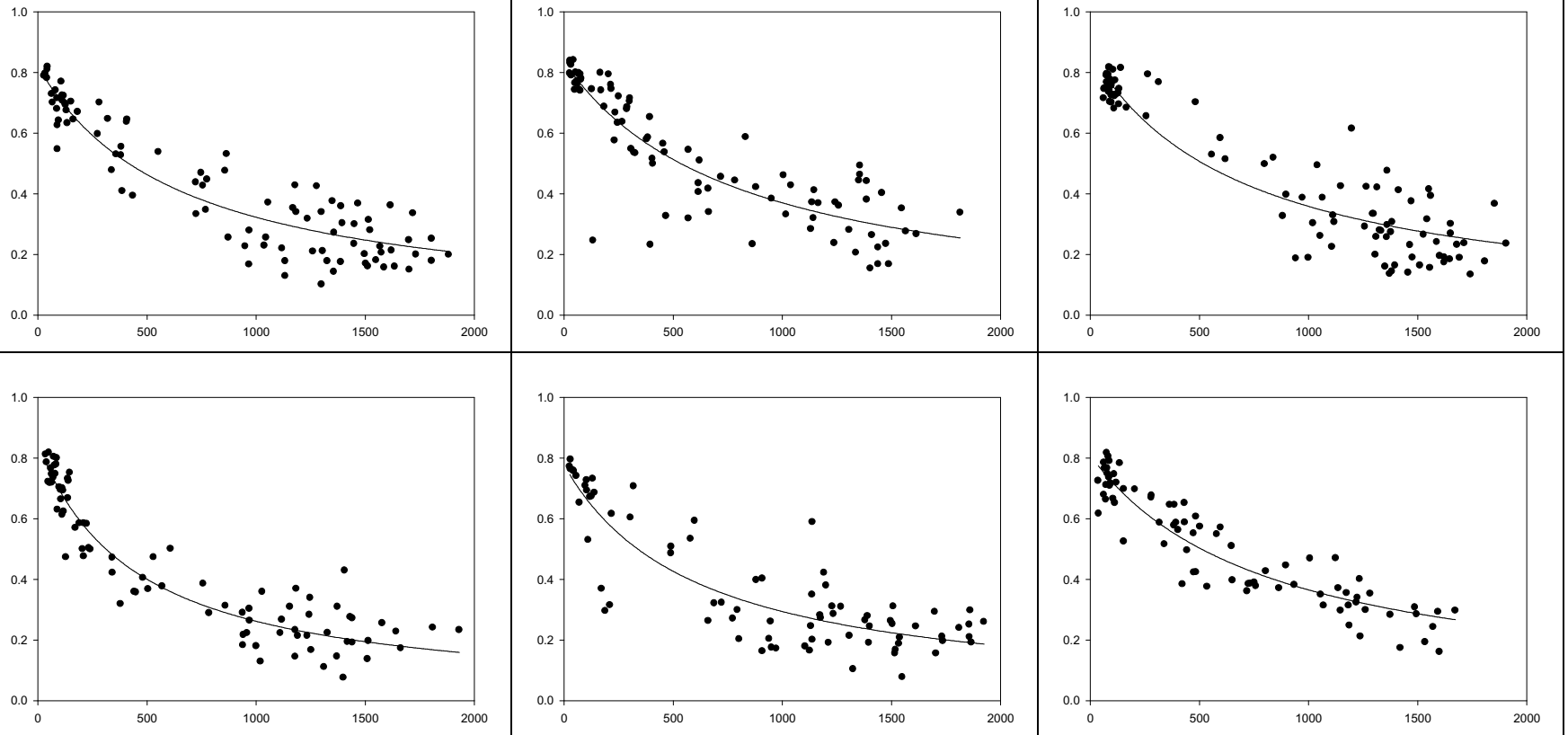

Figure A5.9. $F_{q'}/F_{m'}$ light curves for September 2011. A) Q. rubra, B) Q. velutina, C) Q. alba, D) A. rubrum E) U. alata. Curves were fit to a line by Formula (5.2), YLD = (*a***b*)/(*b*+x). Where *a* sets magnitude (*a* = F_v/F_m @ 0 ppfd) and *b* sets bending degree.

*

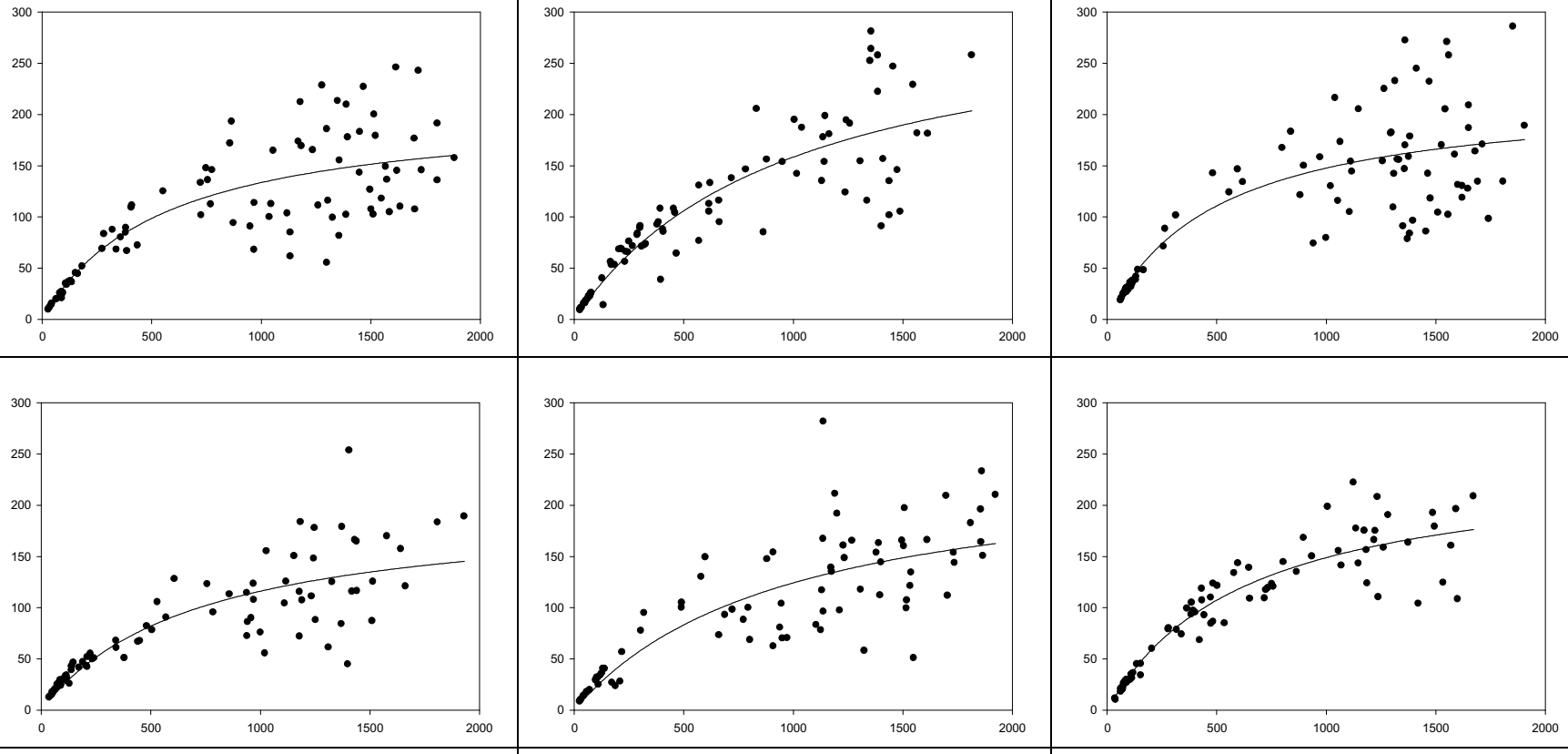

Figure A5.10. ETR light curves for September 2011. A) Q. rubra, B) Q. velutina, C) Q. alba, D) A. rubrum E) U. alata, and F) P. serotina. Curves were fit to a line by Formula (5.3), ETR = (a*x)/(b+x). Where a sets magnitude and b sets bending degree.

Tables for September 2011

Table A5.21. Calculated cardinal points for September 2011.

Species	PPFDmax	ETRmax	Rank	Fv/Fm	Rank
Q. rubra	1339	146.7	4	0.268	4
Q. velutina	1494	189.5	1	0.290	3
Q. alba	1258	158.4	3	0.312	1
A. rubrum	1361	130.5	6	0.210	6
U. alata	1450	146.7	4	0.230	5
P. serotina	1366	166.1	2	0.304	2

ETRmax = ETR @ 2000 mol * 0.9

Table A5.22. Cardinal points for PPFD 83.9 µmol m^{-2} s^{-1}.

Species	PPFD	ETR	Rank	Fv/Fm	Rank
Q. rubra	83.9	27.9	3	0.729	4
Q. velutina	83.9	25.0	4	0.753	2
Q. alba	83.9	31.7	1	0.774	1
A. rubrum	83.9	21.1	5	0.715	5
U. alata	83.9	19.8	6	0.686	6
P. serotina	83.9	28.0	2	0.733	3

Table A5.23. Cardinal points for PPFD 746 µmol m^{-2} s^{-1}.

Species	PPFD	ETR	Rank	Fv/Fm	Rank
Q. rubra	746	119.2	4	0.382	4
Q. velutina	746	135.6	1	0.431	1
Q. alba	746	132.7	2	0.421	3
A. rubrum	746	101.8	6	0.318	6
U. alata	746	106.4	5	0.350	5
P. serotina	746	131.5	3	0.423	2

Table A5.24. Cardinal points for PPFD 466 µmol m^{-2} s^{-1}.

Species	PPFD	ETR	Rank	Fv/Fm	Rank
Q. rubra	466	95.0	4	0.477	4
Q. velutina	466	101.0	3	0.528	1
Q. alba	466	106.7	1	0.521	2
A. rubrum	466	78.7	6	0.415	6
U. alata	466	79.5	5	0.440	5
P. serotina	466	103.0	2	0.517	3

Tables for October *A* (high temp) 2011

Table A5.25. Calculated cardinal points for Octobrer *A* 2011.

Species	PPFDmax	ETRmax	Rank	Fv/Fm	Rank
Q. rubra	1400	155.8	5	0.26	3
Q. velutina	1600	188.5	1	0.25	4
Q. alba	1450	172.9	2	0.27	2
A. rubrum	950	76.9	6	0.19	6
U. alata	1400	158.1	4	0.24	5
P. serotina	1300	160.5	3	0.30	1

ETRmax = (ETR @ 2000 µmol m^{-2} s^{-1}) * 0.9

Table A5.26. Cardinal points for PPFD 746 μmol m^{-2} s^{-1} for October *A* 2011.

Species	PPFD	ETR	Rank	$F_{q'}/F_{m'}$	Rank
Q. rubra	746	120.0	5	0.38	5
Q. velutina	746	121.5	4	0.40	3
Q. alba	746	128.9	2	0.41	2
A. rubrum	746	72.7	6	0.23	6
U. alata	746	123.4	3	0.39	4
P. serotina	746	132.8	1	0.43	1

Table A5.27. Calculated cardinal points for Octobrer *A* 2011.

Species	PPFDmax	ETRmax	Rank	Fv/Fm	Rank
Q. rubra	700	38.3	6	0.13	5
Q. velutina	1100	97.5	2	0.23	2
Q. alba	1100	78.8	4	0.20	4
A. rubrum	1200	65.1	5	0.12	6
U. alata	750	81.9	3	0.30	1
P. serotina	1100	103.7	1	0.23	2

ETRmax = (ETR @ 2000 μmol m^{-2} s^{-1}) * 0.9

Table A5.28. Cardinal points for PPFD 746 μmol m^{-2} s^{-1} for October *B* 2011.

Species	PPFD	ETR	Rank	$F_{q'}/F_{m'}$	Rank
Q. rubra	35.8	6	6	0.12	5
Q. velutina	87.3	2	2	0.29	2
Q. alba	71.6	4	4	0.23	3
A. rubrum	56.1	5	5	0.16	4
U. alata	81.5	3	3	0.29	2
P. serotina	92.8	1	1	0.30	1

Table A5.29. Calculated cardinal points for April/May 2012

Species	PPFDmax	ETRmax	Rank	Fv/Fm	Rank
Q. rubra	1100	102.7	5	0.24	4
Q. velutina	1350	135.7	3	0.23	5
Q. alba	1250	117.2	4	0.22	6
A. rubrum	1100	110.1	6	0.26	1
U. alata	1350	148.5	2	0.26	1
P. serotina	1250	160.5	1	0.25	3

ETRmax = (ETR @ 2000 μmol m^{-2} s^{-1}) * 0.9

Table A5.30. Cardinal points for PPFD 746 μmol m^{-2} s^{-1} for April/May 2012.

Species	PPFD	ETR	Rank	$F_{q'}/F_{m'}$	Rank
Q. rubra	92.5	92.5	6	0.30	6
Q. velutina	107.1	107.1	3	0.34	3
Q. alba	98.1	98.1	5	0.31	5
A. rubrum	99.6	99.6	4	0.33	4
U. alata	118.6	118.6	2	0.37	1
P. serotina	132.8	132.8	1	0.36	2

Table A5.31. Calculated cardinal points for July 2012

Species	PPFDmax	ETRmax	Rank	Fv/Fm	Rank
Q. rubra	850	84.9	6	0.25	1
Q. velutina	1000	94.6	5	0.25	1
Q. alba	1150	116.5	3	0.25	1
A. rubrum	1200	110.3	4	0.22	4
U. alata	1350	121.5	2	0.20	5
P. serotina	1200	130.6	1	0.22	4

ETRmax = (ETR @ 2000 μmol m^{-2} s^{-1}) * 0.9

Table A5.32. Cardinal points for PPFD 746 μmol m^{-2} s^{-1} for July 2012.

Species	PPFD	ETR	Rank	$F_{q'}/F_{m'}$	Rank
Q. rubra	746	82.8	5	0.28	6
Q. velutina	746	88.9	4	0.30	3
Q. alba	746	103.1	2	0.34	1
A. rubrum	746	95.1	3	0.31	2
U. alata	746	95.1	3	0.30	3
P. serotina	746	113.4	1	0.30	3

Table A5.33. Calculated cardinal points for October 2012

Species	PPFDmax	ETRmax	Rank	Fv/Fm	Rank
Q. rubra	1550	190.6	3	0.27	6
Q. velutina	1250	154.0	6	0.31	4
Q. alba	1400	181.7	4	0.32	3
A. rubrum	1250	154.9	5	0.31	4
U. alata	1400	197.2	2	0.35	1
P. serotina	1550	223.3	1	0.33	2

ETRmax = (ETR @ 2000 μmol m^{-2} s^{-1}) * 0.9

Table A5.34. Cardinal points for PPFD 746 μmol m^{-2} s^{-1} for October 2012.

Species	PPFD	ETR	Rank	$F_{q'}/F_{m'}$	Rank
Q. rubra	746	122.3	6	0.42	4
Q. velutina	746	129.7	5	0.42	4
Q. alba	746	141.0	3	0.45	3
A. rubrum	746	130.0	4	0.42	4
U. alata	746	153.2	1	0.48	1
P. serotina	746	148.0	2	0.48	2

APPENDIX VI – Presentation and Publication of Results

Conferences:

16th Biennial Southern Silvicultural Research Conference
Chalreston, SC February 14-17, 2011

Oral Presentation:

First year response of oak natural regeneration to a shelterwood harvest and midstory competition control in the Arkansas Ozarks.

Publication:

Cunningham, K.K. (2012) First year response of oak natural regeneration to a shelterwood harvest and midstory competition control in the Arkansas Ozarks. In: Butnor, John R., ed. 2012. Proceedings of the 16th biennial southern silvicultural research conference. e-Gen. Tech. Rep. SRS-156. Asheville, NC: U.S. Department of Agriculture Forest Service, Southern Research Station. 393 p.

95th Annual Meeting of Arkansas Academy of Sciences
University of Arkansas at Monticello, April 8 and 9th, 2011

Oral Presentation:

Using Chlorophyll Fluorescence to Compare Irradiance Effects on Photosystem II (PSII) Photochemistry in Advanced Reproduction of Five Upland Hardwood Species
Cunningham K., and Grace S.

17th Biennial Southern Silvicultural Research Conference
Shreveport, LA, March 5 – 7, 2013

Oral Presentation:

Third year response of oak natural regeneration to a shelterwood harvest and midstory competition control in the Arkansas Ozarks. – Cunningham K.

Poster Presentation:

Evaluation of photosynthetic light response curves from two methods of chlorophyll fluorescence sampling in the field using advanced reproduction of six upland hardwood species.
Cunningham K. and Grace S.

Using chlorophyll fluorescence to evaluate light reactions of photosynthesis for hardwood andvanced reproduction in varying understory sunlight environments
Cunningham K. and Grace S.

Publication:

Full paper

Cunningham, K.K. (2014, in print) Third year response of oak natural regeneration to a shelterwood harvest and midstory competition control in the Arkansas Ozarks.

Extended abstract
(In print)Evaluation of photosynthetic light response curves from two methods of chlorophyll fluorescence sampling in the field using advanced reproduction of six upland hardwood species. Cunningham K. and Grace S.

North American Forest Ecology Workshop
Bloomington, IN June 16 – 18, 2013

Oral Presentation:

Using chlorophyll fluorescence to evaluate light reactions of photosynthesis for hardwood andvanced reproduction in varying understory sunlight environments
Cunningham K. and Grace S.

Poster Presentation:

Evaluation of photosynthetic light response curves from two methods of chlorophyll fluorescence sampling in the field using advanced reproduction of six upland hardwood species.
Cunningham K. and Grace S.

Publication:

No proceedings, presentations will be placed on website.

99th Ecological Society of America Annual Meeting
Sacramento, CA August 10 – 15th, 2014

Oral Presentation: Submitted

Using chlorophyll fluorescence to evaluate light reactions of photosynthesis for hardwood andvanced reproduction in varying understory sunlight environments
Cunningham K. and Grace S.

Poster Presentation: Submitted

Evaluation of photosynthetic light response curves from two methods of chlorophyll fluorescence sampling in the field using advanced reproduction of six upland hardwood species.
Cunningham K. and Grace S.

A growing season analysis of photosynthesis for upland hardwood reproduction experiencing drought stress.

APPENDIX VII – Monthly Average Maximum Temperature and Precipitation

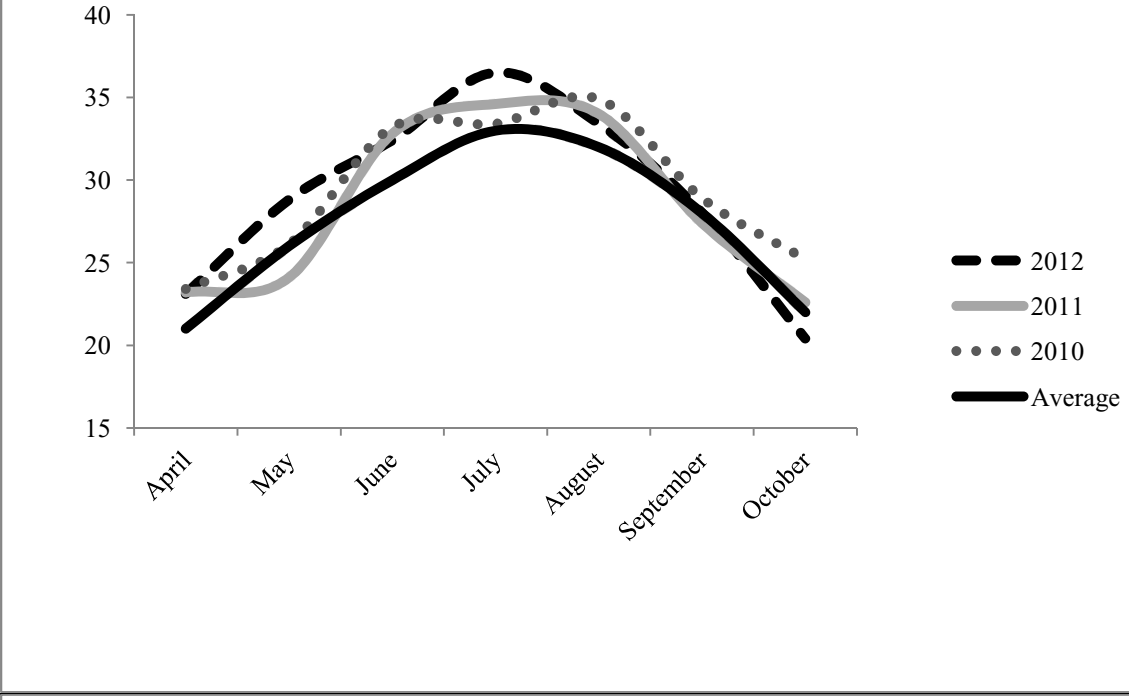

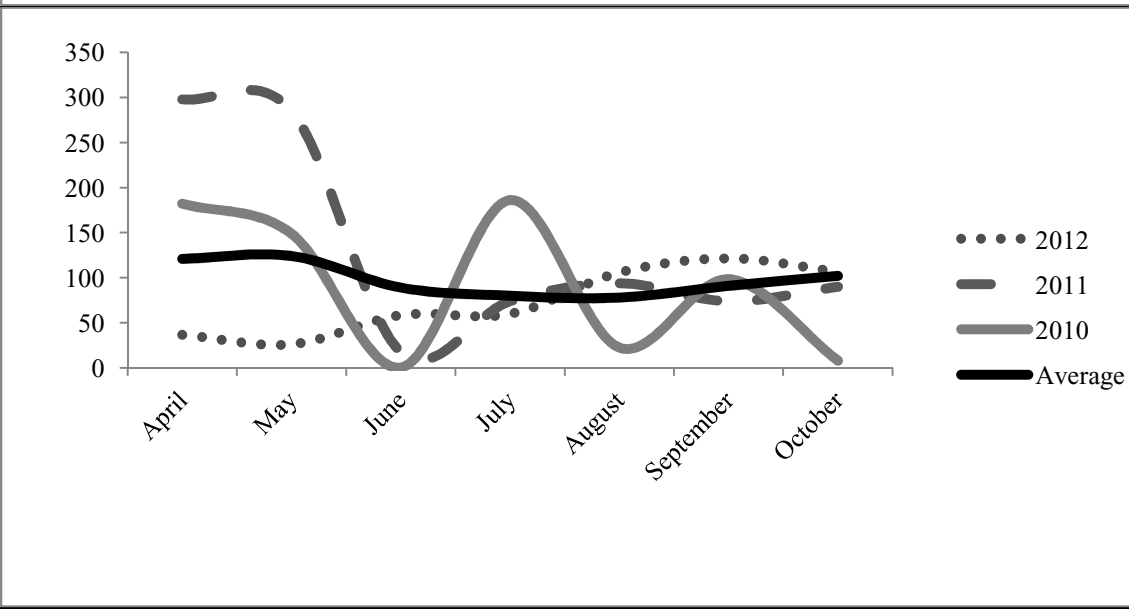

Figure __. A) Monthly average maximum daily temperatures for years 1 – 3 post-harvest. B) Monthly average precipitation (mm) in years 1 -3 post-harvest.